A Perspective on Computational Aeroelasticity 1970s to Now

Guru P. Guruswamy
Computational Physics Branch
NASA Advanced Supercomputing (NAS) Division
Exploration Technology Directorate
Ames Research Center

Symposium on Classical to Computational Aeroelasticity
Indian Institute of Science
Bengaluru, India
Sept 10-13, 2018

http://www.nas.nasa.gov/~guru

Acknowledgements

Research Partners

Byun Chansup (Sun) : HiMAP, FSI, Parallel Computing
Mark Potsdam (US Army) : HiMAP, grids for UH-60A
Pieter Buning (LaRC) : OVERFLOW
Peter Goorjian (ARC) : TSP, GO3D
Doug Boyd (LaRC) : Deforming grid in OVERFLOW, HART-II GRID
Dennis Jespersen (ARC) : MPI on Super-cluster
Sabine Goodwin, Pradeep Raj, Vin Sharma (Lockheed) : L1011, F-16 Computations
Shigeru Obayashi (Tohoku U) : ENSAERO Upwind Flow Solvers
Lloyd Eldred (LaRC) : FEM, NASTRAN
Neal Chaderjian (ARC) : Zonal Grid Options in HiMAP
Rakesh Kapania, Dale MacMurdy (VPI) : FEM
Yehia Rizk (ARC) : Hypersonic
Fred Striz (Okalohoma U) : FEM, Frequency Domain Approach
Manoj Bhardwaj (Sandia, DoE) : FEM
Dave Findlay (US NAVY) : F18
Steve Dobbs, Gerry Miller, Iroshi Ide (Boeing) : B-1, X31
Appa (Northrup) Argyris (Stuttgart) : Flight Dynamics for CFD
David Yeh (Boeing-Military) : Active Controls, X31
Eugene Tu (ARC) : ENSAERO, Stability Derivatives, Active Controls
Lakshmi Sankar: (SA Turbulence model, Parallel version)
Joseph Garcia (ARC) : Nonlinear CSD, Controls, Hypersonic
Mike Myers (Lockheed): Flutter
Ferat Hatay(Sun/Oracle): Parallel Computing
Mehrdad Farhannia (President & CEO, Roxwood Medical) : HiMAP
Max Platzer, Kevin Jones (Naval Post Graduate School, F-18 Abrupt Wing Stall)

Program Managers

(NASA) : HPCC, HSCT, SRW, NAVY, Air Force
Mentors : Drs. Yang (Purdue), Olsen (AFWAL), Ballhaus (NASA), Ashley(Stanford)

Background

- Structural deformations impact vehicle performance
  - High speed civil transports
  - Launch vehicles
  - Rotorcraft
  - Flexible thermal protection system

- Strong fluid/structure interactions occur due to
  - Flow separations, moving shock waves
  - Large structural displacements
  - Aeroelastic instabilities such as flutter

- Current analysis tools for design compute aeroelasticity within linear aerodynamic limitations (NASTRAN)
  - Euler/Navier-Stokes (ENS) based methods are needed

- Many current procedures use ENS as corrections to linear aerodynamic
  - Not adequate when flow non-linearities occur
  - Cannot account for non-linear phase angles
  - Not adequate for transient cases
  - Not suitable for active-controls

- Recently more tendency towards using Reduced Order Method
  - Limited to Euler equations
  - Not robust for Navier-Stokes equations (Stanford)
  - Not shown better than uncoupled modal approach (ENSAERO)

Key References

"Aeroelastic Time Response Analysis of Thin Airfoils by Transonic Code LTRAN2," Computers and Fluids, (1981)

"Efficient Algorithm for Unsteady Transonic Aerodynamics of Low-Aspect-Ratio Wings," J. of Aircraft, (1985),

"Efficient Algorithm for Unsteady Transonic Aerodynamics of Low-Aspect-Ratio Wings," J. of Aircraft, (1985)

"An Integrated Approach for Active Coupling of Structures and Fluids," AIAA J., (1989)

"Unsteady Aerodynamic and Aeroelastic Calculations for Wings Using Euler Equations," AIAA J., (1990),

"Vortical Flow Computations on a Flexible Blended Wing-Body Configuration," AIAA JI., (1992)

.

"Direct Coupling of the Euler Flow Equations with Plate Finite Element Structures," AIAA J., (1995).)

"Navier-Stokes Computations for Oscillating Control Surfaces," J of Aircraft, (1994),

"Convergence Acceleration of a Navier-Stokes Solver for Efficient Static Aeroelastic Computations," AIAA J., (!995)

"CFD/CSD Interaction Methodology for Aircraft Wings ", AIAA J (1998)

"Aerodynamic Influence Coefficient Computations Using ENS Equations on Parallel Computers," AIAA J., (1999)

"Development and Applications of a Large Scale Fluids/ Structures Simulation Process on Clusters," C & Fluids (2007)

"Time-Accurate Aeroelastic Computations of a Full Helicopter Model RANS" J. of Aerospace Innovations, (2013).

"Dual Level Parallel Computations for Database to Design Aerospace Vehicles," NASA TM-2013-216602, (2013).

"Dynamic Stability Analysis of Hypersonic Transport during Reentry," AIAA J (2017)

"Time Accurate Coupling of 3-DOF Parachute System using Navier-Stokes Equations," J Spacecraft and Rockets, (2016)

"N–S Equations-Based Aeroelasticity of Supersonic Transport Including Short-Period Oscillations, "" AIAA J, (2018)

Objective

- To present a summary of frequency domain and time domain procedures for aeroelasticity by using non-linear flow equations
  - Transonic small perturbation theory
  - Euler/Navier-Stokes Equations
  - Suitable for frameworks
  - Focus on efforts at Ames Research Center since 1975
  - 100 person-year effort!

Levels of Fidelity

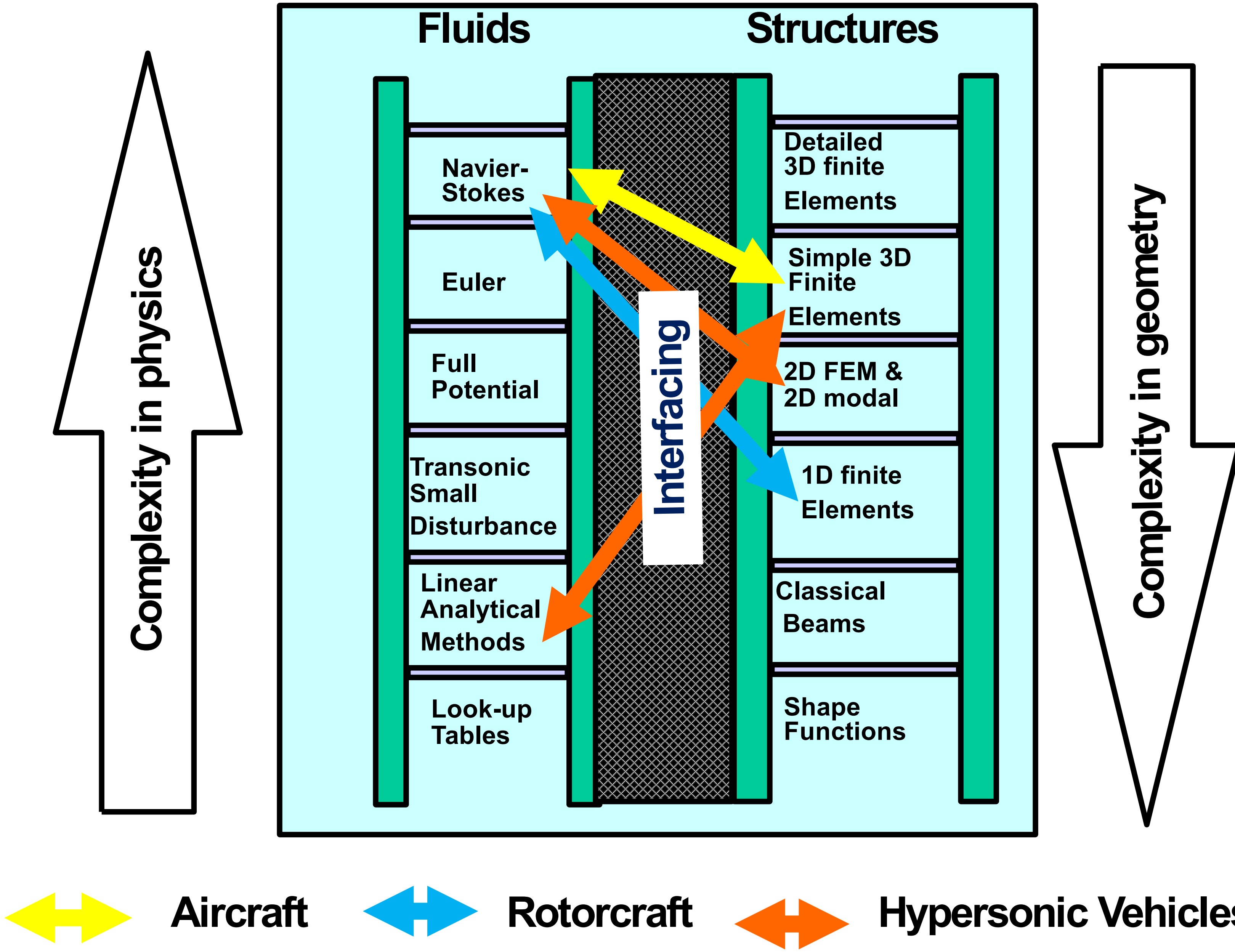

Solver Approaches

- Transonic Small Perturbation Equations
  - Limited to transonic flows
  - Robust since no grid movements
  - Super fast and still good for conceptual design

- Euler/Navier-Stokes equations
  - Reynolds averaged Navier-Stokes (RANS) equations
  - Baldwin-Lomax & Spalart-Allmaras turbulence models
  - Diagonal form of Beam-Warming central difference solver
  - Stream-wise upwind algorithm of Obayashi and Goorjian
  - Structured grids, patched & overset
  - Implemented in NASA codes HIMAP, OVERFLOW

  Grids are validated for space and temporal accuracies

- Lagrange's structural equations
  - Finite element and modal form

- Trajectory Equations

  3 DOF - Parachutes

  Phugoid Motion – Supersonic Transport

Coupled Aeroelastic Equations of Motion

- Lagrangian equations of motion

$$[m]\{\ddot{d}\} + [g]\{\dot{d}\} + [k]\{d\} = \{f\}$$

Where [m], [g], and [k] Are mass, damping, and stiffness matrices
{d} and {f} are the nodal displacements and aerodynamic force

- [M], [g] and [k] are computed using FEM
- {F} is computed solving ENS equations
- Solved using direct time integration

Modal equations of motion

From Rayleigh-Ritz analysis, the displacement vector {d} can be expressed as:

$$\{d\} = [\psi]\{q\}$$

where $[\psi]$ is the modal matrix and {q} is the generalized displacement vector. The final modal form of Lagrange's equations of motion is:

$$[M]\{\ddot{q}\} + [G]\{\dot{q}\} + [K]\{q\} = \{F\}$$

where [m], [g], and [k] are modal mass, damping, and stiffness matrices respectively. {F} is the generalized aerodynamics force vector defined as

$$\frac{1}{2}\rho U^2 [\psi]^T [A]\{C_P\}$$

where C_p is the pressure coefficient [A] is the diagonal area matrix of the aerodynamic control points, ρ the free-stream density, and U is velocity.

Coupled Procedures Using CFD/CSD

- Can be grouped into two categories based on type of fluid/structure coupling

TA-time Accurate

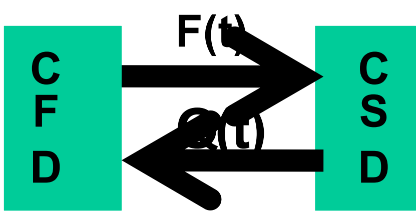

Every step

HB-Hybrid Methods

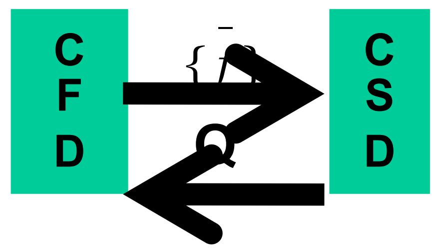

Ad-hoc

- In both methods CFD is computed time accurately
- In TA, airloads {f(t)} is directly from CFD in same time frame as CSD

$$[m]\{\ddot{q}\}+[c]\{\ddot{q}\}+[k]\{q\}=\{f_{CFD}\}$$

- In HB, $\{\bar{f}\}$ is modified using non-CFD (look –up tables!)

$$[m]\{\ddot{q}\}+[C]\{\dot{q}\}+[k]\{q\}=\{\bar{f}\}=g(\{q\})+\{\Delta f_{CFD}\}$$

- G is based on linear theory, look-up tables etc.
- CFD and CSD are not in the same time frame

Uncoupled Aeroelastic Procedure

- Onset of instability starts as a small perturbation phenomenon
- Unsteady aerodynamic forces for all frequencies are computed using fast indicial response approach
- Primary stability depends on rigid body pitch and plunge motions
- Fast generation of indicial responses is accomplished using dual-level parallel computations
- Stability analysis is performed in frequency domain using pre-computed unsteady aerodynamic data. (uncoupled analysis)

Two Degrees-of-Freedom Model
Rigid Body Plunge-Pitch modes

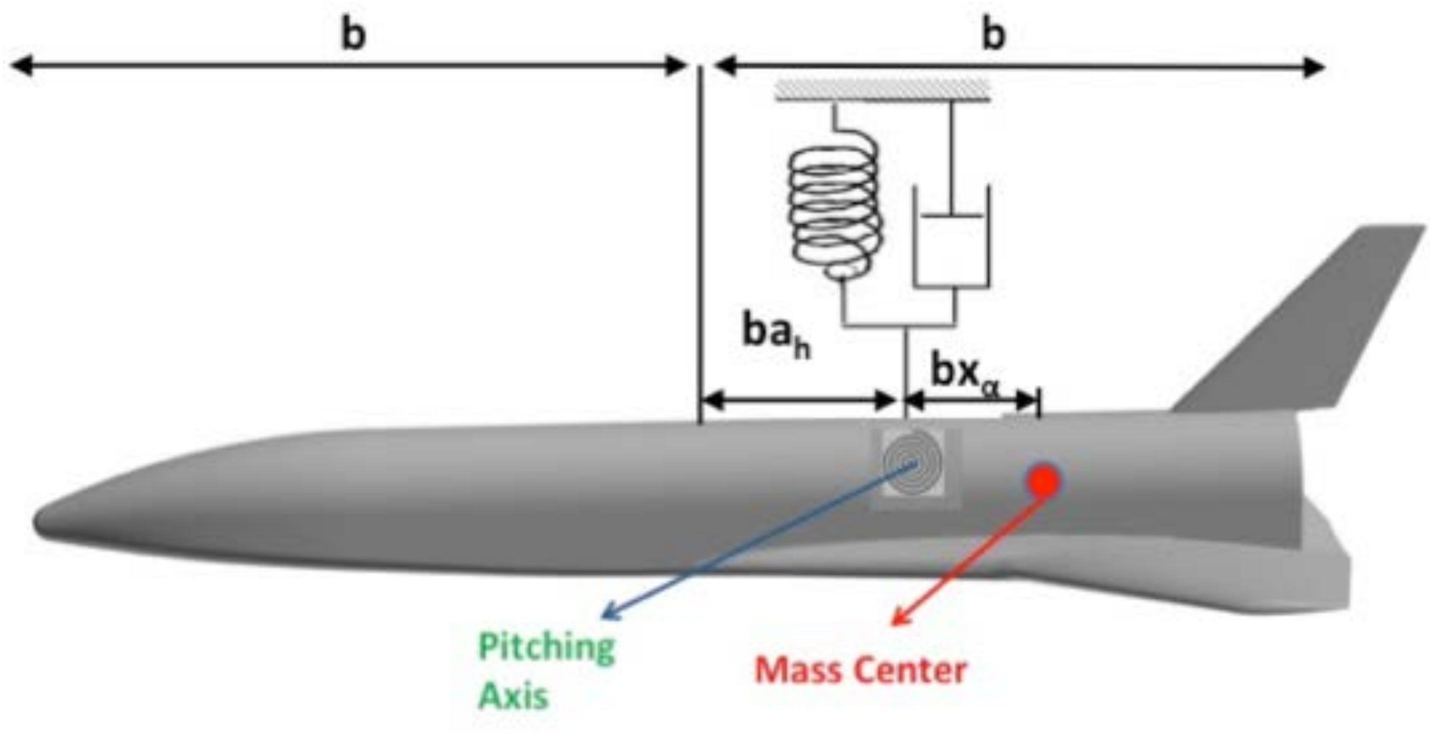

- **Distances are measured from mid-length +ve towards tail**

Stability Analysis Equations

- **Frequency domain Eigenvalue Equations**

$$\left[\mu k_b^2[M]-[A]\right]\begin{Bmatrix}\delta\\ \alpha\end{Bmatrix}=\lambda[K]\begin{Bmatrix}\delta\\ \alpha\end{Bmatrix}$$

k_b = reduced frequency, ωb/U, ω is circular frequency in rad/sec, U is speed in feet per sec, and b is semi-length. δ = h/2b and α are displacements corresponding to plunging and pitching motions, The mass-to-air density ratio $\mu = m/(\pi\rho b^2)$ where ρ is the air density and m is the total mass.

$$[M]=\begin{bmatrix}1 & x_\alpha\\ x_\alpha & \gamma_\alpha^2\end{bmatrix}\quad [A]=\frac{1}{\pi}\begin{bmatrix}0.5C_{l\delta} & C_{l\alpha}\\ -C_{m\delta} & -2C_{m\alpha}\end{bmatrix}\quad [K]=\frac{1}{\omega_r^2}\begin{bmatrix}\omega_h^2 & 0\\ 0 & \omega_\alpha^2\gamma_\alpha^2\end{bmatrix}$$

where ω_h, ω_α and ω_r are plunging, pitching and reference oscillatory frequencies. γ_α radius of gyration. The eigenvalue λ is defined as $\mu(1+ig)(b\omega_r^2/U)$ where g is the artificial structural damping.

- **Solved using classical U-g method**

Indicial Response Method

- **History**
  - **Introduced for computing unsteady airloads - Lomax (1950s)**
  - **Extended to flight stability analysis – Tobak (early 60)**
  - **TSP based unsteady aerodynamics - Ballhaus &Goorjian (mid 70s)**
  - **Airfoil flutter boundary - Guruswamy and Yang (late 70s)**
  - **NS based wing flutter boundary – Guruswamy and Tu (mid 80s)**
  - **Stability analysis of spacecraft – Guruswamy (2016)**

- **Assumptions**
  - **Unsteadiness is small-linear perturbation about a non-linear steady-state solution.**

- **Advantages**
  - **Data for multiple frequencies is extracted from a single response**

- **Derivatives**
  - **Pulse transfer technique - Edwards (mid 80s)**
  - **Rotorcraft – Leishman (late 80s)**
  - **Non-linear perturbation - Cummings et. al. (current)**

Classical Indicial Method

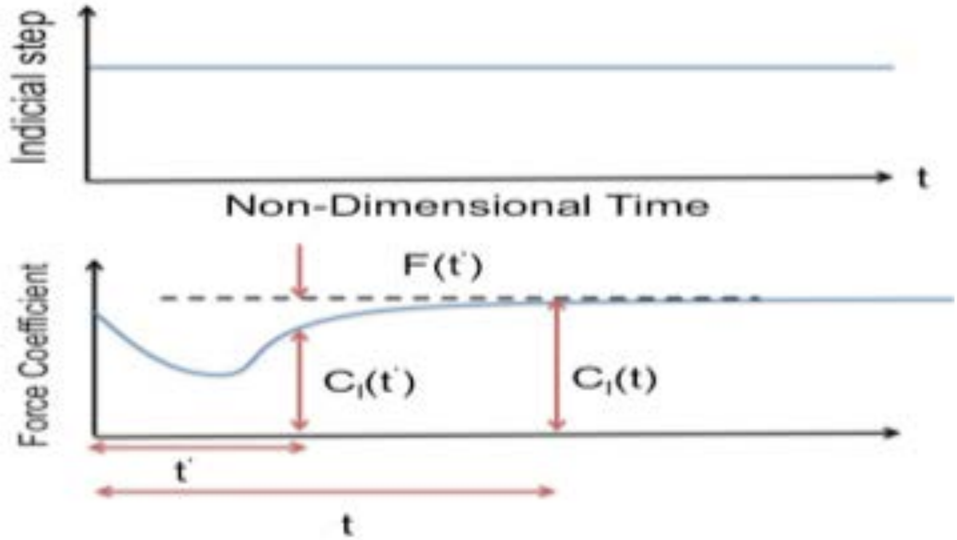

- **Assuming sinusoidal pitching motion**

$$\alpha(t) = \alpha_0 + \alpha_1 e^{i\omega t}$$

$$Re[C_{l\alpha}] = C_{l\alpha}(\infty) - \omega \int_0^{\infty} F(t')\sin(\omega t')\,dt'$$

$$Im[C_{l\alpha}] = -\omega \int_0^{\infty} F(t')\cos(\omega t')\,dt'$$

- **Similar equations apply for the moment coefficient**
- **Values for plunge motion are computed using the relation that induced angle** $\alpha_i = \frac{h}{U}$

Typical Finite Elements Used

In-house NASA 1D, 2D and 3D CSD models
- BEMBLD : 10dof rotating beam element
- SPARH: shear panel for spars and ribs
- PLTSHL: 18-dof skin/plate/shell fem
- TET3D: 12-dof tetrahedron solid element (future)
- NASTRAN

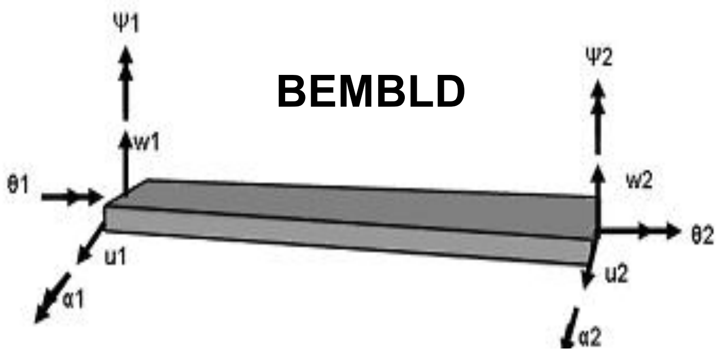

SPARH

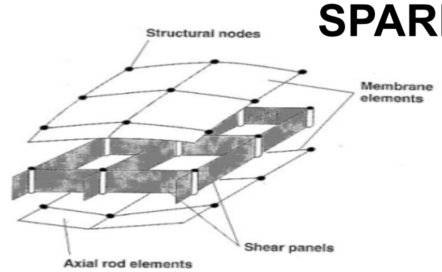

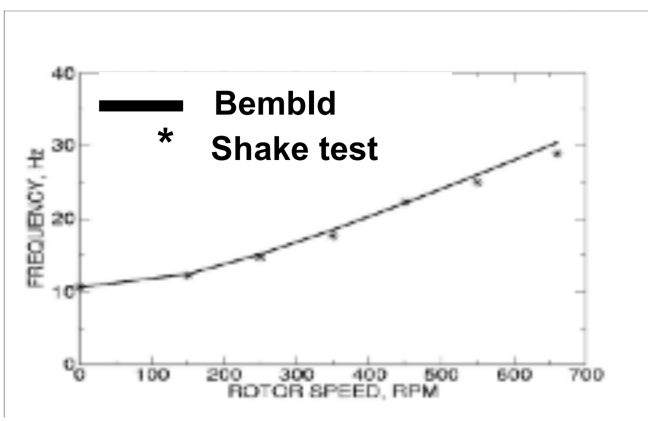

First flapping frequency

PLTSHL

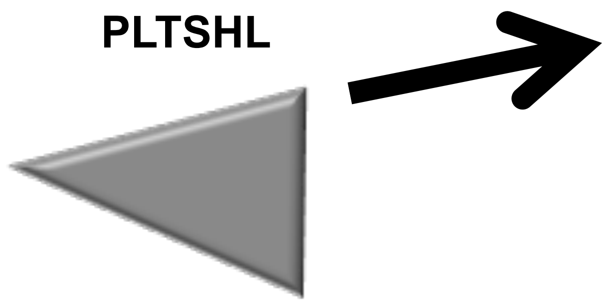

TET3D

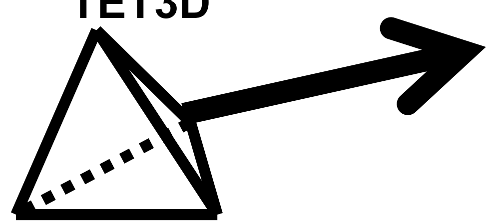

CFD/CSD Interactions (FSI)

Consistent load approach
Illustration for transverse DOF

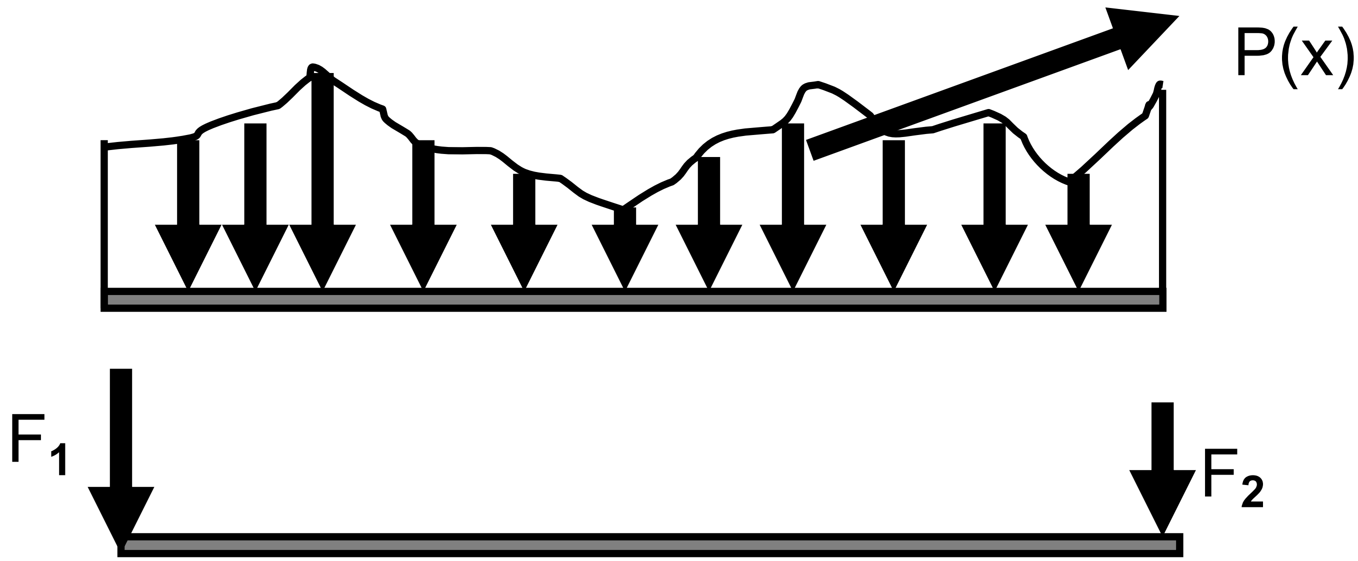

- $F_i = \int p(x)\, s_i(x)\, dx \quad 0 < x < l$

  where i denotes the deg of freedom p(x) is the distributed load and $S_i(x)$ IS ith shape function

- **Work is conserved between CFD and CSD**
- **Extensions using virtual surface method**

Guruswamy, G. P.," Coupled Finite-Difference/Finite-Element Approach for Wing-Body Aeroelasticity," AIAA 92-4680, n, September 21-23, 1992, Cleveland, Ohio.
Guruswamy, G.P. ," A Review of Numerical Fluids/Structures Interface Methods for Computations using High Fidelity Equations, "Computers and Fluids, (80) 2002 (Editor Prof Bathe, MIT)

Fluid/Structure Interface

- **Lumped load approach**
  - Fast, needs fine grids, adequate for uncoupled method

- **Consistent load approach (conserves loads)**
  - Accurate for coupled methods, expensive

• Transformation matrix : $T = Y_A [D^{-1} K + Y_S^T Y_S]^{-1} Y_S^T$

• Deflections at cfd grid : $Q_A = T\, Q_S$

• Nodal forces at fe grid : $Z_S = T^T Z_A$

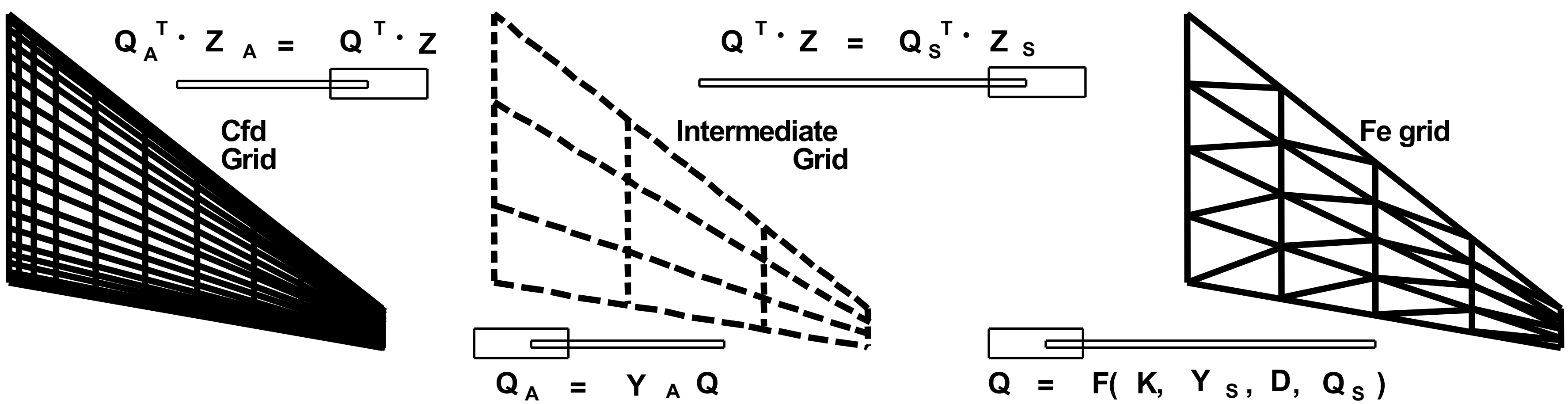

Guruswamy, G.P, and Byun, C. "Direct Coupling of the Euler Flow Equations with Plate Finite Element Structures," AIAA J, Vol. 33, No 2, Feb 1995.

Newmark's Time Integration

- **Assuming linear acceleration:**

$$\{\ddot{q}\}_t = [D](\{F\}_t - [G]\{v\} - [K]\{w\})$$

$$[D] = \left([M] + \left(\frac{\Delta t}{2}\right)[G] + \left(\frac{\Delta t^2}{6}\right)[K] \right)^{-1}$$

$$v = \{\dot{q}\}_{t-\Delta t} + \left(\frac{\Delta t}{2}\right)\{\ddot{q}\}_{t-\Delta t}$$

$$w = \{q\}_{t-\Delta t} + (\Delta t)\{\dot{q}\}_{t-\Delta t} + (\Delta t)\{\ddot{q}\}_{t-\Delta t} + \left(\frac{\Delta t}{2}\right)\{\ddot{q}\}_{t-\Delta t}$$

$$\{\dot{q}\}_t = \{\dot{q}\}_{t-\Delta t} + \left(\frac{\Delta t}{2}\right)\{\ddot{q}\}_{t-\Delta t} + \left(\frac{\Delta t}{2}\right)\{\ddot{q}\}_t$$

$$\{q\}_t = \{q\}_{t-\Delta t} + (\Delta t)\{\dot{q}\}_{t-\Delta t} + \left(\frac{\Delta t^2}{3}\right)\{\ddot{q}\}_{t-\Delta t} + \left(\frac{\Delta t^2}{6}\right)\{\ddot{q}\}_t$$

- **Above can be made implicit, assuming constant acceleration. This is NOT loose coupling as referred by Chopra's, group at UMD, ,Barun's group at Georgia Tech etc**

FSI Implicit (staggered) algorithm

- **Algorithm**

  a) Compute deformations using loads at t

  b) Using a) advance CFD from time *t* to *t* + Δ*t*

  c) Compute deformations using loads at *t* + Δ*t*

  d) Repeat a) b) c) until converge (use Newton method)

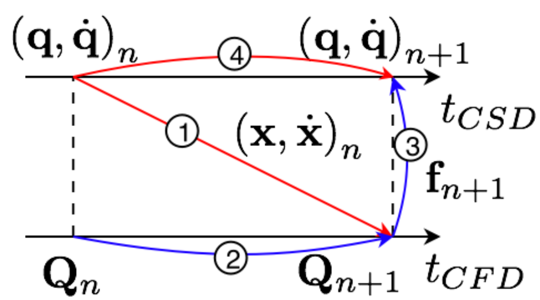

- **Increases book-keeping and dds significant computational expense**

- **No impact on CFD and CFD (linear and geometrically non-linear) computations**
  - In-house research
  - NASA sponsored research grants (UMD, Stanford)

Some Related Developments

(in-house and/or sponsored)

- Sheared grids for swept tapered wings (TSP)
- Characteristics BCs for supersonic flows (TSP & ENS)
- Stream-wise upwind algorithm for ENS solvers
- Pipe-line Gauss-Seidel algorithm for parallel CFD
- Parallel direct & sub-structure solver for CSD (NASTRAN)
- MPIRUN, for parallel fluid/structure/control simulation
- Parallel version of SA turbulence model
- Virtual surface method for FSI
- Virtual surface method for sliding CFD grid zones (controls)
- Area co-ordinate method for FSI(wing-box)
- Tcl/Tk, C++ for CFD/CSD communications (GUI)
- Staggered FSI (rotorcraft)

Dual-Level Parallel Computing

- **Efficient single-job environment for multiple cases, each running on multiple cores:**
  - **Reduces system start/end overhead**
  - **Makes sure that cores do not overlap**
  - **All cases are completed at the same time, enabling designer to plan his work accordingly rather than "baby-sitting" multiple jobs**

- **Facilitates fast generation of indicial response data for use in stability analysis**

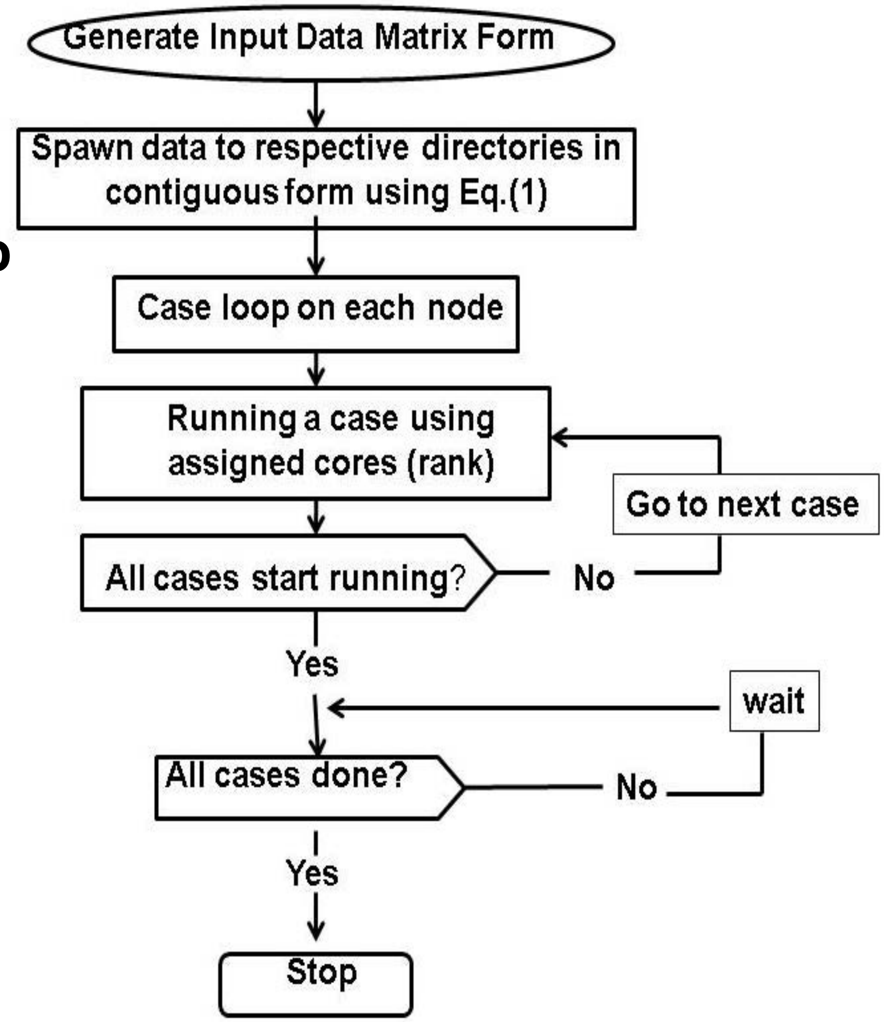

Guruswamy, G.P., "Dual Level Parallel Computations for Large Scale High-Fidelity Database to Design Aerospace *Vehicles," NASA/TM-2013-216602,* Sept. 2013.

An Intercube Communication Between Fluid and Structural Domains

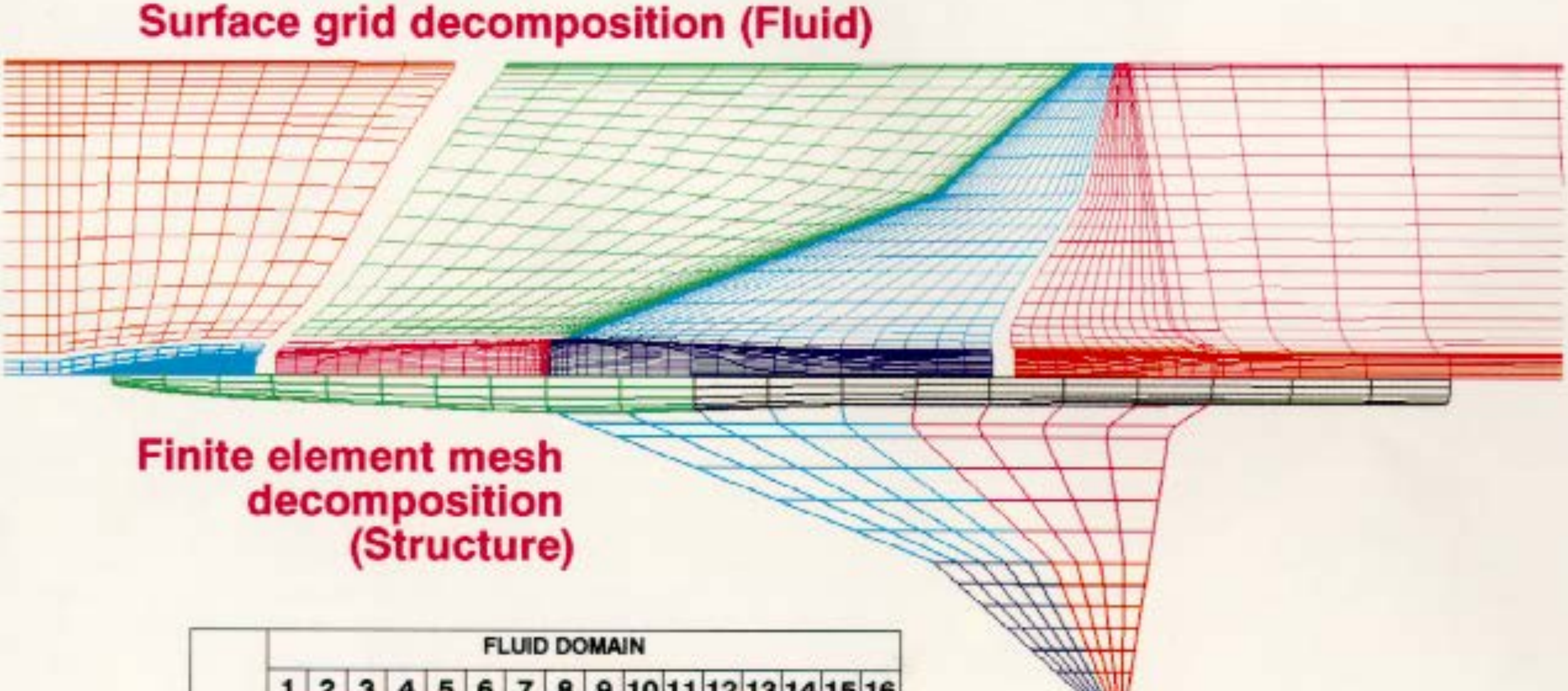

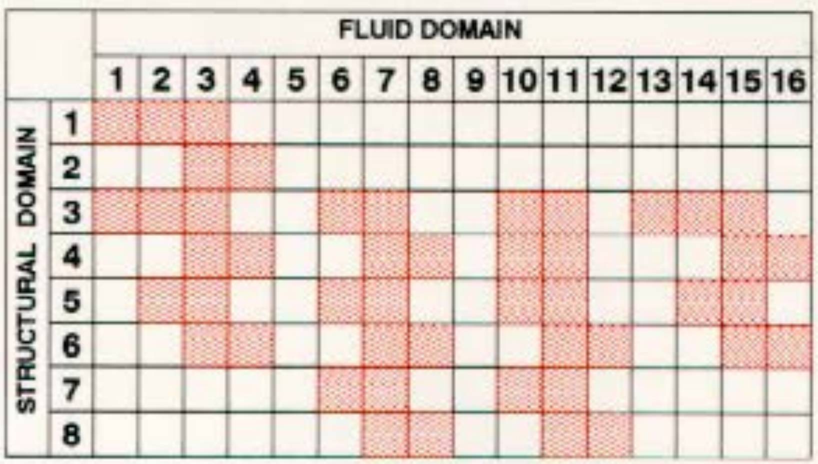

active communication
no communication
1 – 16 : processor numbers

Load Balancing Scheme in HiMAP

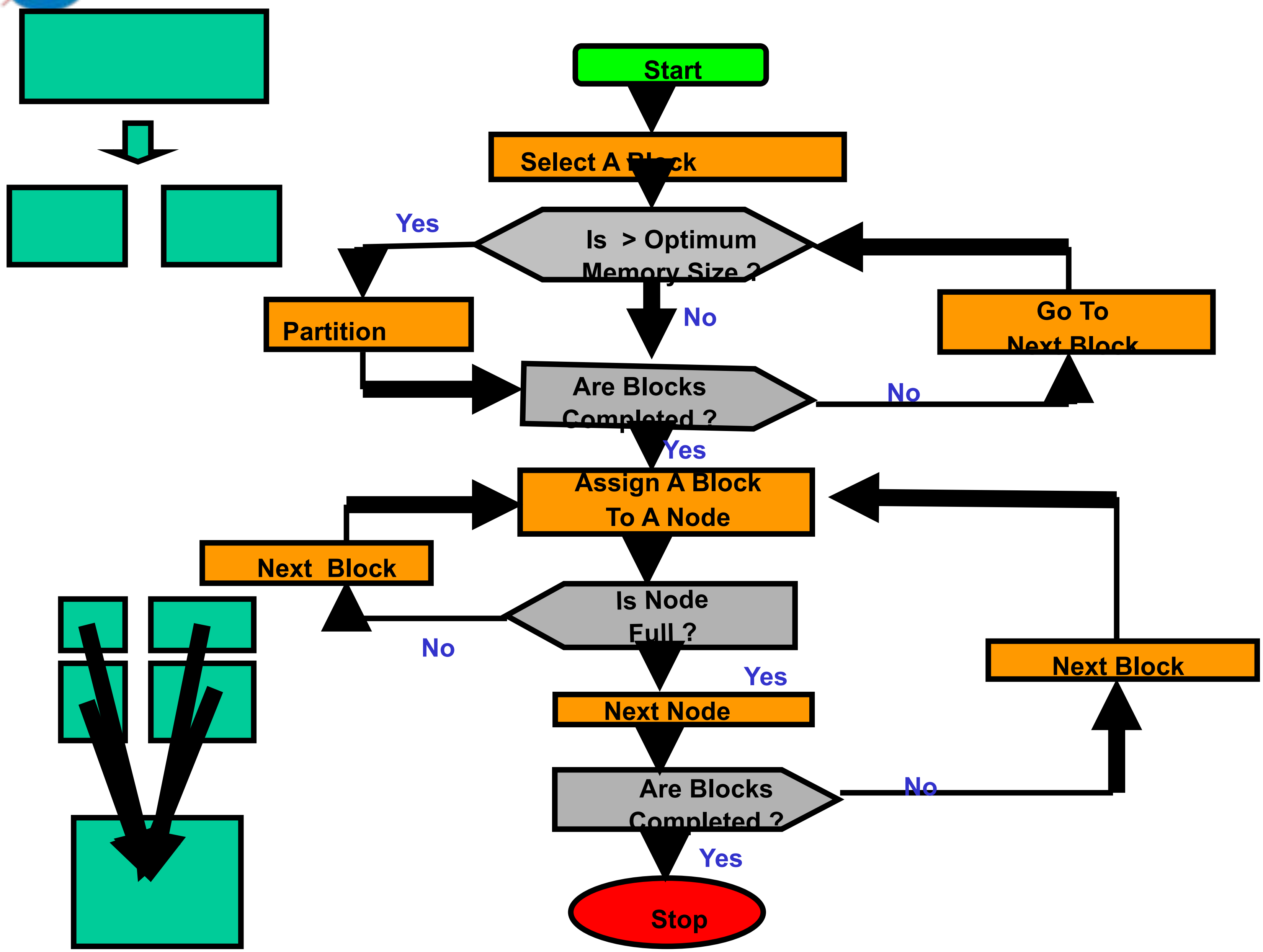

LOAD BALANCING

- Node filling algorithm for cfd zonal grids
- Mesh partitioning for csm

Typical 34 Zone CFD10m Mesh

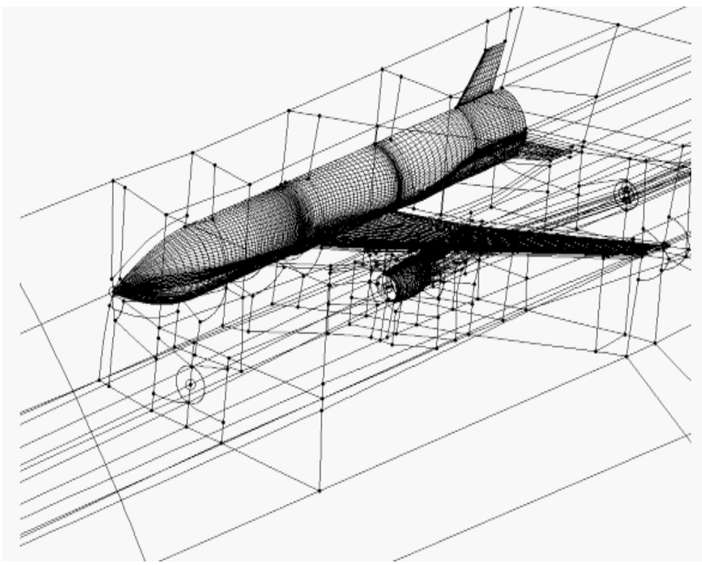

Results Of Load Balancing

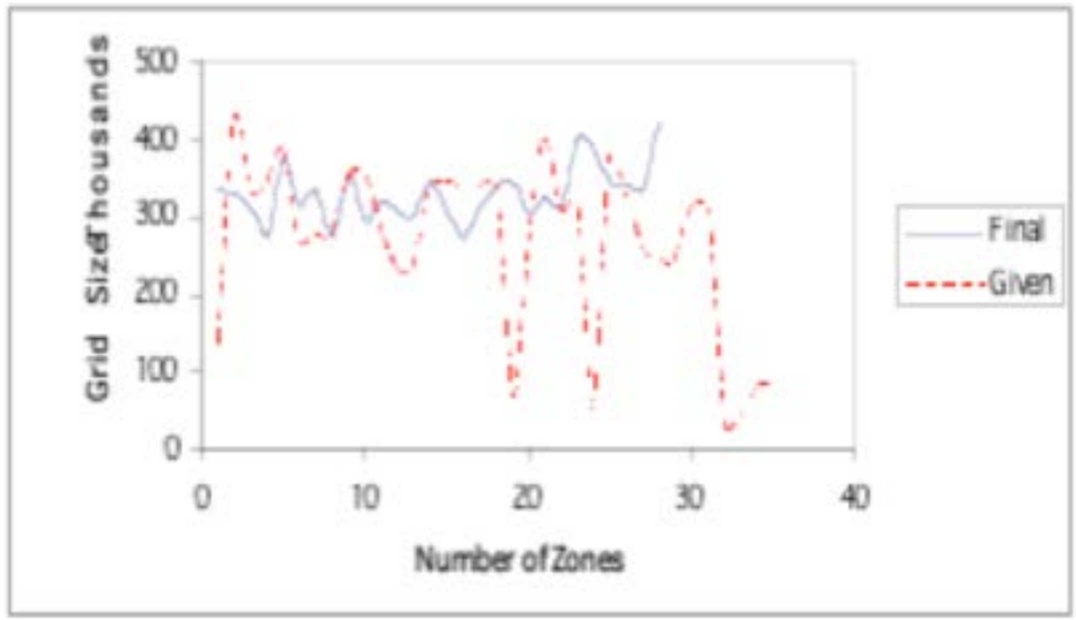

.

Number nodes were reduced

To 28 from 34

Three Level Parallel Computing

Description of Higfidelity Multidisciplinary Analysis Process (HiMAP)

A 3-level parallel, meta modular, multidisciplinary analysis software that runs on single-image shared / distributed memory supercomputers using MPIAPI middleware

Accomplishments

Can handle disciplines based on time accurately coupled high fidelity methods

- Structured/unstructured grid-based Euler/Navier-Stokes solvers (ARC3D, GO3D,USM3D) with parallel multi-block moving grid
- Modal and parallel finite element structures (NASTRAN)
- Time domain controls
- Winner of NASA Sofware Release award

Applications

Demonstrated for full F-18, L1011, 777, HSCT, X-31 and UCAV configurations

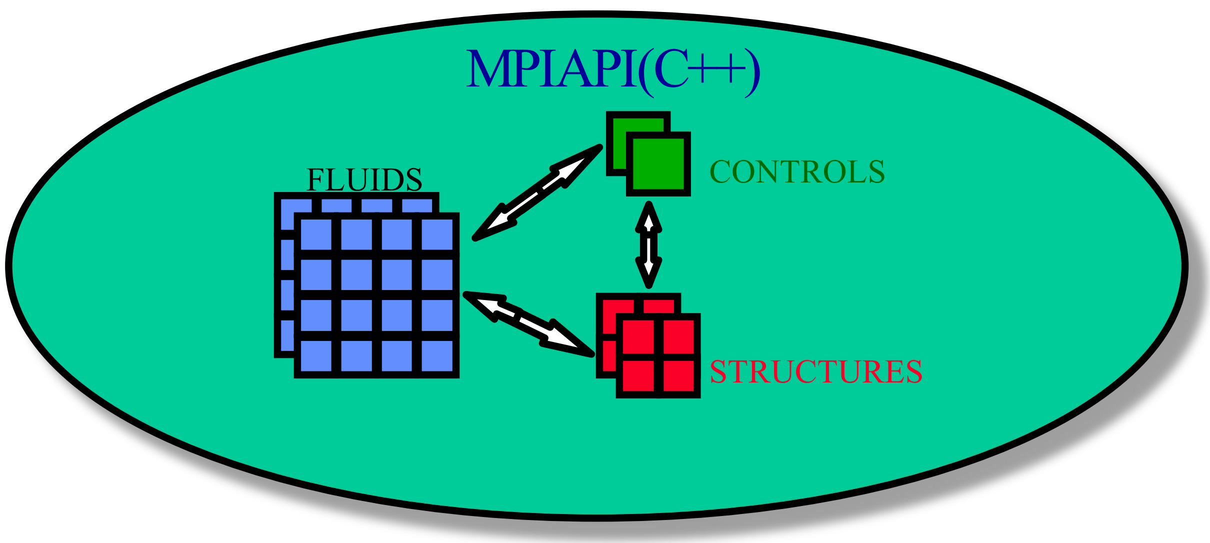

Multizonal/Multidiscipline Parallel Communication in HIMAP

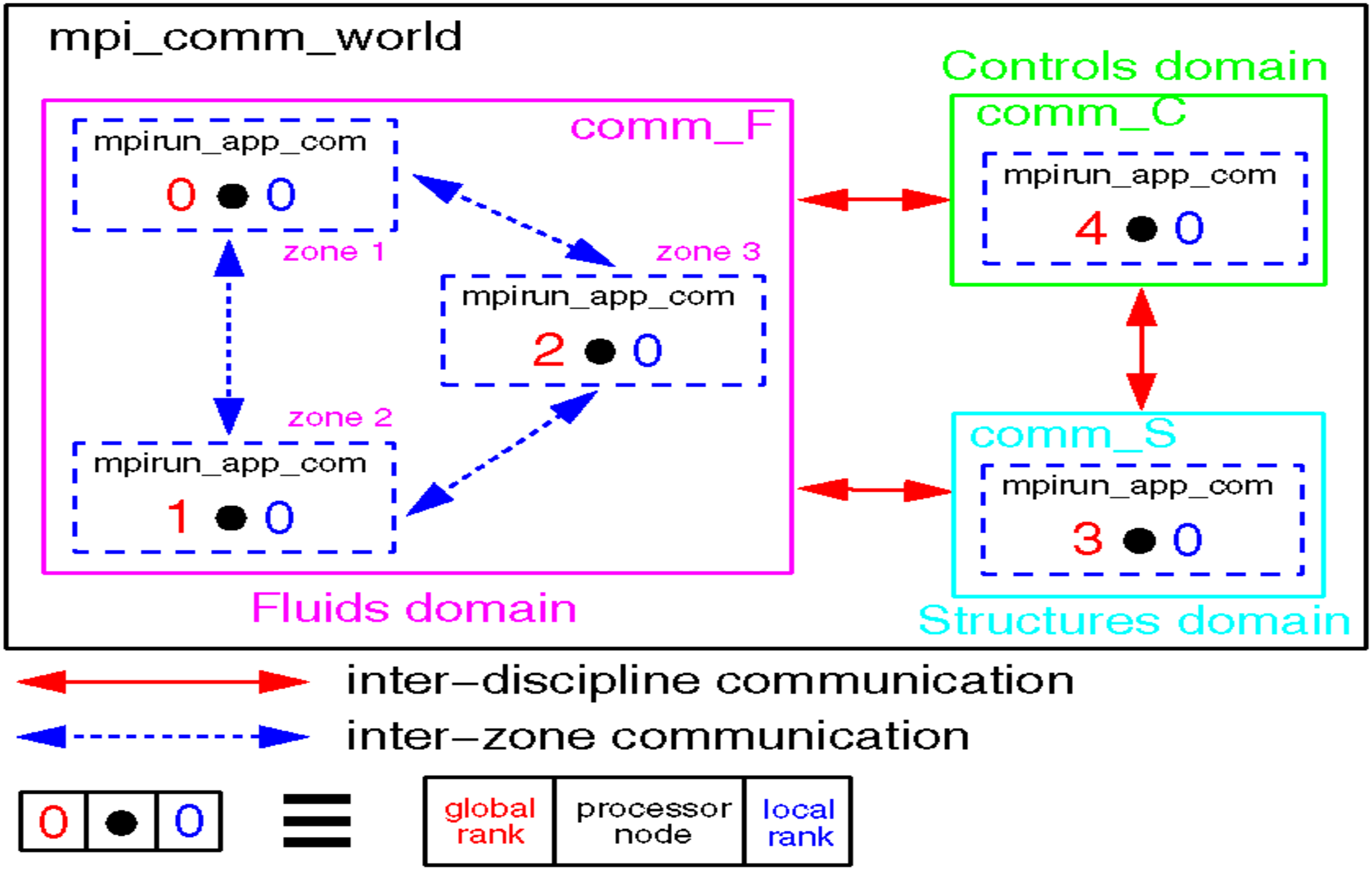

3-level Parallel Communication In HiMAP

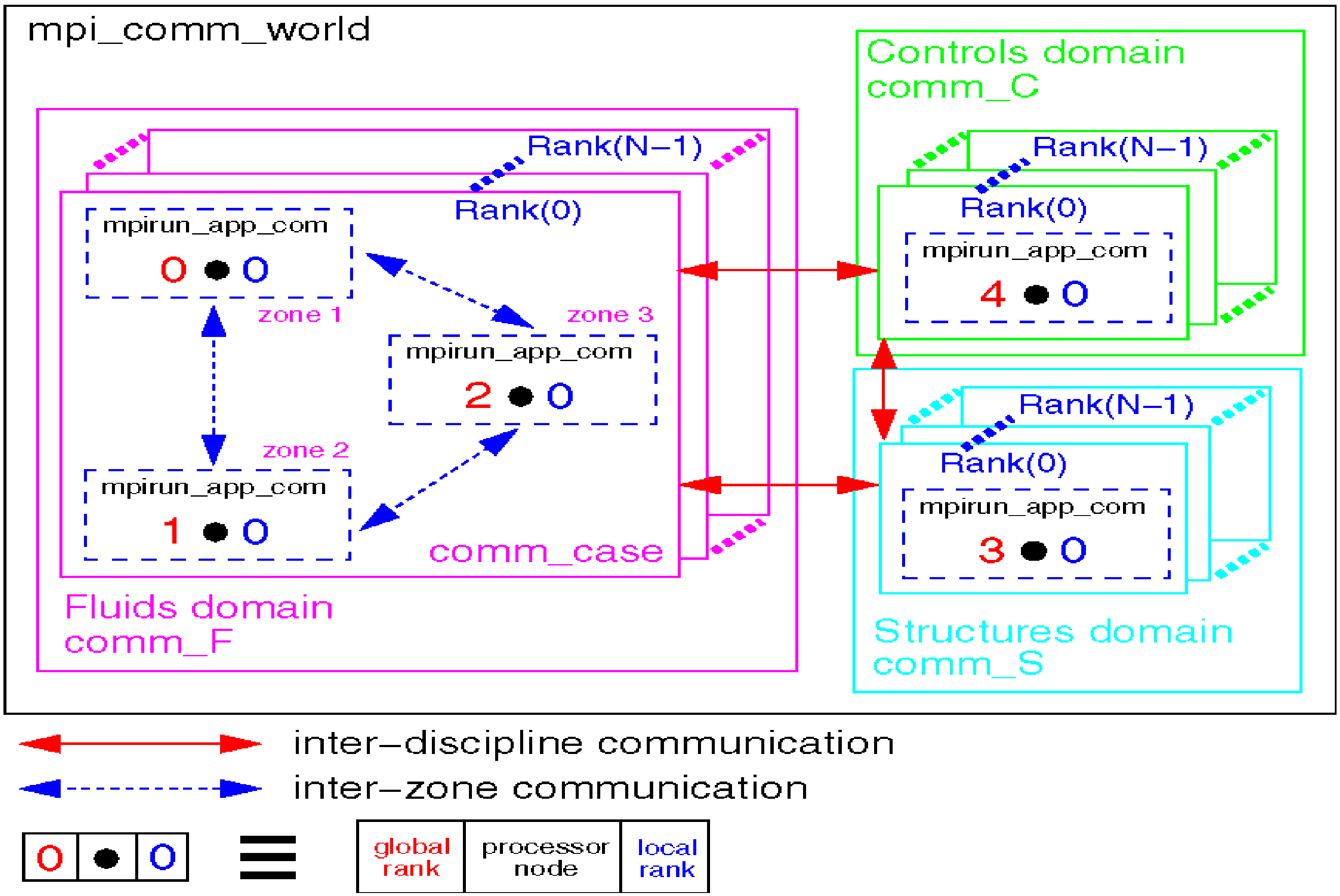

Effort towards Framework

RUNEXE - C++ Based Super Modular Process

- All modules are treated separately as objects and executed using C++ system commands
- Communication among modules is accomplished using I/O, MPI and/or TCL/TK
- On-the-fly based graphics, xmgrace, opengl
- Manages data for visualization (field view)

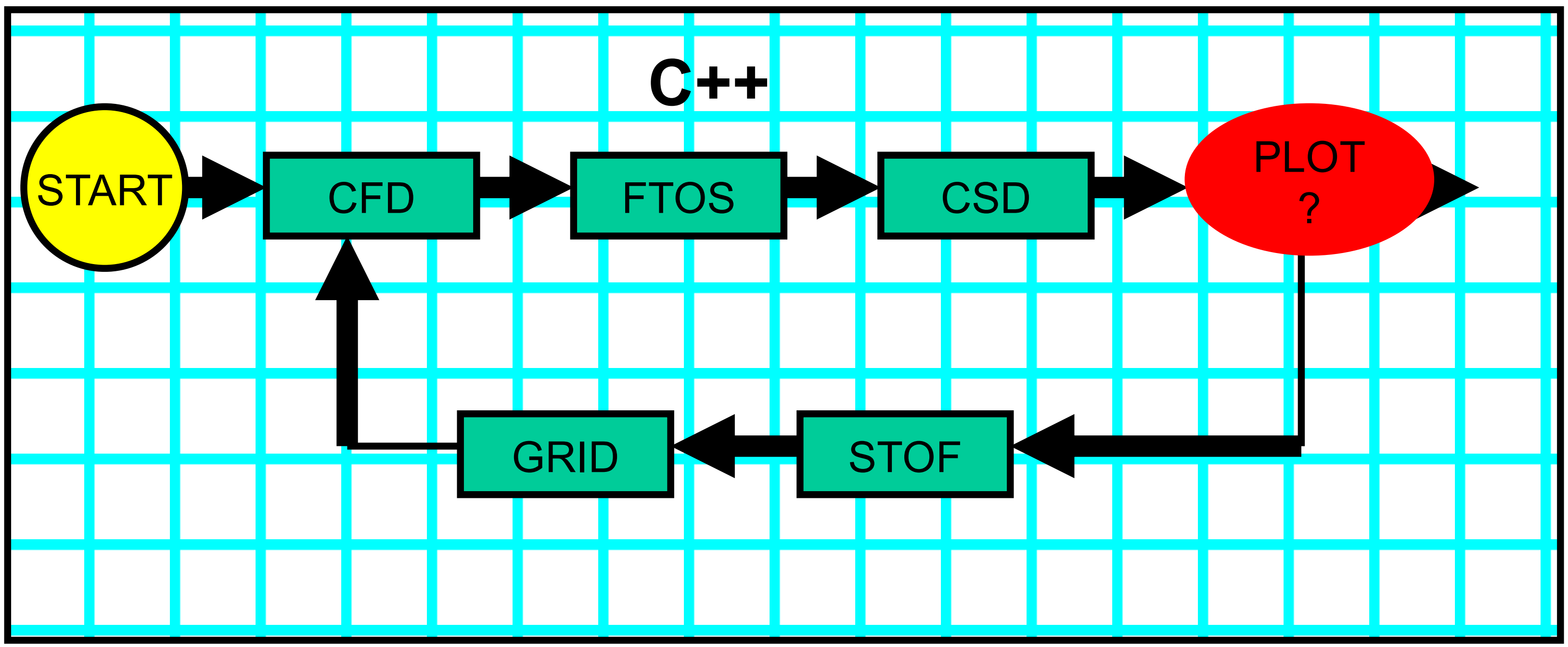

CURRENT FORTRAN 95 HAS SOME SIMILAR CAPABILITIES

Illustration of RUNEXE Process

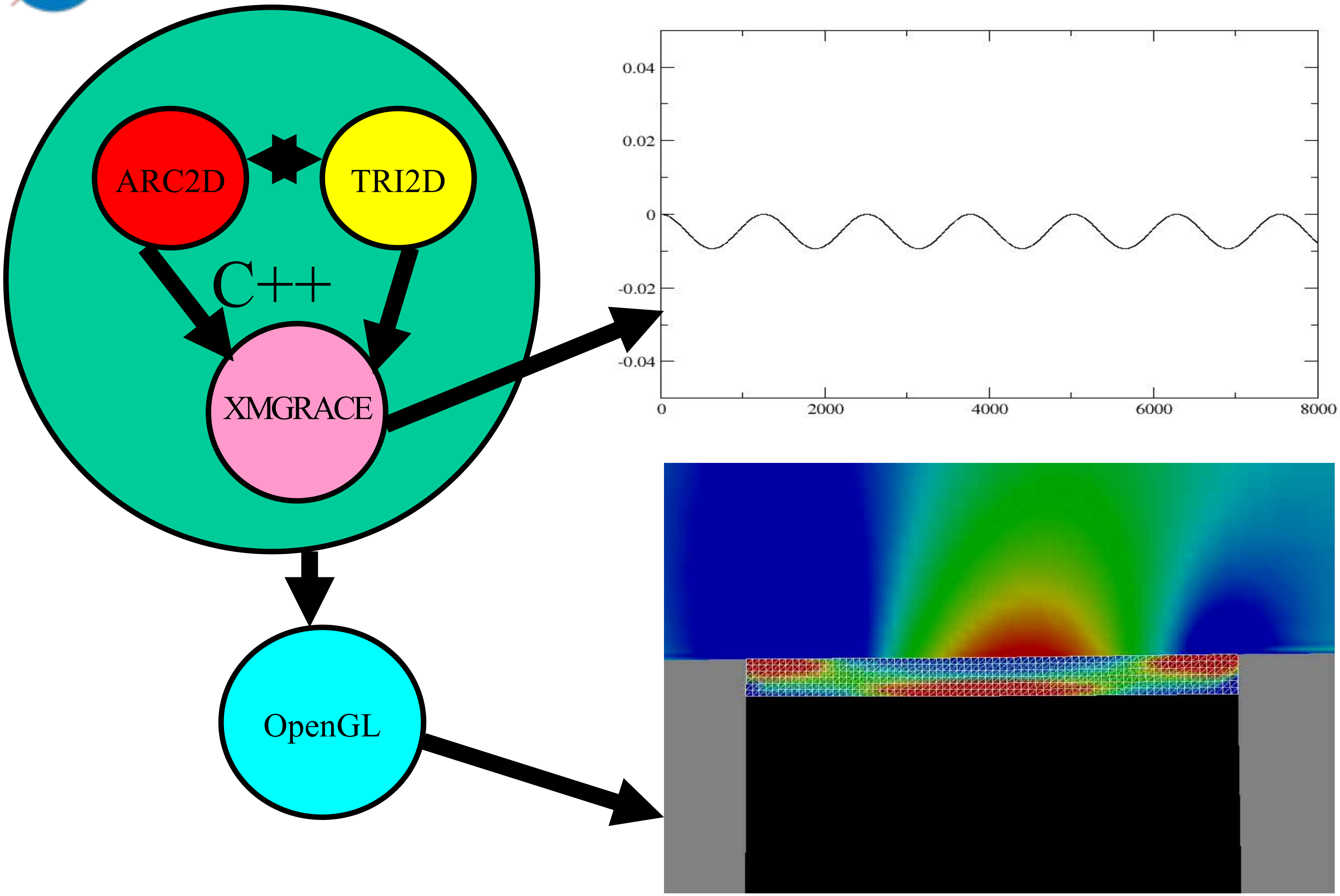

2D Transonic Small Perturbation Theory
ATRAN2S (1977)

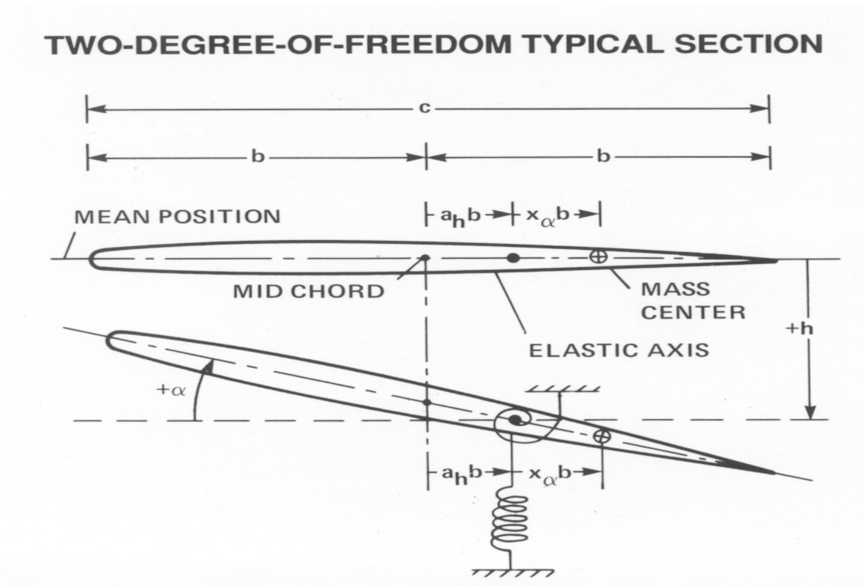

Aerodynamic Coefficients for Flat Plate Pitching about Mid-Chord at M = 0.7.

Aerodynamic Coeff.	Method	Reduced Frequency $k_c = \omega c/U$ 0.05 Real	0.05 Imag.	0.10 Real	0.10 Imag.	0.15 Real	0.15 Imag.
c_{ℓ_δ}	1	0.0669	0.4225	0.1700	0.8000	0.3038	1.134
	2	0.0616	0.3974	0.1666	0.7190	0.2719	0.9876
c_{ℓ_α}	1	8.449	-1.338	8.001	-1.701	7.557	-2.025
	2	7.964	-1.133	7.240	-1.488	6.671	-1.570
c_{m_δ}	1	0.0151	0.0952	0.0479	0.1787	0.0954	0.2486
	2	0.0174	0.0990	0.0501	0.1780	0.0865	0.2425
c_{m_α}	1	1.904	- .3016	1.787	- .4788	1.657	- .6361
	2	1.985	- .3500	1.794	- .5117	1.640	- .5996

Method 1: Time Integration by LTRAN2 (linear).
Method 2: Kernel Function Method.

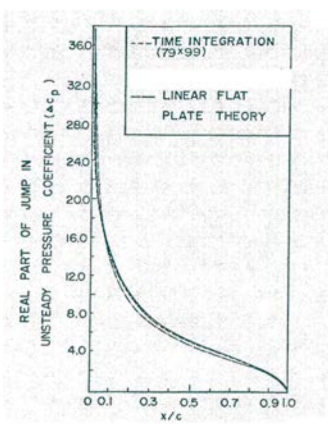

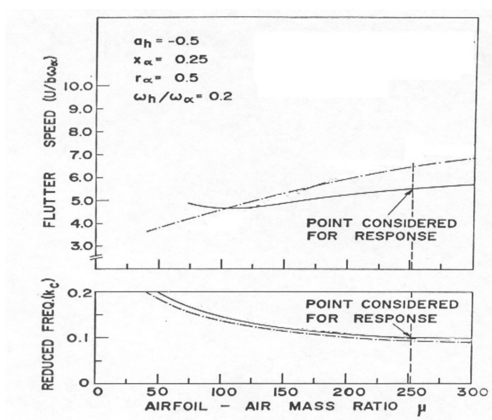

Effect of Airfoil-Air Mass Ratio on Flutter Speed for NACA 64A006 Airfoil at M = 0.85.

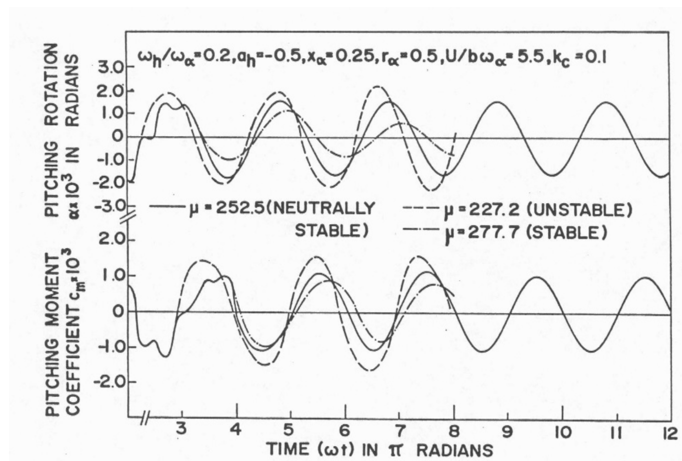

Effect of Airfoil-Air Mass Ratio (Altitude) on Pitching Rotation and Pitching Moment for NACA 64A006 Airfoil at M = 0.85

Guruswamy, G. P. and Yang, T. Y.," Aeroelastic Time Response Analysis of Thin Airfoils by Transonic Code LTRAN2," Computers and Fluids, Vol. 9, No. 4, Dec. 1981,

3D Transonic Small Perturbation Theory ATRAN3S (1984)

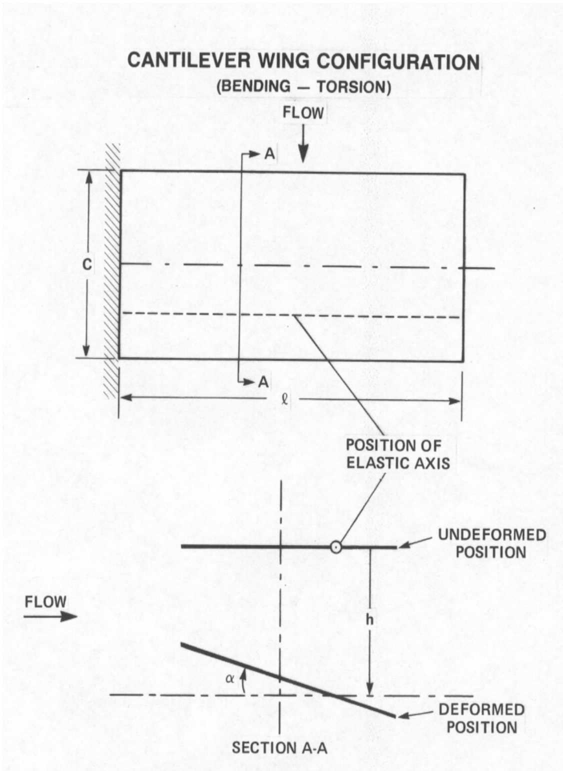

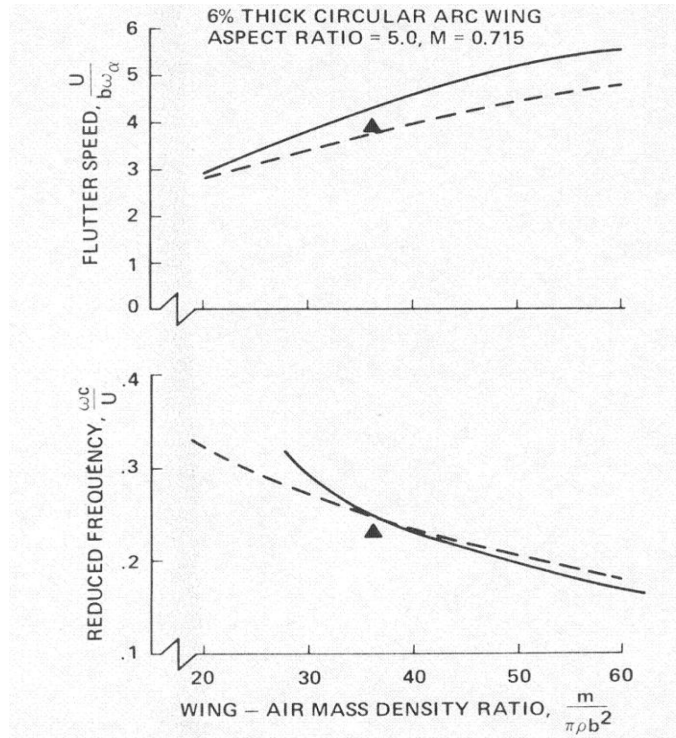

Guruswamy, G. P. and Goorjian, P. M. " Computations and Aeroelastic Applications of Unsteady Transonic Aerodynamics About Wings," Jl. of Aircraft, Vol. 21, No. 1, Jan. 1984, pp. 37-43.

Fluid/Structures Interaction
HiMAP with NASTRAN

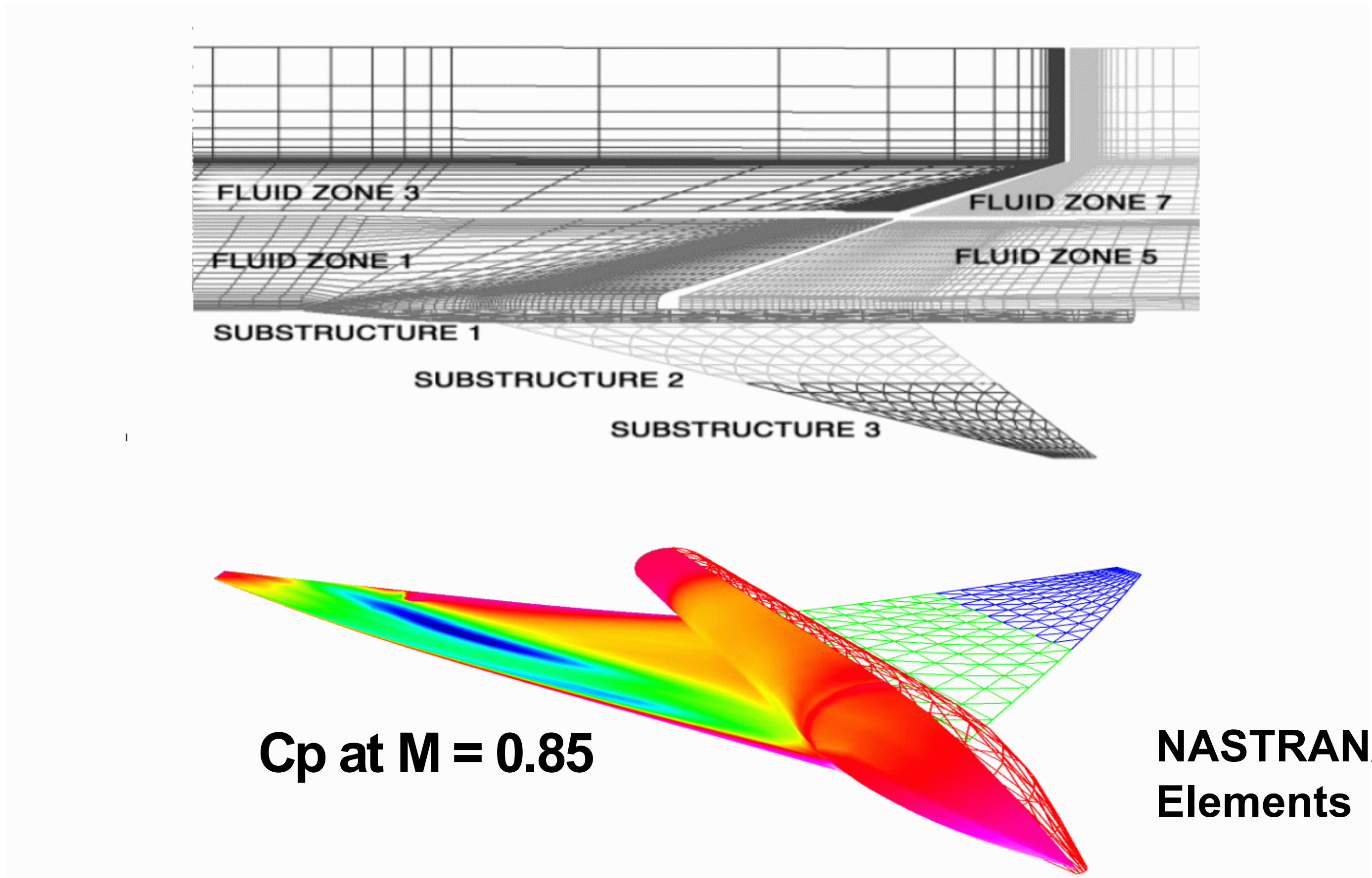

NASTRAN/ANS4 Elements

- **Demonstrated for HSCT model with 5 million grid points fluid and 20k DOF ELFINI FEM**

Eldred, L. , Guruswamy, G.P. and Byun, C, "Parallel Aeroelastic Analysis Using ENSAERO and NASTRAN," HPCCP/CAS Workshop 98, NASA/CP-1999-208757, Jan 1999.

Parallel FSI Demonstration for HSCT

- **Nastran Based Parallel Sub-structure Solver Is Developed**

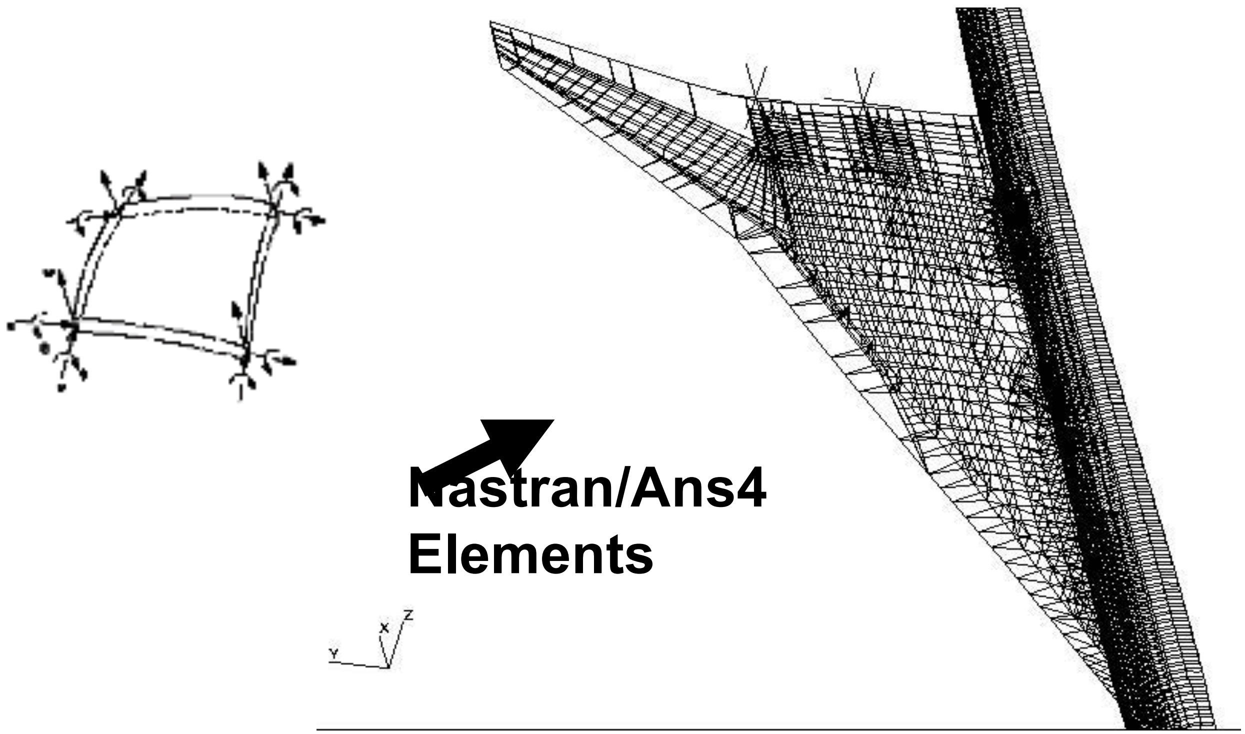

Tca6 20k Dof Fem

- **Demonstrated for a HSR Model With 5 M Pt Fluid and 20K DOF FEM**

Validation Of Unsteady Pressures

NASA TND 344 WING, M = 0.90, k = 0.26

UNSTEADY Cp AT 50% SEMISPAN

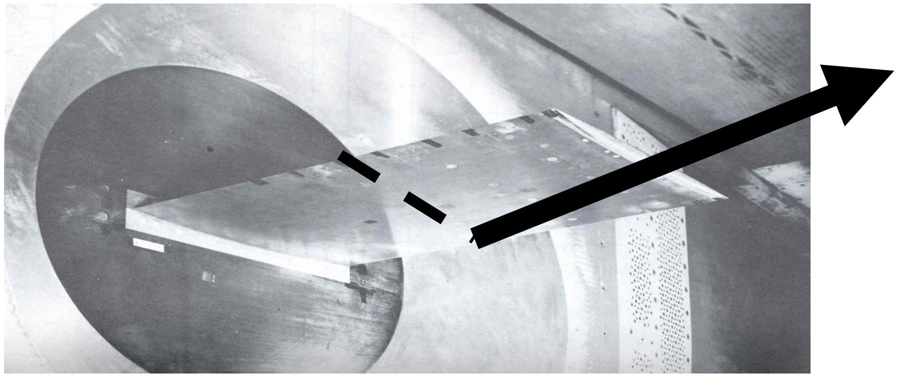

WING IN FIRST BENDING MODE

MOTION

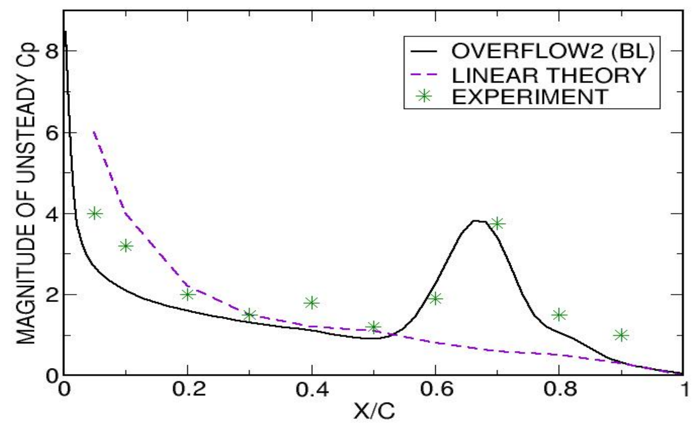

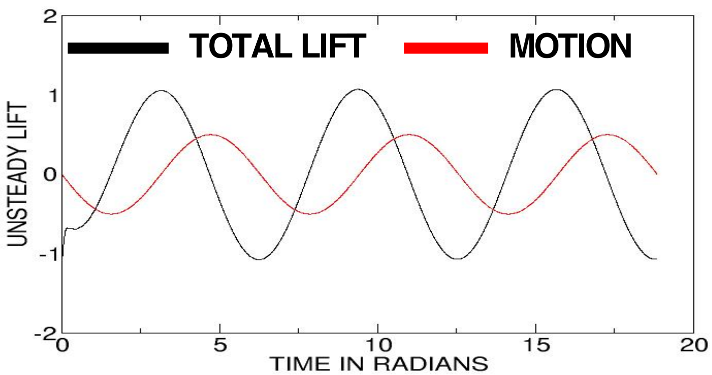

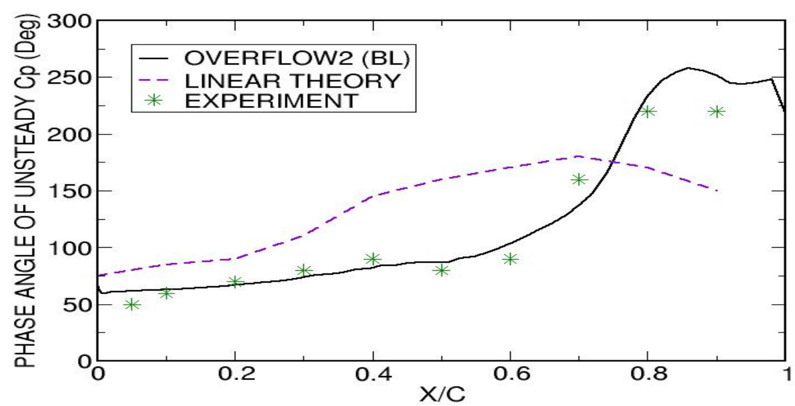

Guruswamy, G. P. ,"Unsteady Aerodynamic and Aeroelastic Calculations for Wings Using Euler Equations ," AIAA Jl., Vol. 28, No. 3, March 1990, pp 461-469. (also AIAA Paper 88-2281)

Rectangular Wing

Aeroelasic validation

NASA TMX-79, AR =5, M = 0.715, re = 4.5 million

Modes

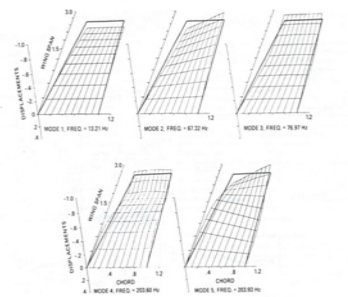

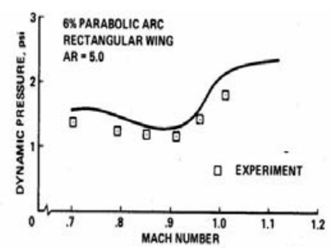

Dynamic Aeroelastic Responses

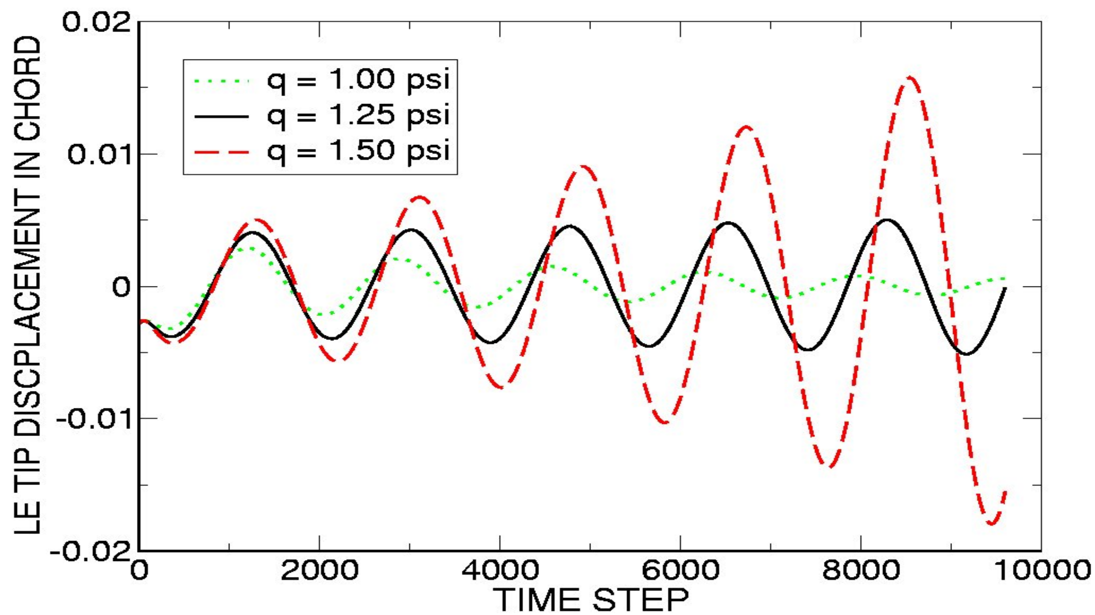

MEASURED DYNAMIC PRESSURE q =1.31psi

PLATE FEM AND MODAL GIVE SIMILAR RESULTS

Guruswamy, G.P.,"Computational-Fluid-Dynamics and Computational-Structural-Dynamics Based Time-Accurate Aeroelasticity of Helicopter Blades," Jl. of Aircraft, Vol. 47, No. 3, May-June 2010

Validation For Aeroelastic Research Wing

HIMAP, M = 0.80, α = 2.98 deg, Re = 1.3M, q = 0.72 psi

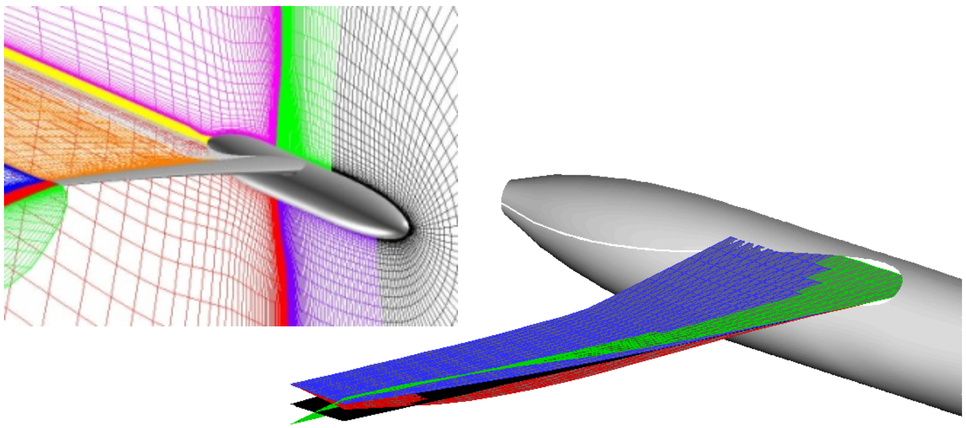

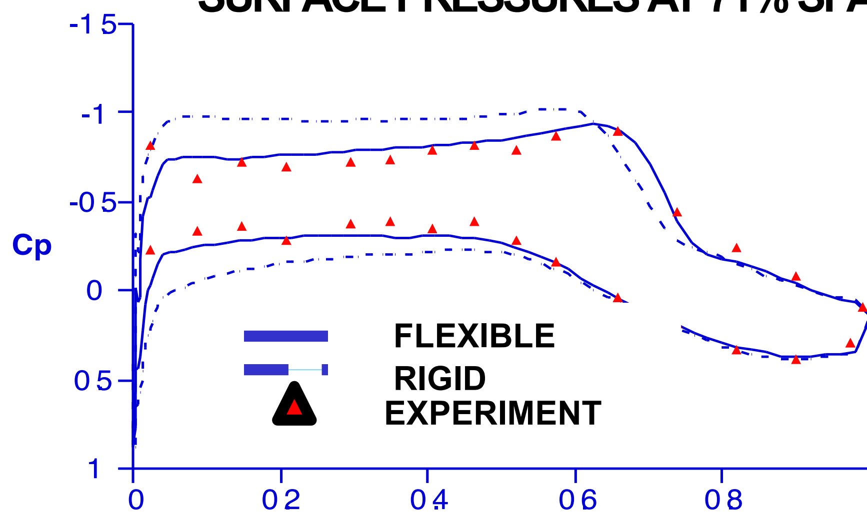

FEM MODEL OF WING - 400 DOF

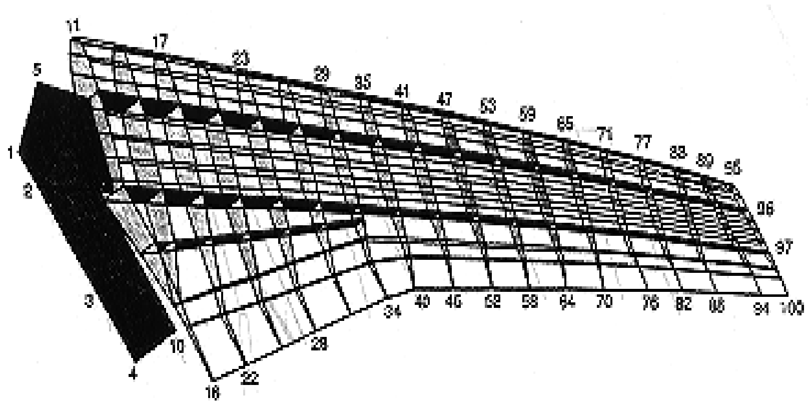

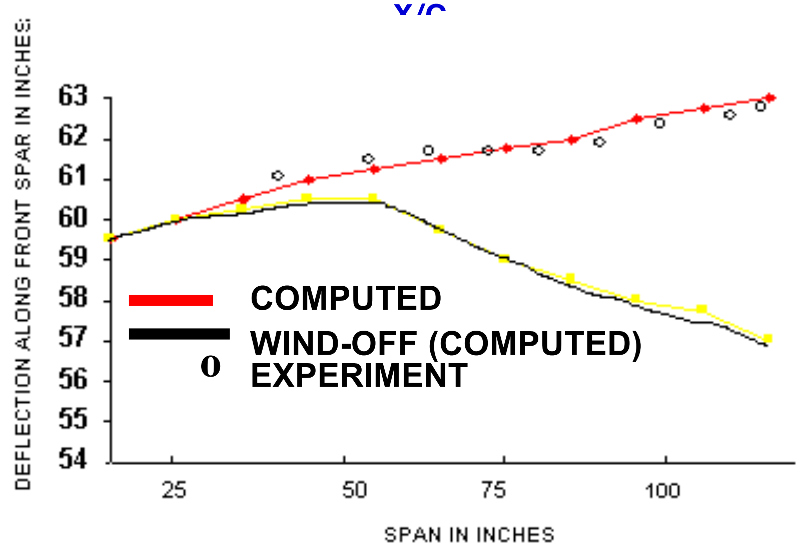

Bhardwaj, M., Kapania, R., Reichenbach and Guruswamy, G.P., "CFD/CSD Computational Interaction Methodology for Aircraft Wings," AIAA JI Vol 36, No 12, Dec 1998.

6 MODES FROM GVT GIVES SIMILAR RESULTS

Vortex Induced Aeroelastic Oscillations of Supersonic Aircraft

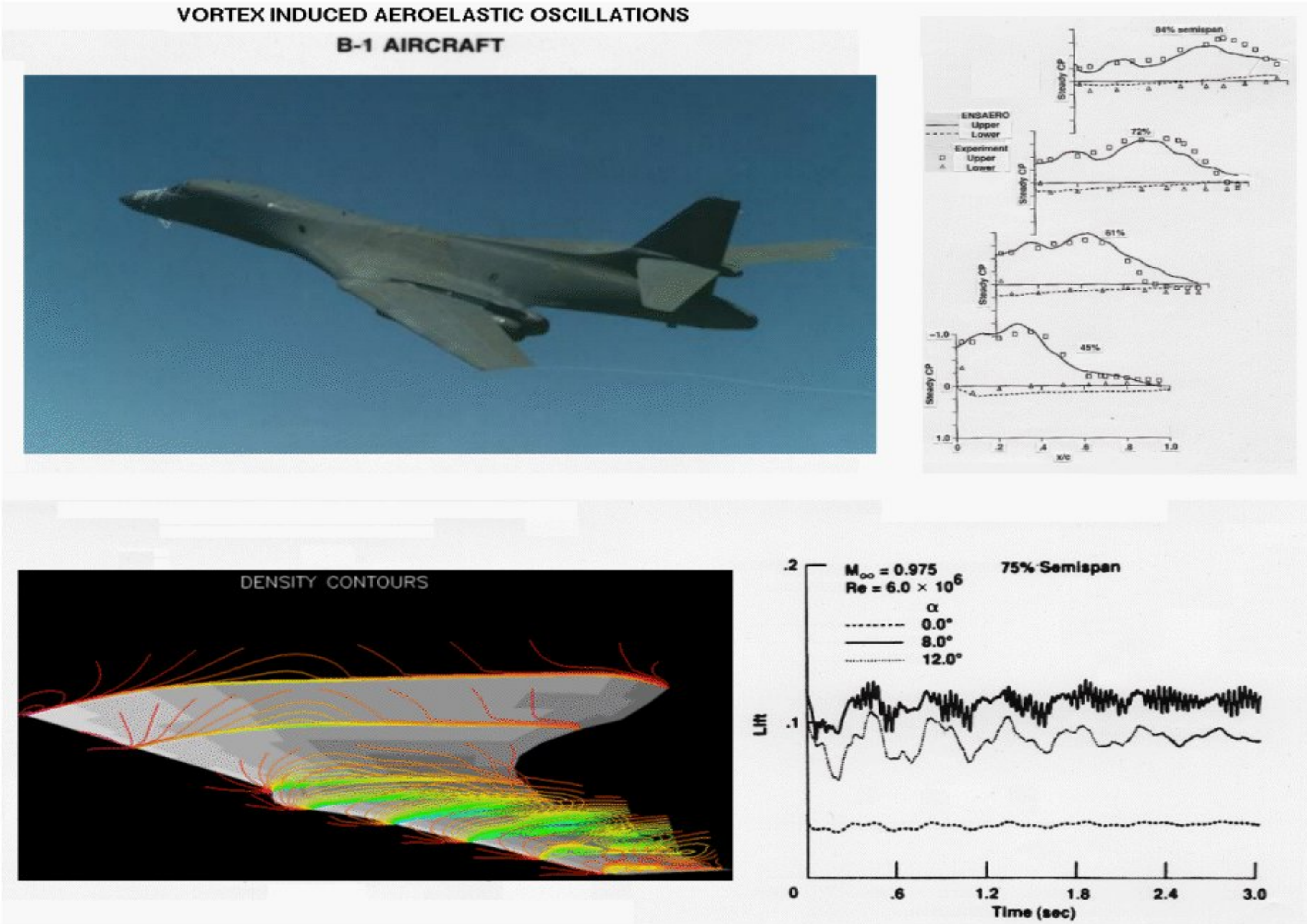

Guruswamy, G. P., ,"Vortical Flow Computations on a Flexible Blended Wing-Body Configuration," AIAA Jl., Vol. 30, No. 10, October 1992. pp 2497-2503

Demonstration for Full Aircraft
(HIMAP, L1011 Wind Tunnel Model, M = 0.85)

- 9m grid pts, 38 fluid zones
- 5 structural modes, 700 nodes with 3dof per node

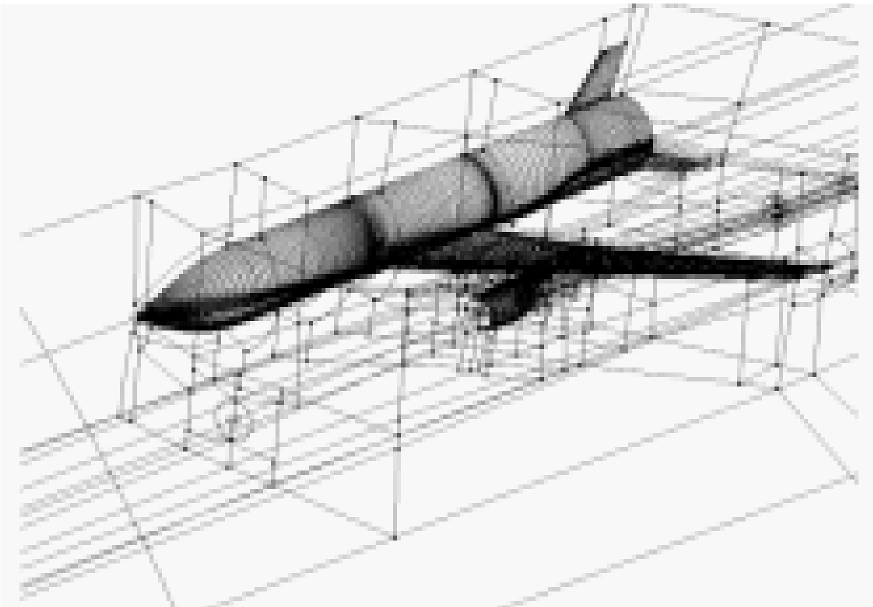

Cp deformed configuration

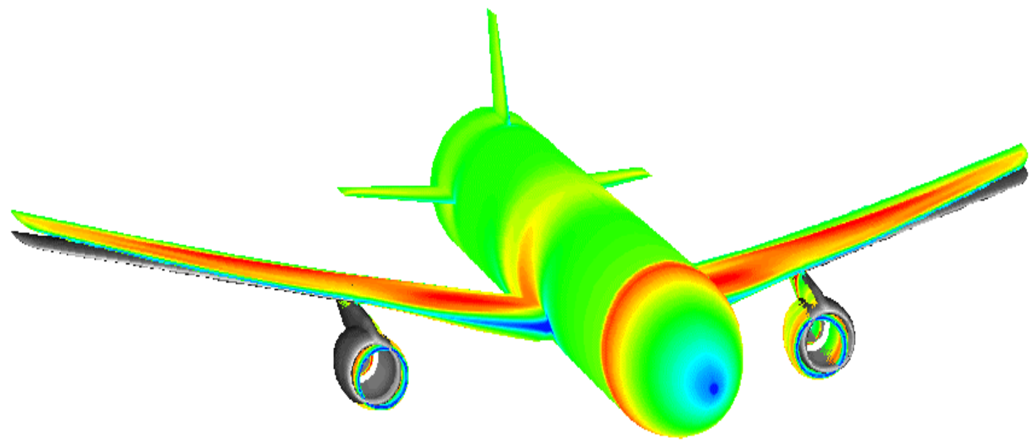

- Typical aeroelastic computation using 34 nodes of parallel computer requires
  - 15 minutes with memory efficient load balance scheme
    or 10 CPU hrs without load balance scheme

(Potsdam, M.A. and Guruswamy G.P , " A Parallel Multiblock Mesh Movement Scheme for Complex Aeroelastic Applications, " AIAA 2001-0716, Jan 2001.)

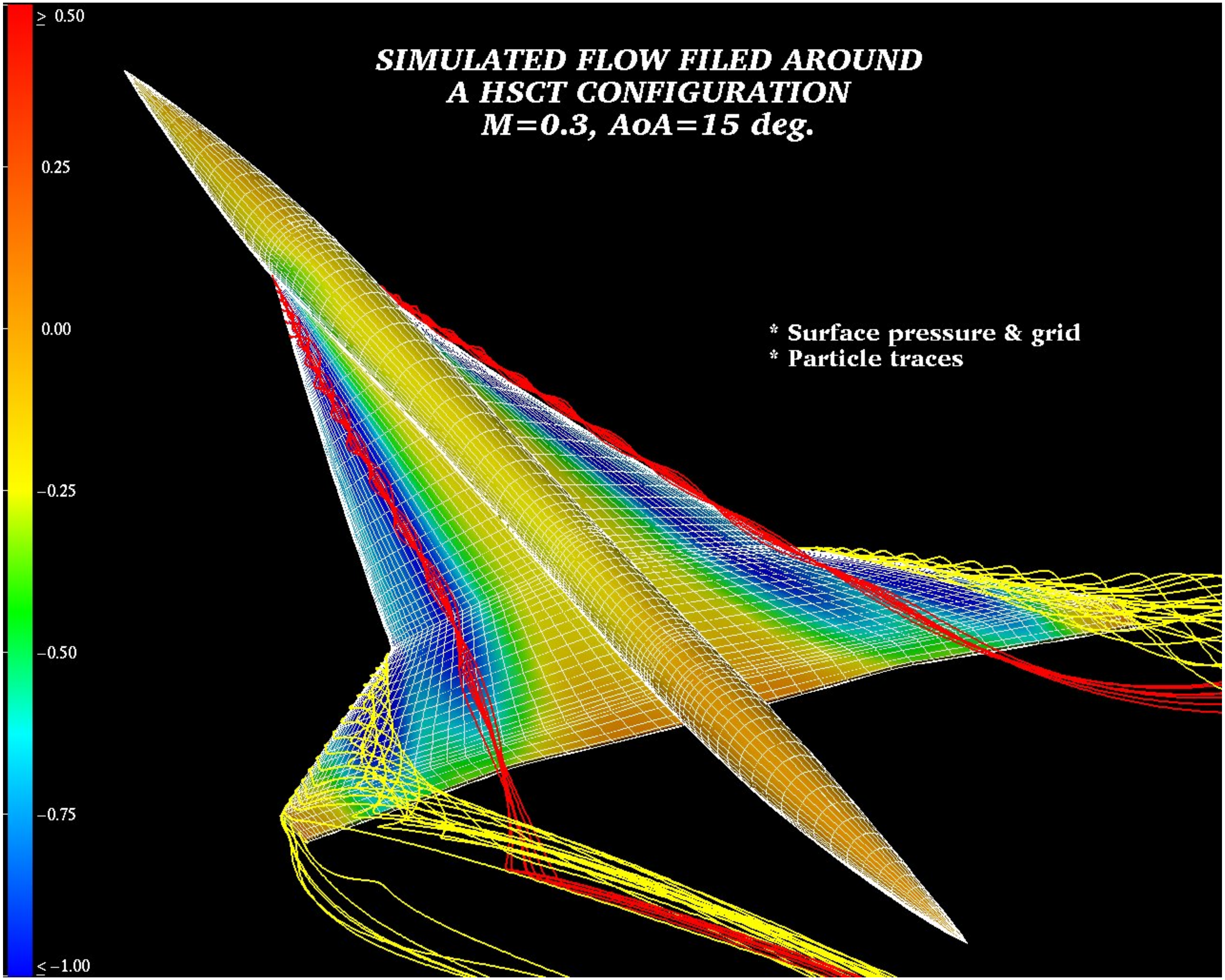

SIMULATED FLOW FILED AROUND
A HSCT CONFIGURATION
M=0.3, AoA=15 deg.
* Surface pressure & grid
* Particle traces
≥ 0.50
0.25
0.00
−0.25
−0.50
−0.75
≤ −1.00

X-31- Pressure Distribution

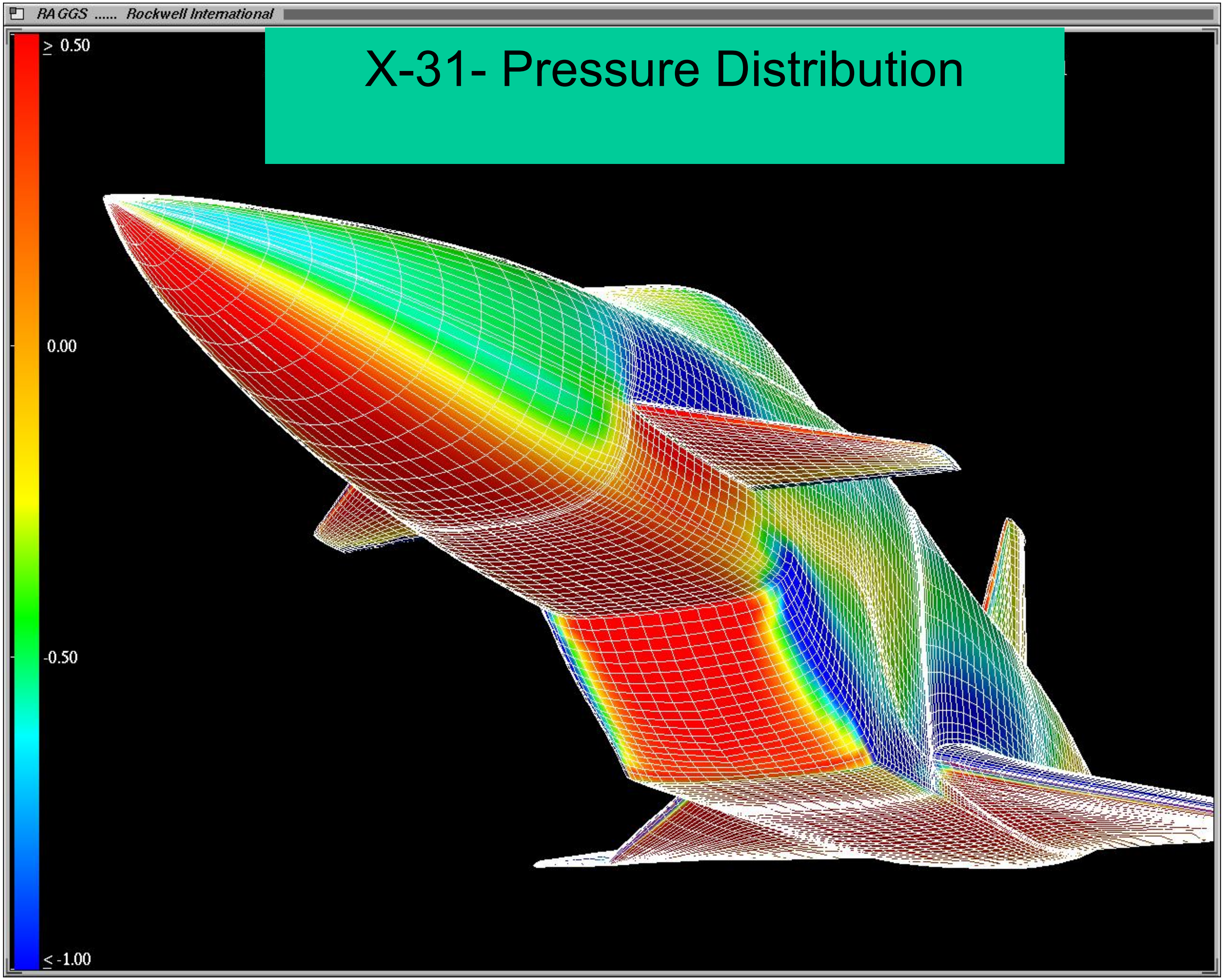

HiMAP Applications

HSCT -12 M GRID POINTS
ELFINI FEM

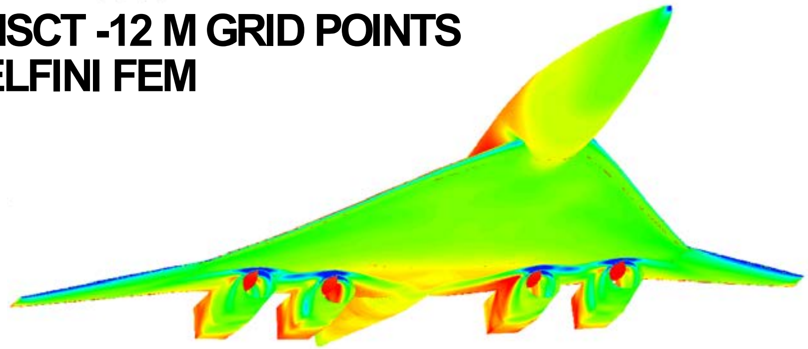

L1011, 10M PTS
MODALSTRUCTURES

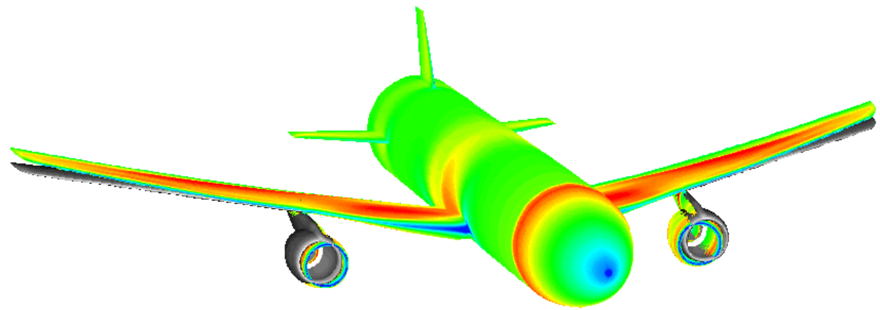

UCAV 14M GRID POINTS

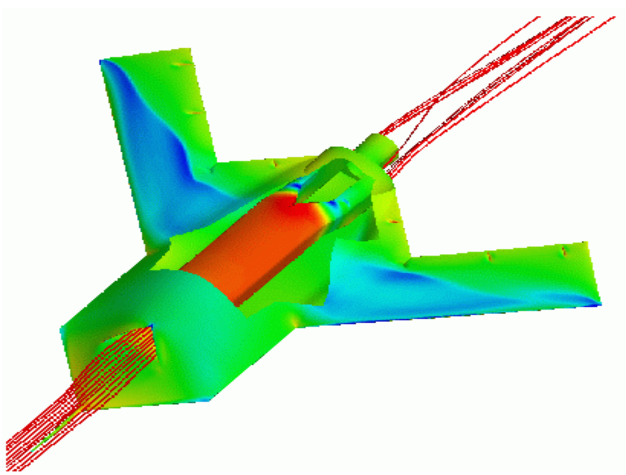

F18E/F, 17M PTS
FEM STRUCTURES

Rotating Blades

Unsteady Validation- Caradonna-tung Blade, AR =16, Re = 3.93m, RPM =1500, θ = 0.0deg

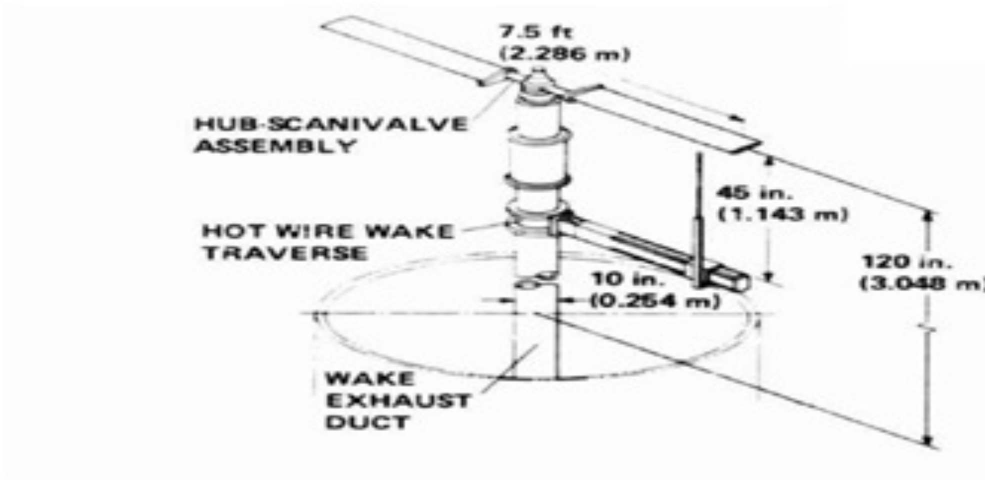

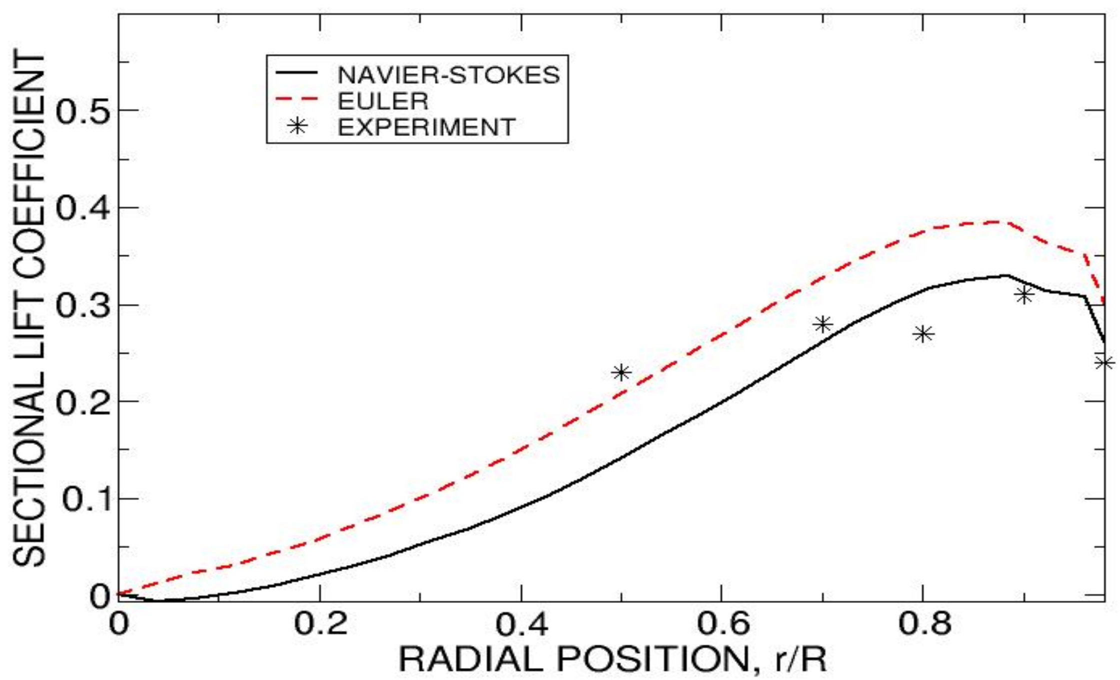

Aeroelastic Validation for Rotating Blade

Advancing Blade, Japan/MIT

Ω =100 RAD/SEC, M = 0.40, Flexible Blade, Θ_c = 0 Deg

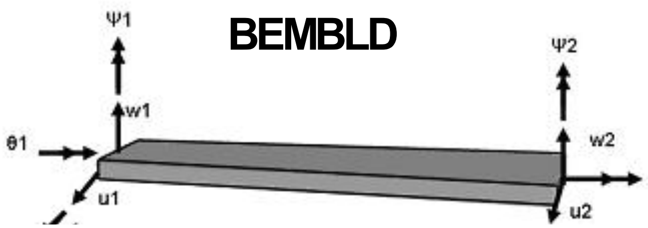

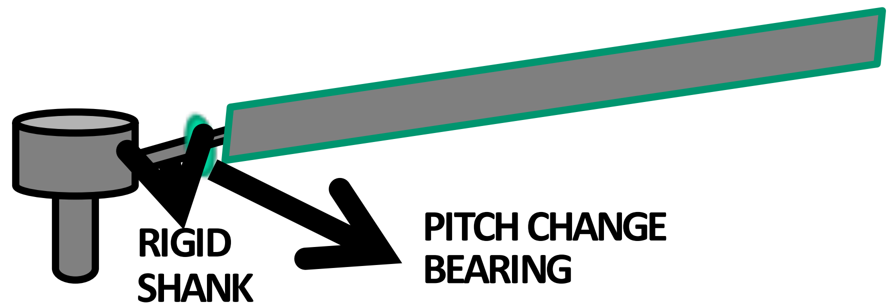

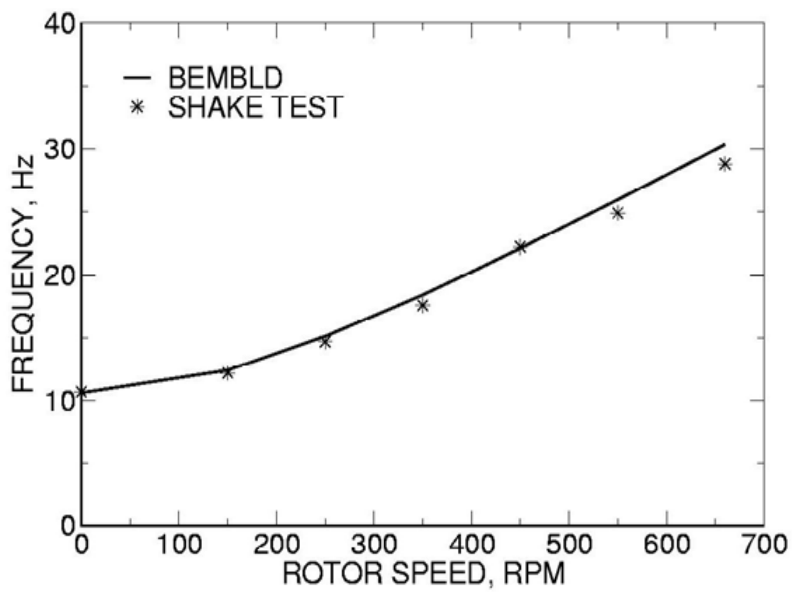

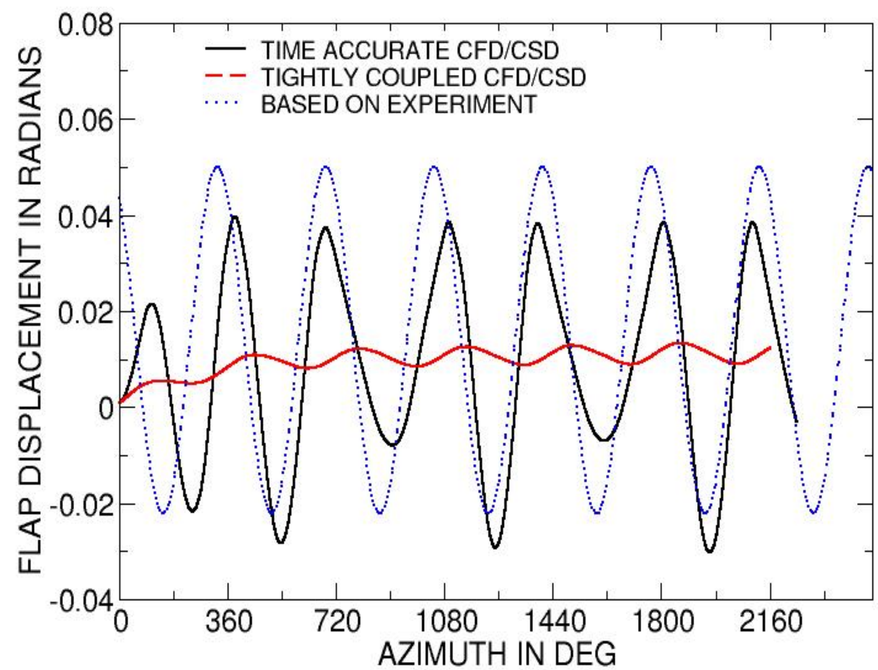

Guruswamy, G.P.,"Computational-Fluid-Dynamics and Computational-Structural-Dynamics Based Time-Accurate Aeroelasticity of Helicopter Blades," Jl. of Aircraft, Vol. 47, No. 3, May-June 2010

HART II Configuration

Advance Ratio = 0.15, RPM = 1041, Shaft Angle = 4.5°

Wind Tunnel Model

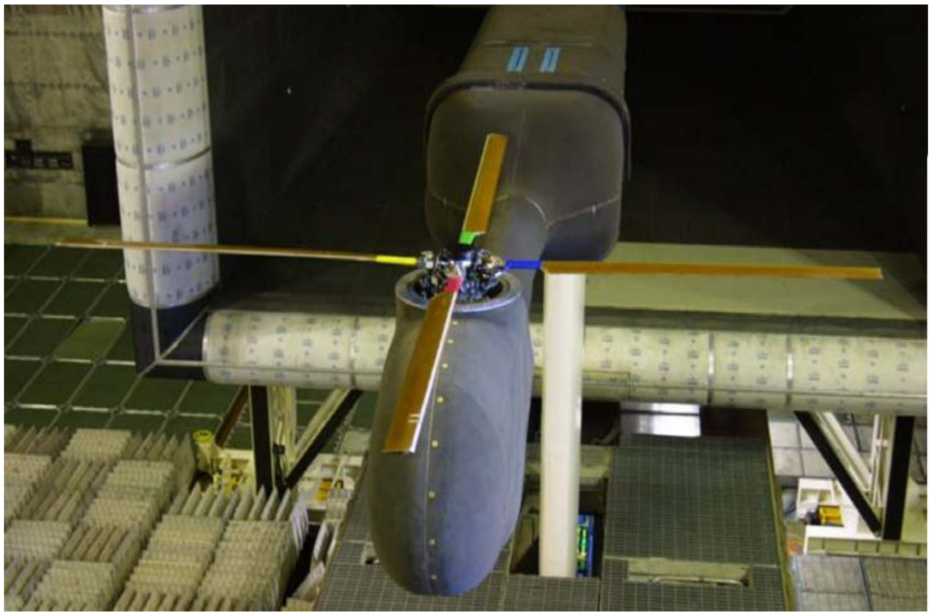

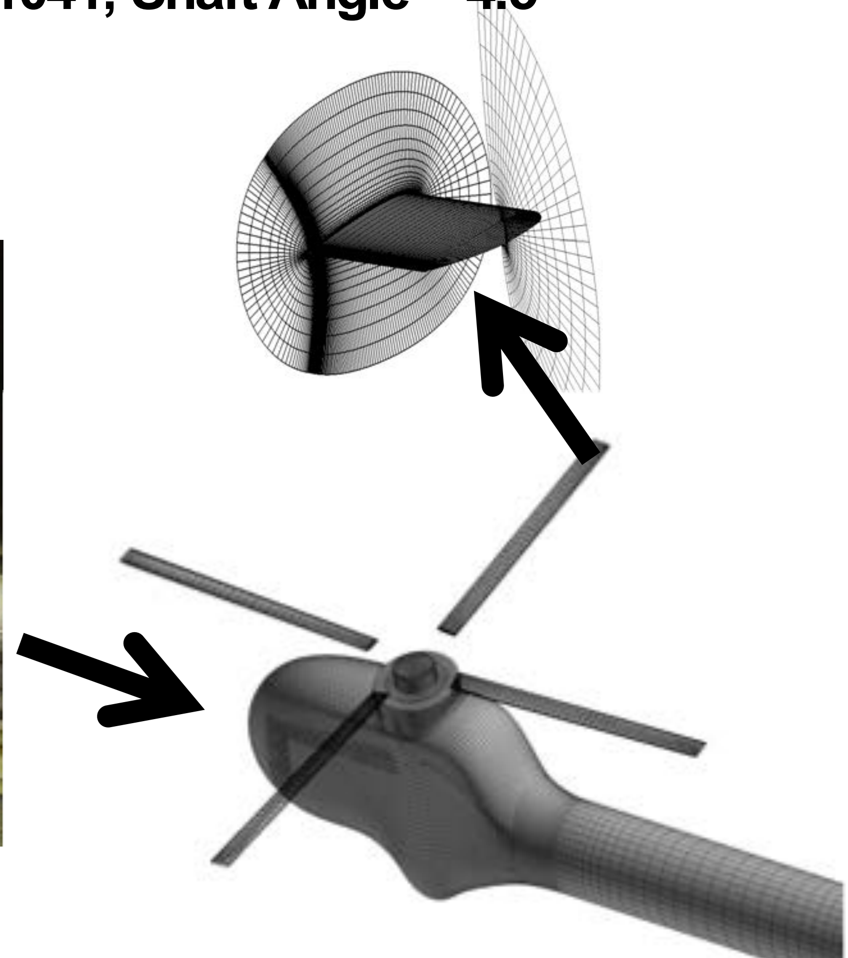

- **- 27m points with 32 near body grid blocks**
  - 23 m points outer grids

Guruswamy, G. P, "Time-Accurate Aeroelastic Computations of a Full Helicopter Model using the Navier-Stokes Equations," International Jl. of Aerospace Innovations, Vol. 5, No 3+4, Dec 2013, pp. 73-82

Air loads for Hart II Configuration

Baseline, Advance Ratio = 0.15, RPM = 1041

TA responses
- Isolated blade
- 2m grid points, 50DOF FEM

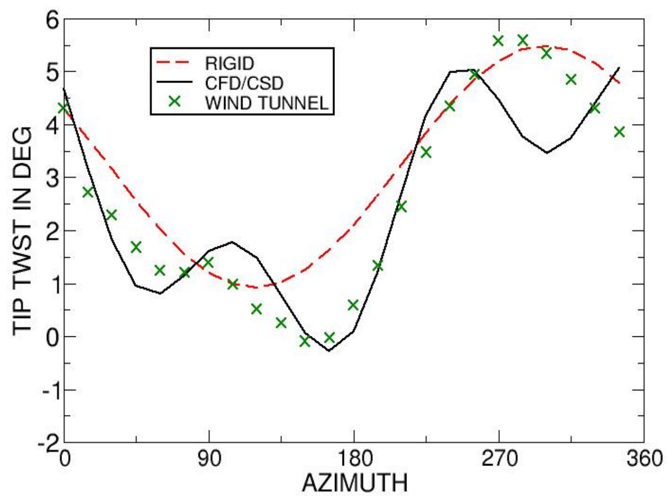

Converged response at 6th revolution
- 7200 time steps per revolution
- 250 cpu hours
- 4 hours wall clock time with 64 processors

Fourier Analysis (Full Configuration)

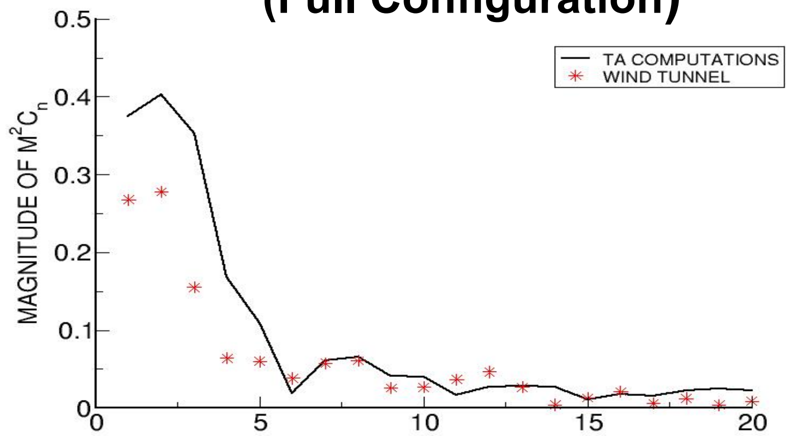

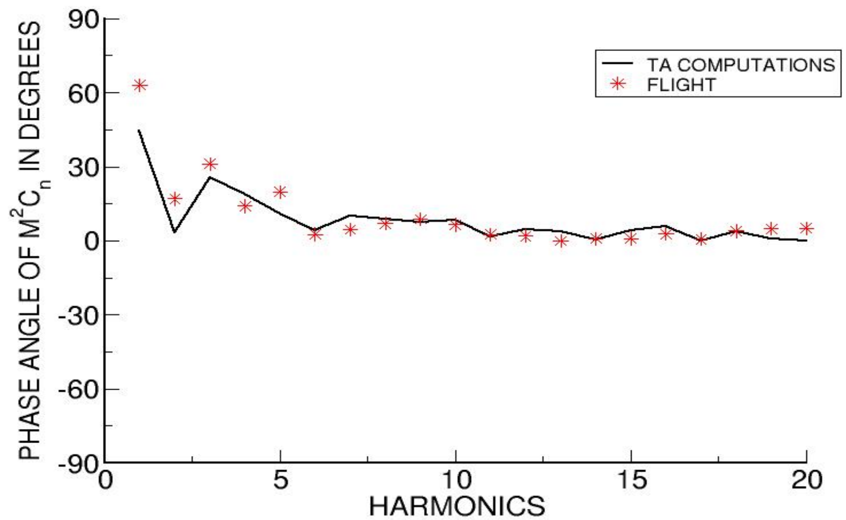

Demonstration for Launch Vehicles

EFFECT OF MODES ON TRANSONIC AIRLOADS

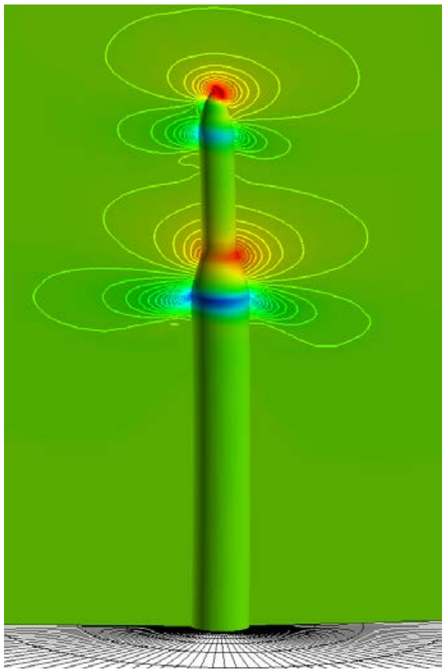

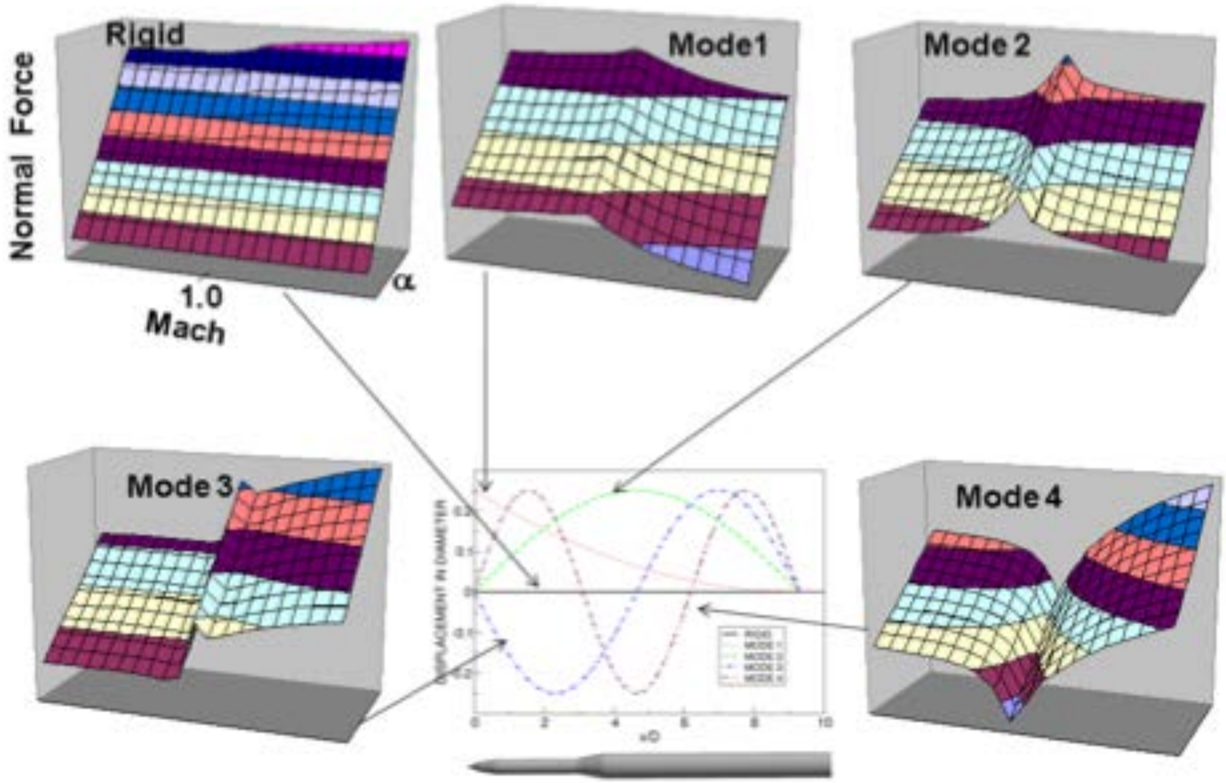

- **1,000 Transonic aeroelastic responses computed with 30 minutes of wall-clock time by using 1,000 nodes each with 4-openmp cores and MPIEXEC utility developed at NAS**

Guruswamy, G.P., "Large-Scale Computations for Stability Analysis of Launch Vehicles Using Cluster Computers," Jl of Spacecraft And Rockets, Aug 2011.

Demonstration for Launch Vehicles Unsteady Motions

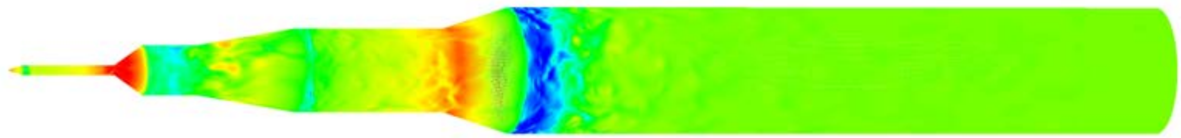

Snap shot of unsteady pressure contours (*V*= 0.005, L, *H*= 0.005L, *k* = 0.5, M = 1.8,) when *h* and *v* are maximum

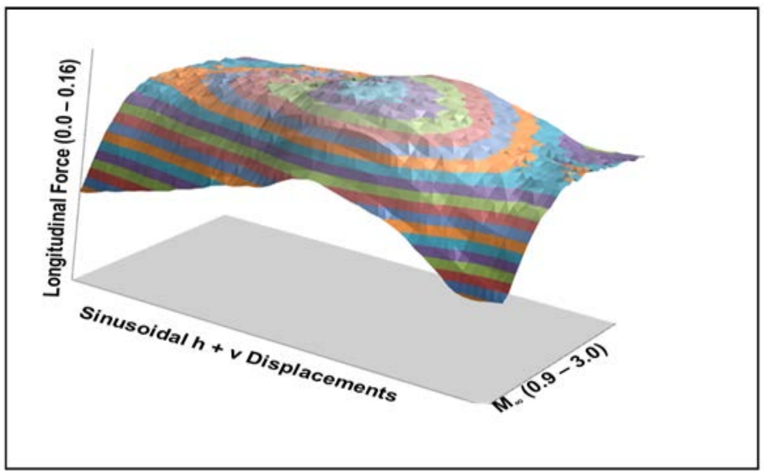

Effect of M on longitudinal forces

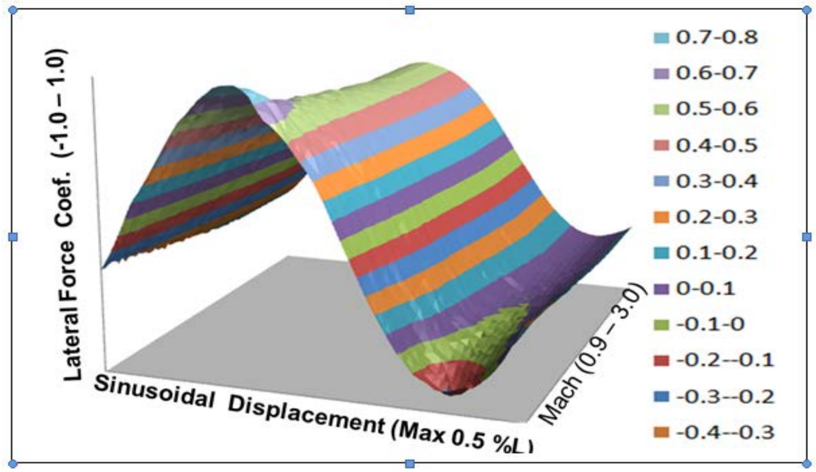

Effect of M on lateral forces

- Each 42-case (13M grid pts 5 cycles) job required a total 25 hrs of wall clock

Guruswamy, G.P Navier-Stokes based Unsteady Aerodynamic Computations of Launch Vehicles undergoing Coupled Oscillations., AIAA Jan 2013.

Trajectory Motion of Parachute

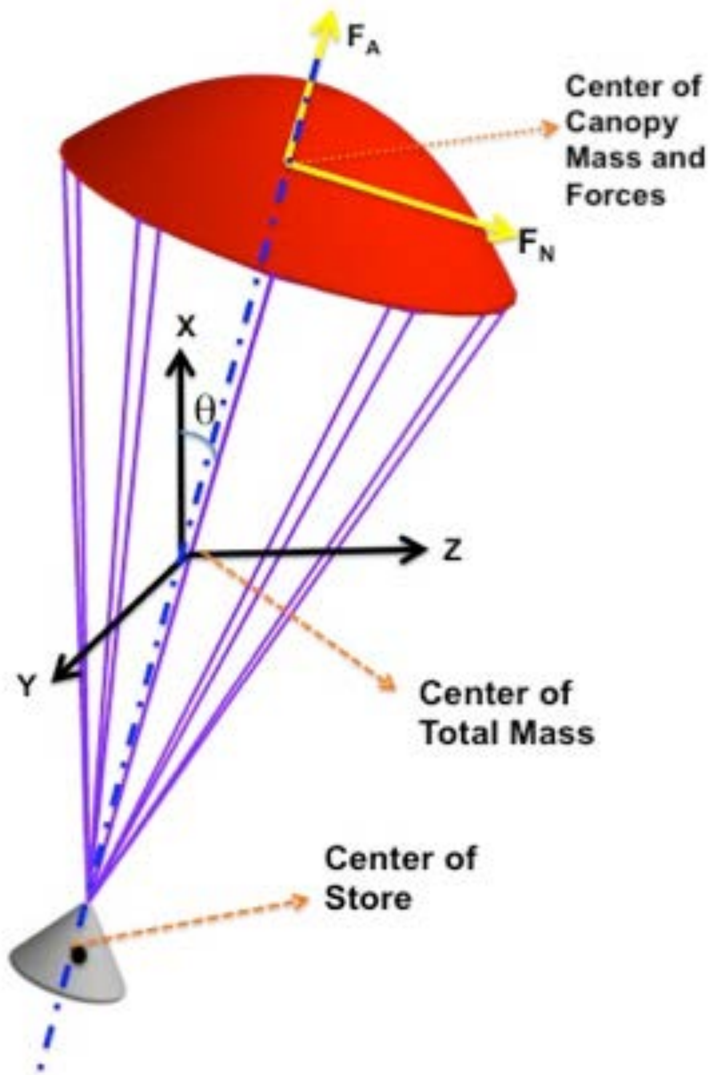

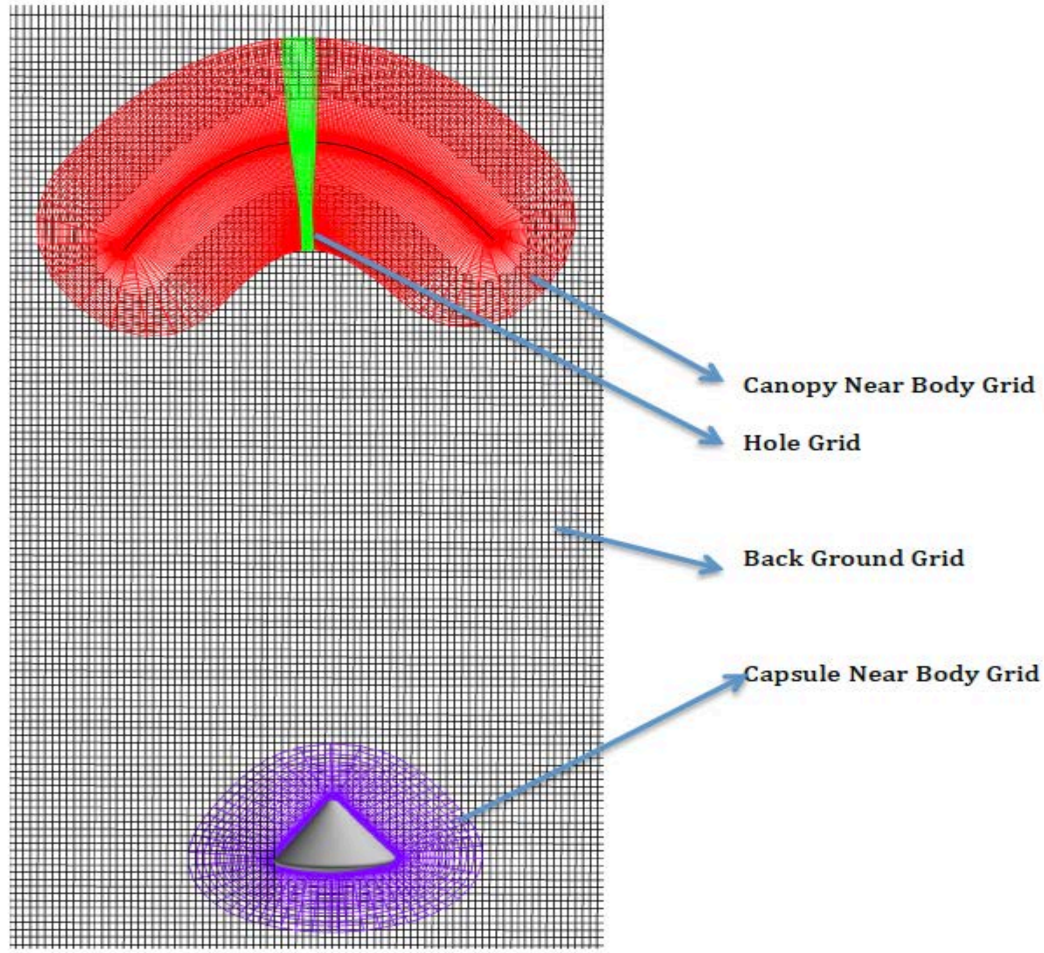

Trajectory Equations of Motion

The following assumptions are made:

a) m_a depends only on the canopy.
b) The centers of m_c and m_a are coincident.
c) m_c and m_p are at a fixed distance apart of L.
d) The centers of forces on canopy and its mass are coincident)
e) The aerodynamic force on payload smaller compared to canopy

The equations of motion governing the system are written as:

$$\frac{d^2\theta}{dt^2} + \left[\frac{g}{L(1+m_c m_a^{-1})}\right]\theta - \frac{F_N}{L(m_a+m_c)} = 0 \quad (1)$$

$$m_s \frac{d^2x}{dt^2} - m_t g + F_A \cos\theta - F_N \sin\theta = 0 \quad (2)$$

$$m_s \frac{d^2z}{dt^2} + F_A \sin\theta + F_N \cos\theta = 0 \quad (3)$$

Parachute Trajectory Motion
M = 2.0

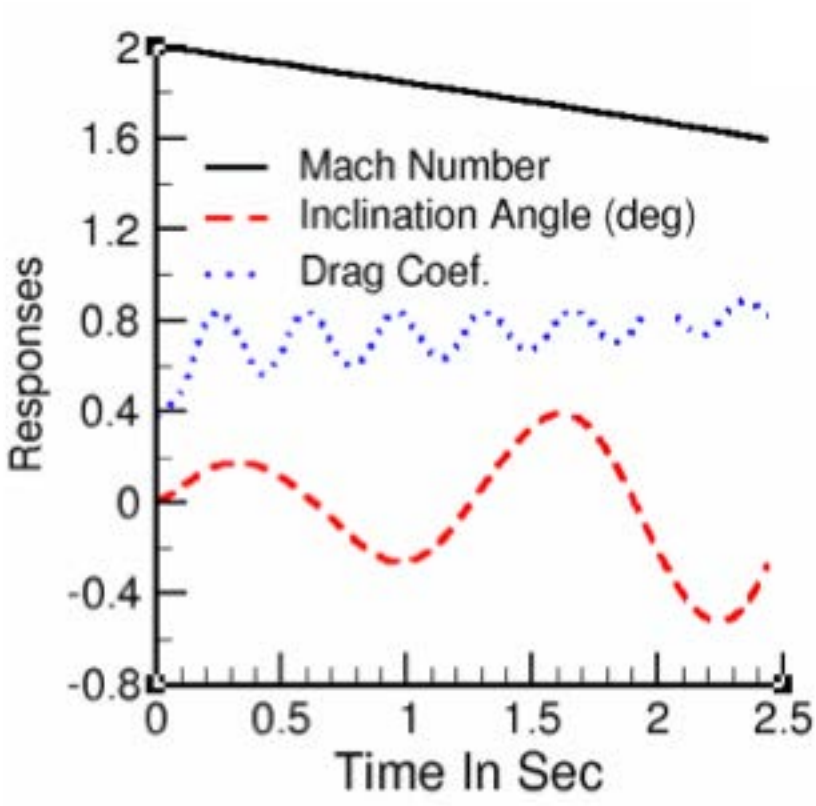

Responses during descent from $M_\infty = 2.0$.

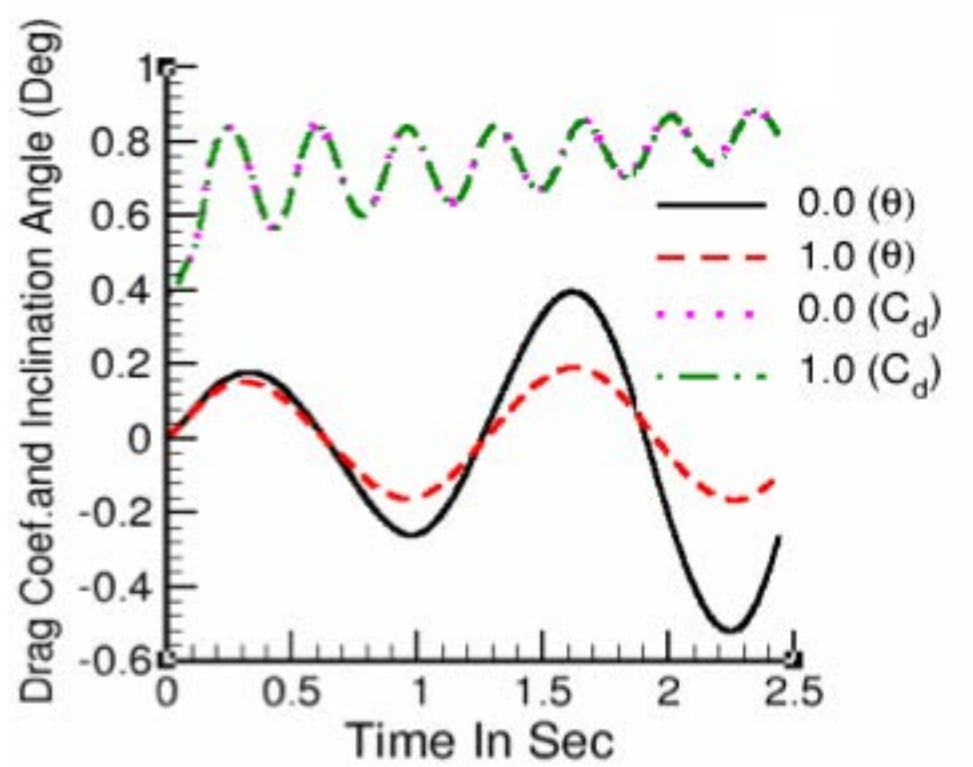

Effect of structural damping on responses.

Parachute Cluster

- Positions of canopies are initialized by applying transformations and rotations to undeflected canopy using Config.xml input file of OVERFLOW
  - Radius of rotation for all canopies 2D
  - Canopy_1 by 15 degrees in the X-Z plane,
  - Canopy_2 by -15 degrees in the X-Z plane then -15 degrees in the X-Y plane,
  - Canopy_3 by 15 degrees in the X-Y plane

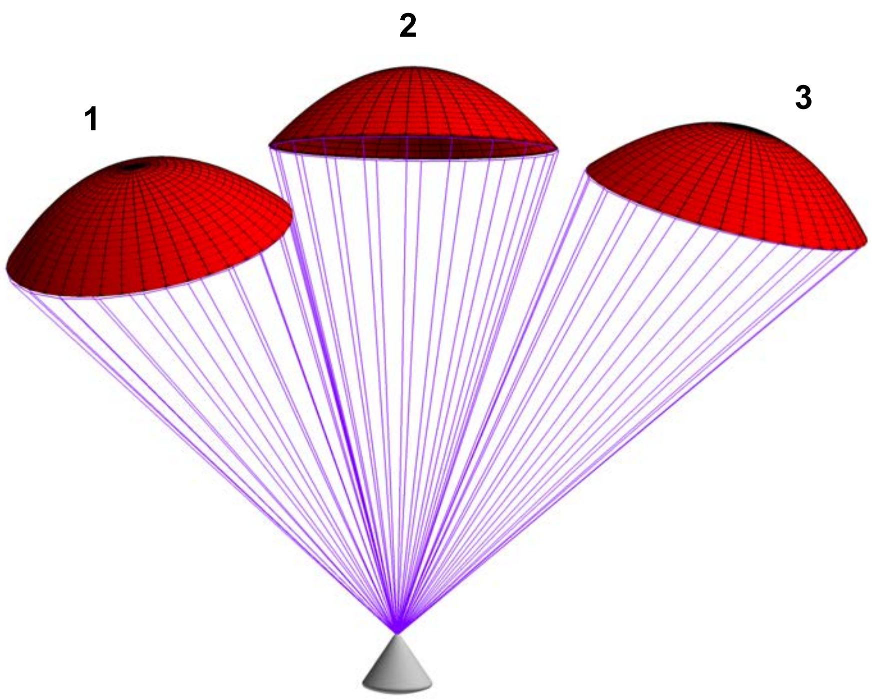

Parachute Cluster Grid

- Xray and Hole Cutting tools of OVERFLOW are used to blend near body grids with off-body grid.

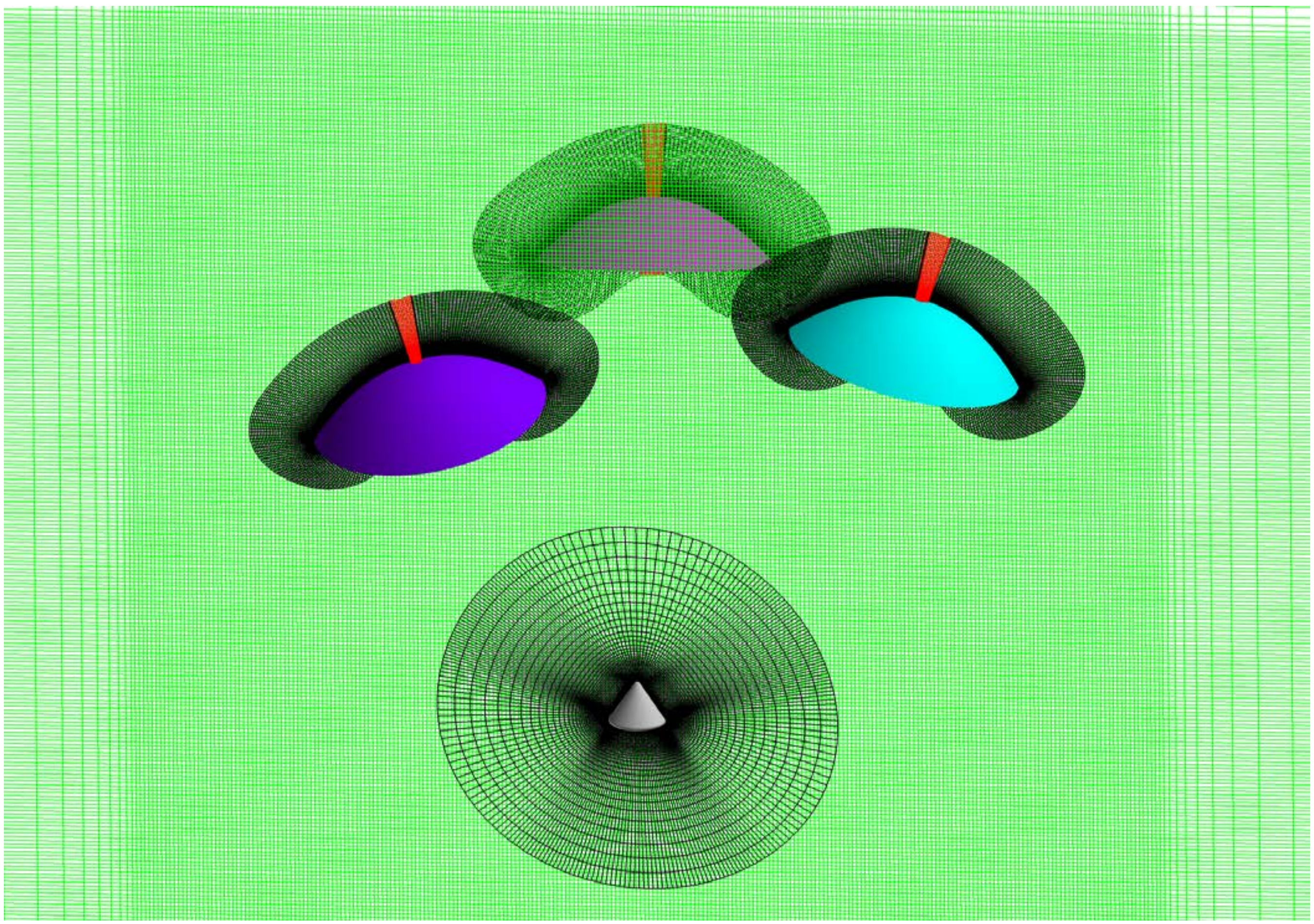

Parallel Computations

Steady state computations on isolated canopy

12000 iterations, 26.5 miilion grid points

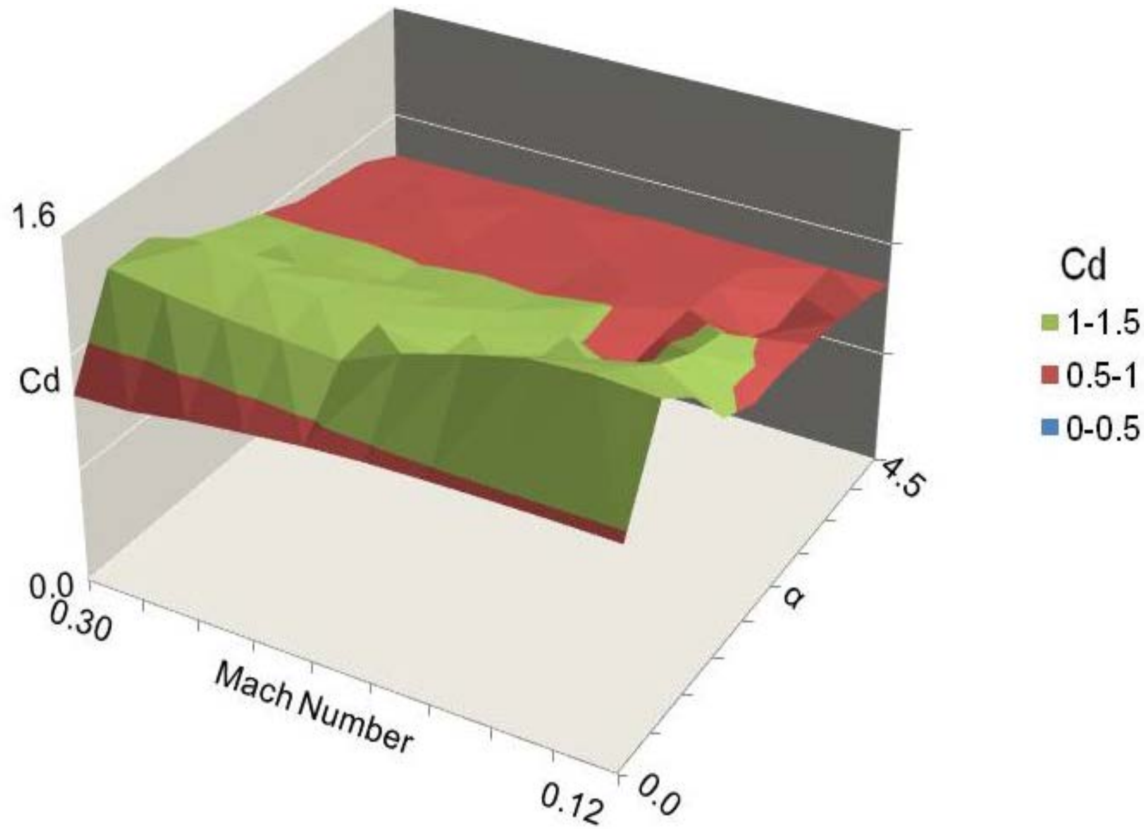

- 100 cases using 4000 cores with 40 cores per case requires 4.61 hrs
  - 1.8% more time than to run a single cases

- Coupling with trajectory motions is in progress

Example for Uncoupled Computations

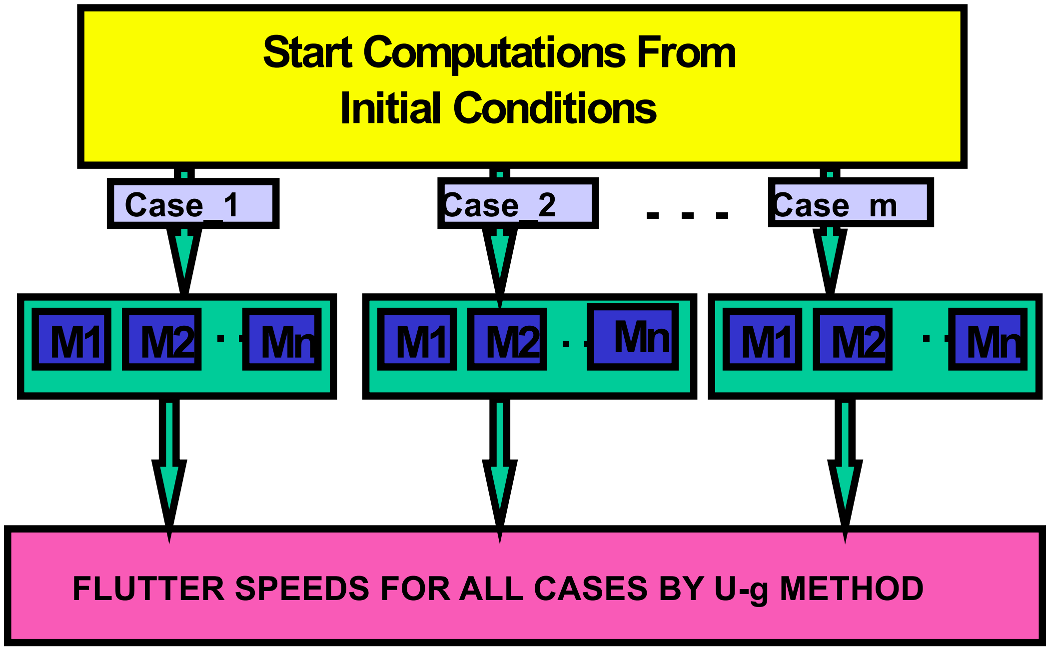

Mn N Modes = Number Of Modes X Number Of Frequencies Selected

Case_m Each Case May Have Different Flow Conditions

Flutter Boundary
Of A Typical Wing

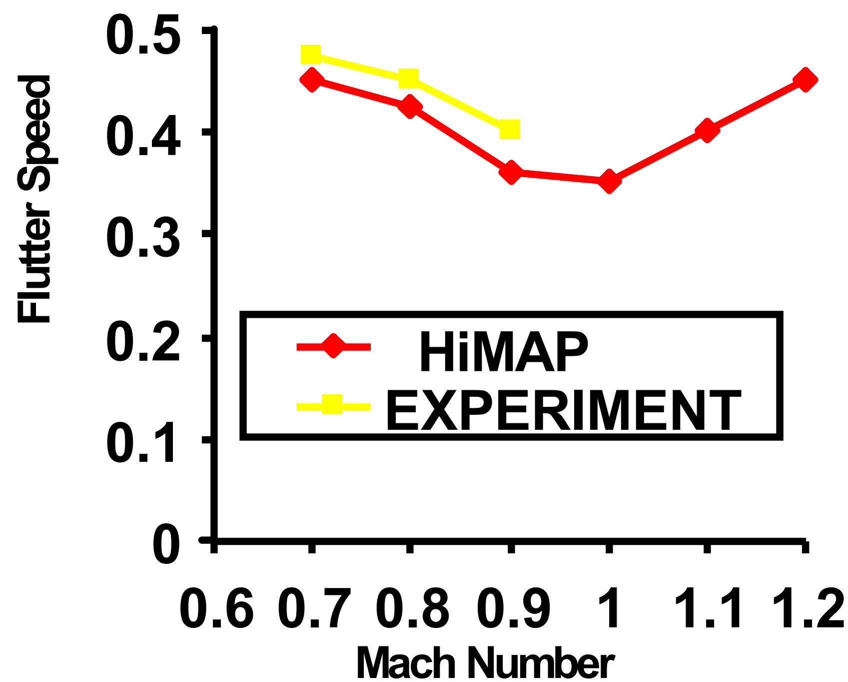

Note : 100 Gflop Performance On 1024 Nodes On O2000
Suitable Low- Fidelity Computations To Fill Design Space

Where CFD/CSD made a Difference

- Transonic flutter-dip of transport aircraft
- Lateral vortex motion coupled with bending motion of blended wing body configuration (B-1, HSCT, BWB)
- Control-reversal due to moving shock-waves
- Jump in phase angles near shock-wave
- Leading edge vortex induced vertical tail oscillations (F18)
- Nacelle oscillations of aircraft in transonic regime (L1011)
- Blade vortex interactions of rotorcraft
- Flexible thermal protection system (in progress)

Phugoid Motion Simulation of a Supersonic Transport using Navier-Stokes Equations

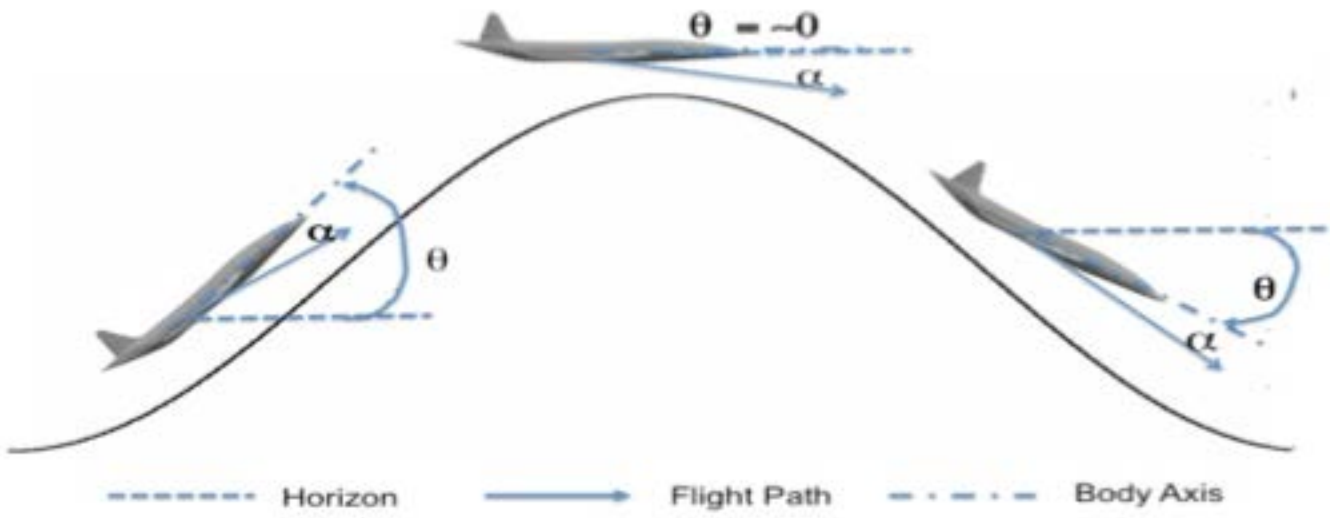

Oscillation in altitude due to the exchange between potential energy and kinetic energy is called phugoid oscillation. Beginning at the bottom of the cycle, pitch angle (θ) increases as the aircraft gains altitude and losses forward speed (V). During phugoid motion, the angle of attack (α) remains constant so that a drop in forward speed amounts to a decrease in lift and flattening of the pitch attitude.

Phugoid Motion Equations

Assuming that the phugoid motion starts with level flight, the equations of motion are written as:

$$\frac{d}{dt}\begin{Bmatrix} u \\ \theta \end{Bmatrix} = \begin{bmatrix} X_u & -g \\ {-Z_u}/{u_0} & 0 \end{bmatrix}\begin{Bmatrix} u \\ \theta \end{Bmatrix} \quad (1)$$

where u is the change in the velocity from the initial velocity u_0, θ is the flight-path angle, and g is acceleration due to gravity. X_u and Z_u are defined as:

$$X_u = -\frac{QS}{mu_0}\left[2C_{L0} + MC_{LM}\right] \quad (2)$$

$$Z_u = -\frac{QS}{mu_0}\left[2C_{D0} + MC_{DM}\right] \quad (3)$$

Equation system (1) are combined into a single ordinary differential equation with u as a variable by using $\theta = \frac{X_u u - u}{g}$ which results in:

$$\ddot{u} - X_u\dot{u} - \frac{Z_u g}{u_0}u = 0.0 \quad (4)$$

In this work, Eq. (4) is solved using the Newmark's time integration method

Typical Supersonic Transport

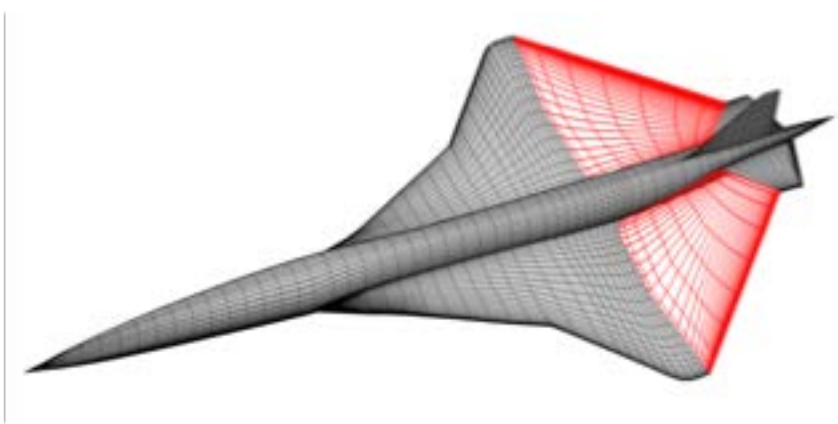

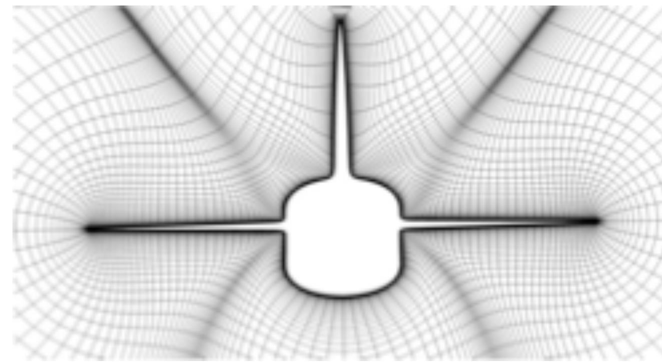

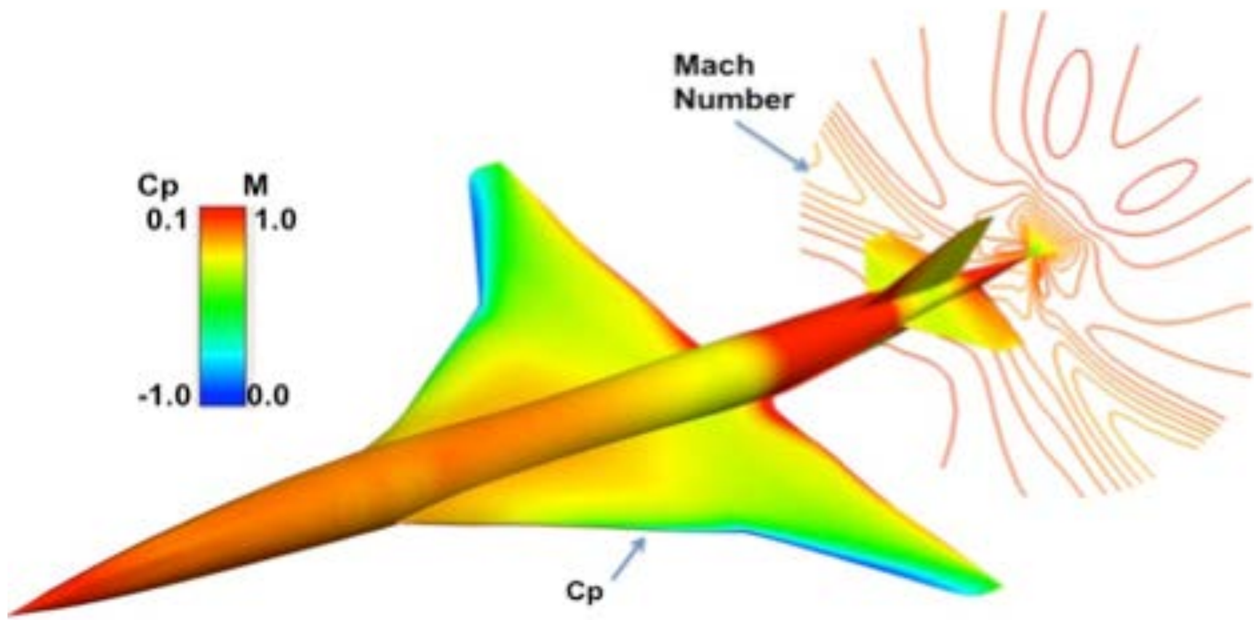

Effect of Mach Number on Phugoid Responses

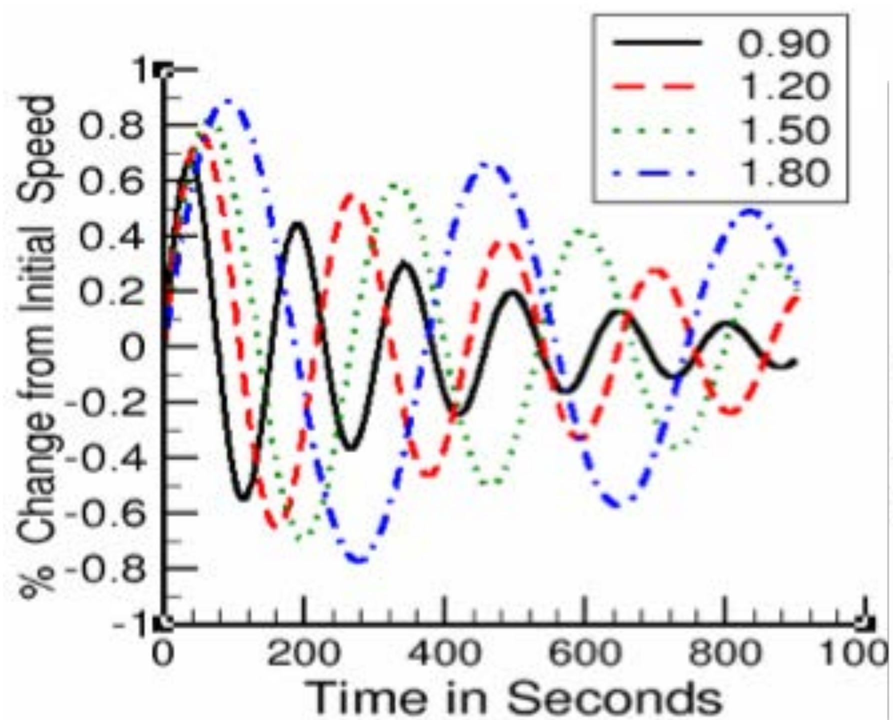

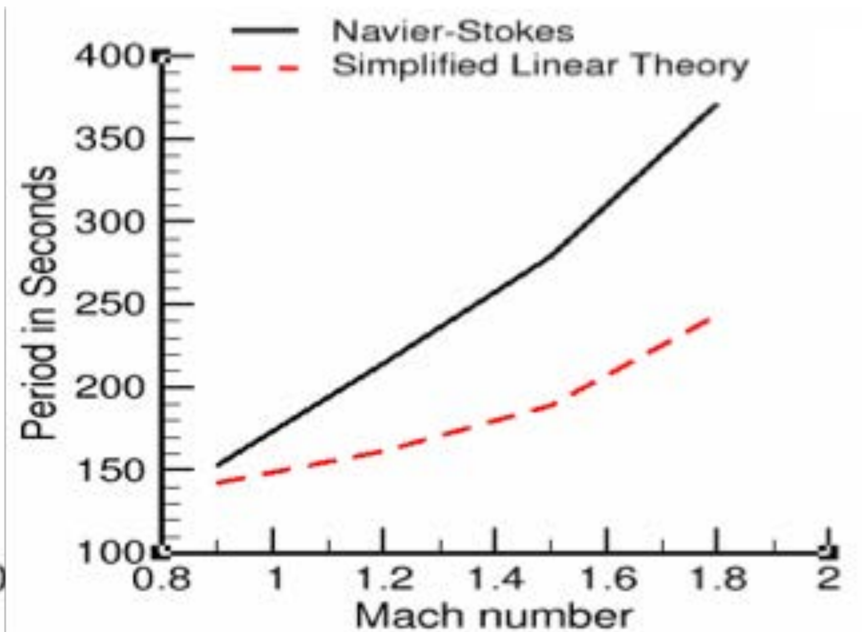

Effect of Mach numbers on change in speed at α = 5 deg.

Effect of Mach number on oscillation period α = 5deg

Dynamic Stability Analysis
Hypersonic Transport During Reentry

- Strong need exists for development of faster civil-transport
  - Supersonic transports
    - Boeing program, Next generation Concorde
  - Hypersonic Civil Transport (HCT)
    - NASA programs, European SKYLON

- Successful NASA Space Shuttle Transport (SST)
  - Limited passenger capability, 6 crew members
  - Lower length to width ratio
  - Stable atmospheric re-entry trajectory

- Current HCT
  - Planned for larger passenger capability, ~50 passengers
  - Larger length to width ratio
  - Aeroelastic stability plays more important role

Dynamic Stability Analysis Background

- Stability characteristics of high speed vehicles during re-entry
  - Centre of pressure (x_{CP}) shifts significantly and affects stability
  - Trimming is not practical due to rapid changes
  - Often expensive approaches such as moving the fuel location are needed for stable flights
- Computational approaches
  - Current stability analysis are limited to use linear aerodynamics
  - Fast methods based on Navier-Stokes flow equations are needed

Typical Reentry Scenarios

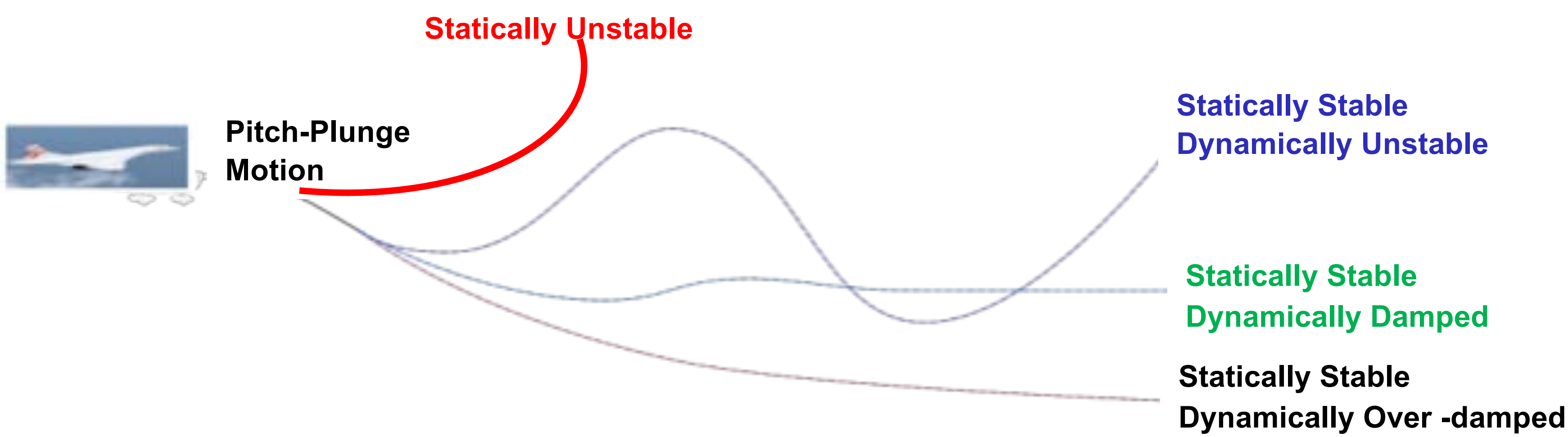

Hypersonic Civil Transport (HCT)

- Configuration
  - Topology of Langley Glide Back Booster (LGBB)

- Grids are generated using OVERGRID following accepted engineering procedures (NASA/TM-2013-216601)

- Body-fitted structured overset 19 near-body grid blocks (20 million points)
  - A normal spacing of 0.000025 of wing chord
  - Surface stretching factor of 1.125
  - Typical y+ value (one grid point away from the surface) is around 1

- Cartesian overset back ground grid blocks (25 million points)
  - Resolution of Level 1 grid is 0.5 % of length
  - Outer boundary location 12 lengths

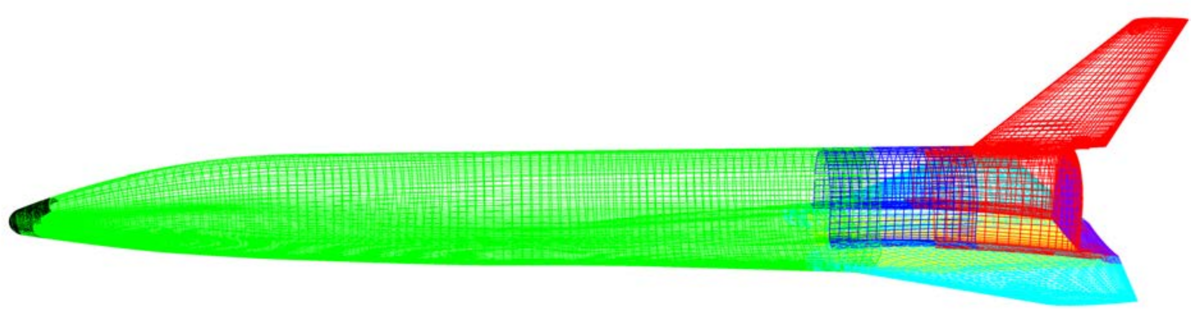

Parameters for Test Cases
(Final 30 seconds of typical atmospheric reentry)

- Mach number (M_∞) 5.5 to 0.5

- Angles of attack (α) 12.0 to 2.0 degrees

- Oscillating frequencies (f)
  plunge : 2 Hz, Pitch = 8hz

- Coefficients validated
  - Steady pressure C_p, Unsteady force coefficients

- Stability parameters computed
  - Flutter speed and frequency

Reentry – Steady- State Computations

Full Configuration, M_∞ = 5.5 to 0.5, α = 12 to 2 deg

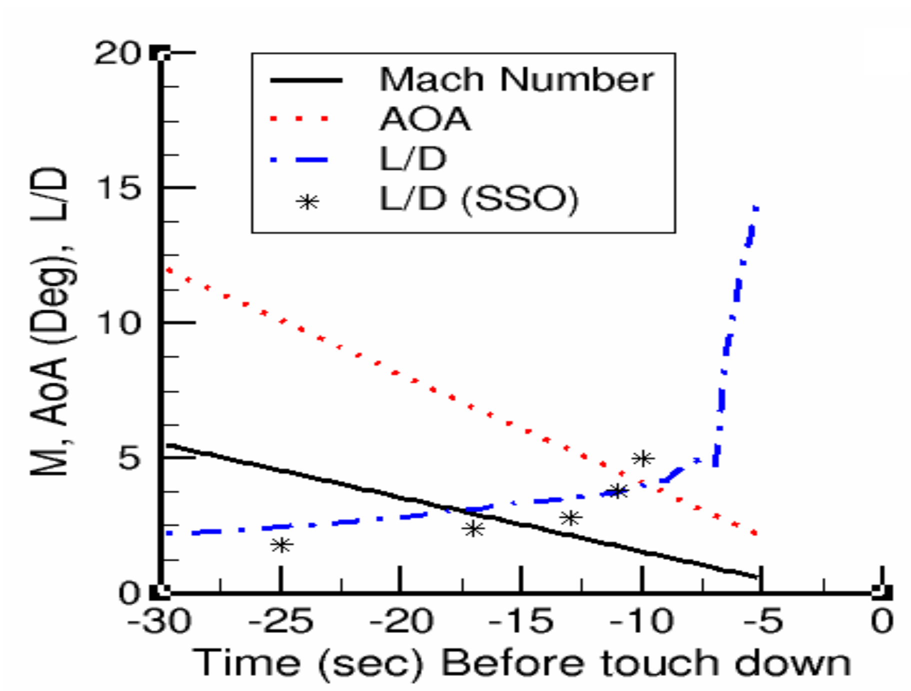

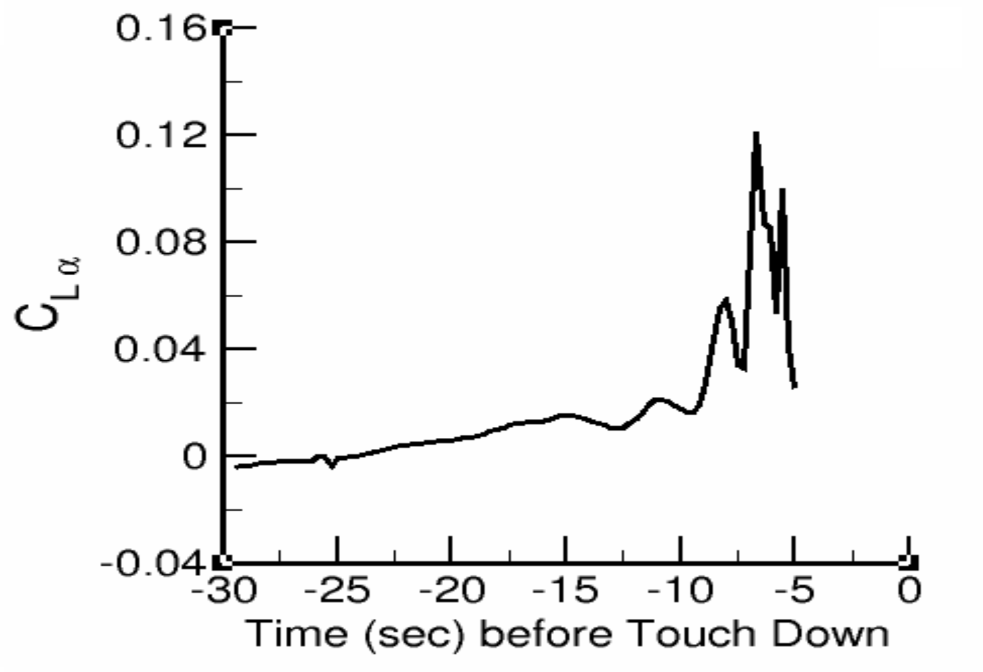

- **Using ~4,000 cores**
  - 100 cases in 2.5 hrs wall clock time

Validation of Indicial Computations with Experiment

Oscillating NACA64010 Airfoil

M_∞ = 0.8, Amplitude of α = 1.0 degs, Re_c = 2.0 million

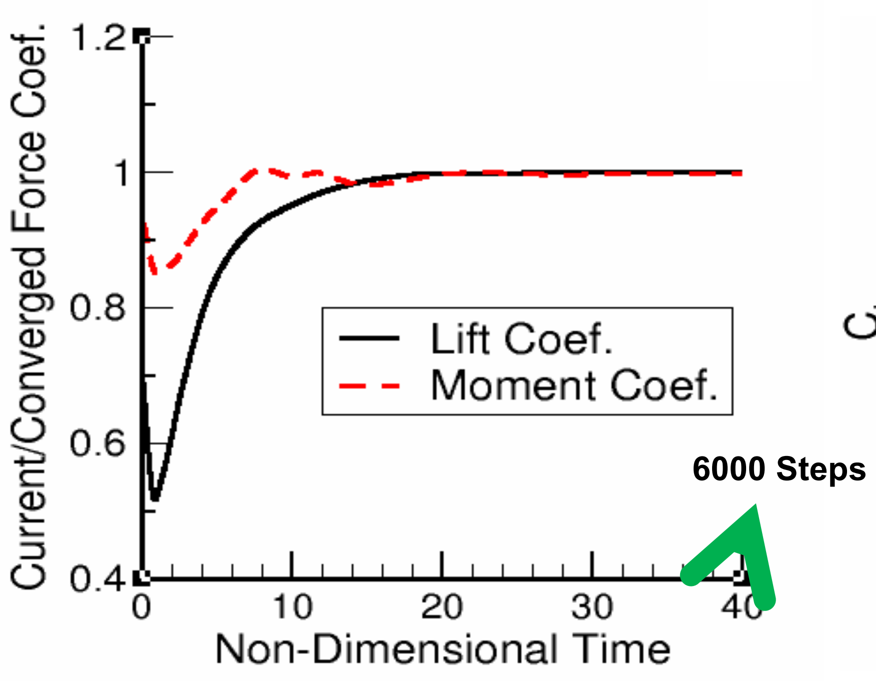

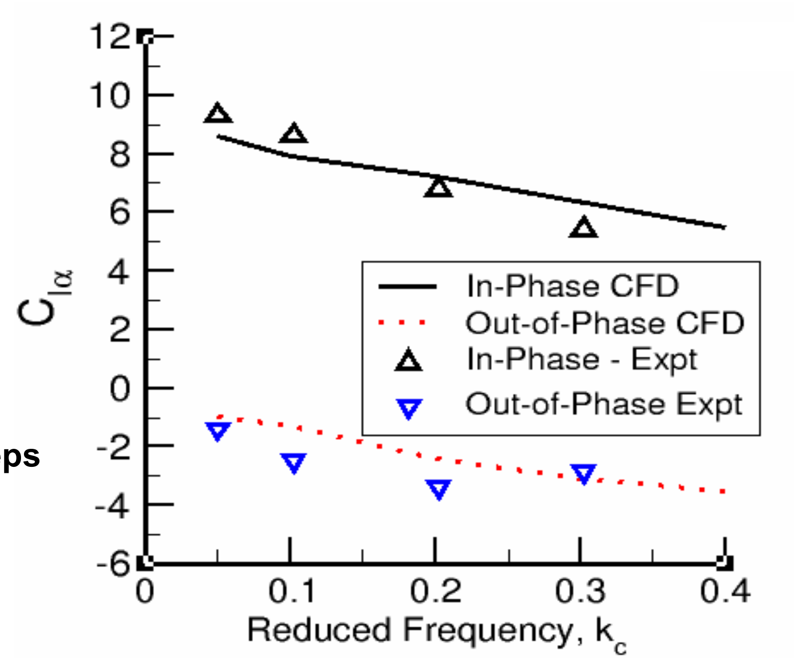

Validation of Indicial Computations with Time Integration

Oscillating, 50% Semi span section of HCT Wing

M_∞ = 0.9, Amplitude of α = 0.5 degs, Re_c = 2.0 million

Table 1: $C_{l\alpha}$ for section of the wing at 50% semispan.

Reduced-Frequency k_c	0.1	0.2	0.3	0.4	0.5
Indicial – In-Phase	8.440	8.001	7.557	6.891	6.127
Time-Integration – In-Phase	8.051	7.712	7.237	6.567	5.978
Indicial – Out-of-Phase	-1.338	-1.701	-2.025	-2.401	-3.001
Time-Integration – Out-of-phase	-1.233	-1.654	-1.934	-2.350	-2.905

- **Indicial response (IN) converged in 3000 steps**
- **Time-integration (TI) required 3 cycles with 3600 steps per cycle for each frequency**
- **Flutter speed differed by 5%**
- **Computational speed-up of IN (TI/IN) = (3x5x3600)/3000 = 18**

Indicial Response Computations for Reentry

Full Vehicle, 100 cases with M_∞ = 5.5 to 0.5, α = 12.0 to 2.0 degs

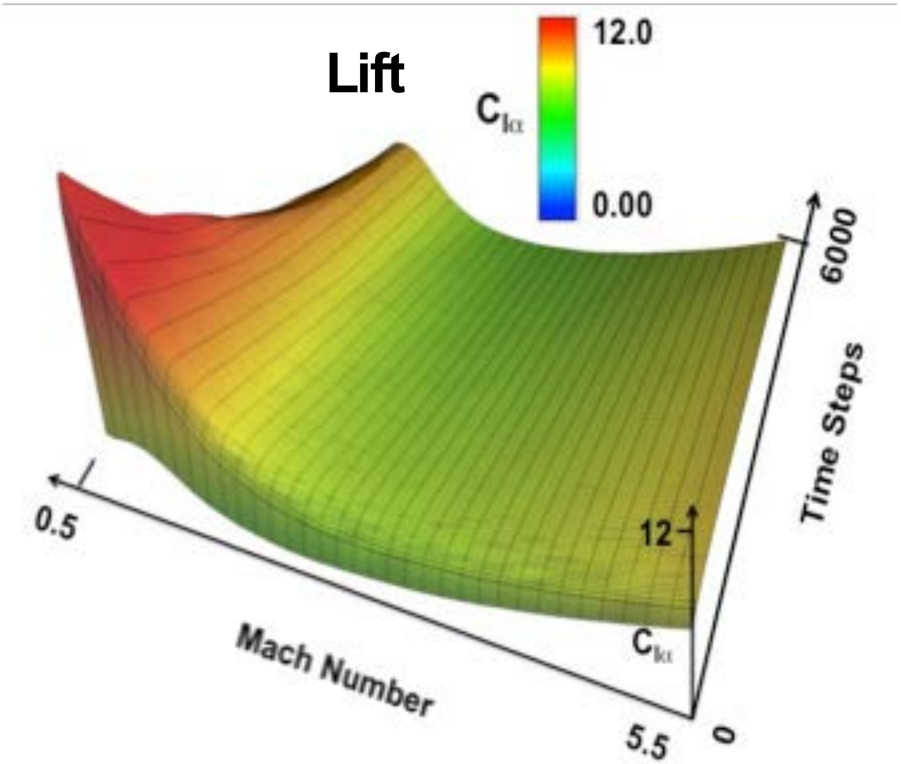

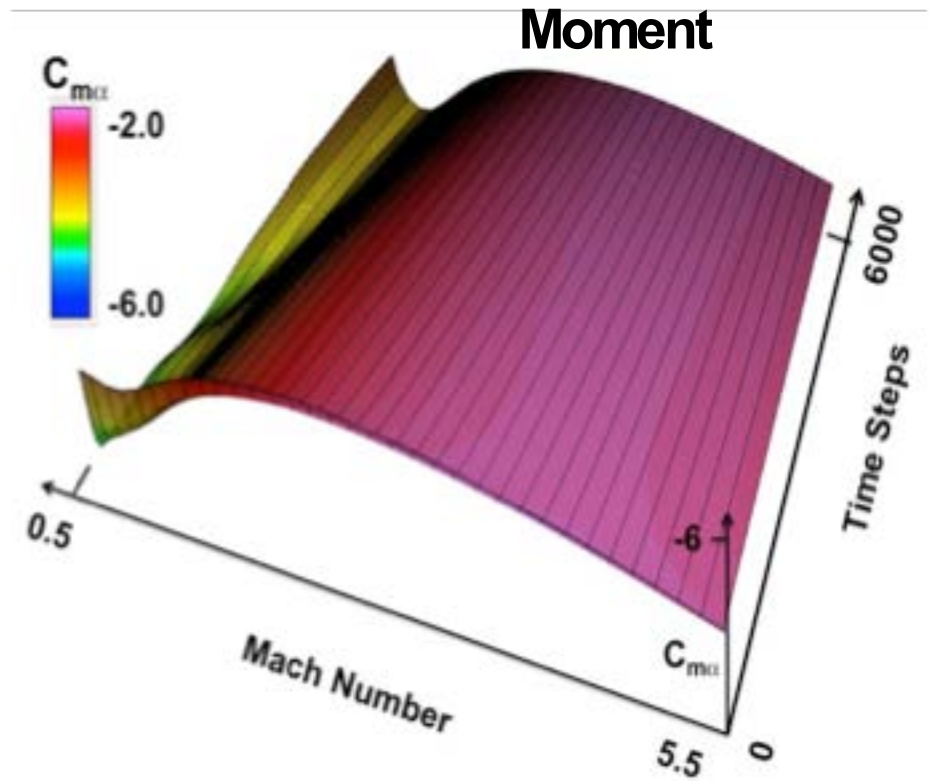

- Using ~4,000 cores.
  - 100 indicial responses in 17.5 hrs wall clock time

Flutter Boundary Computations during Reentry
Elastic axis is at 67% of length from nose
100 cases with M_∞ = 5.5 to 0.5, α = 12.0 to 2.0 degs

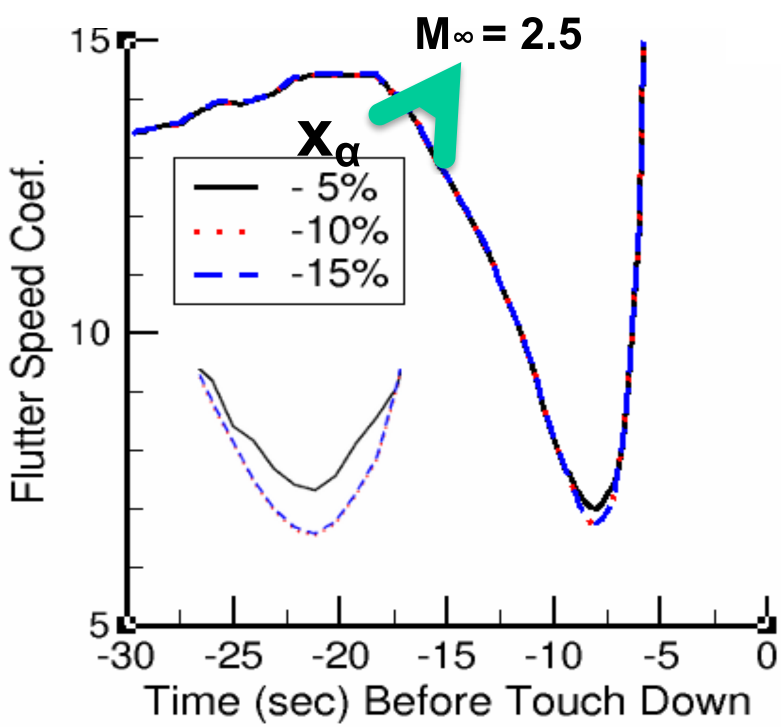

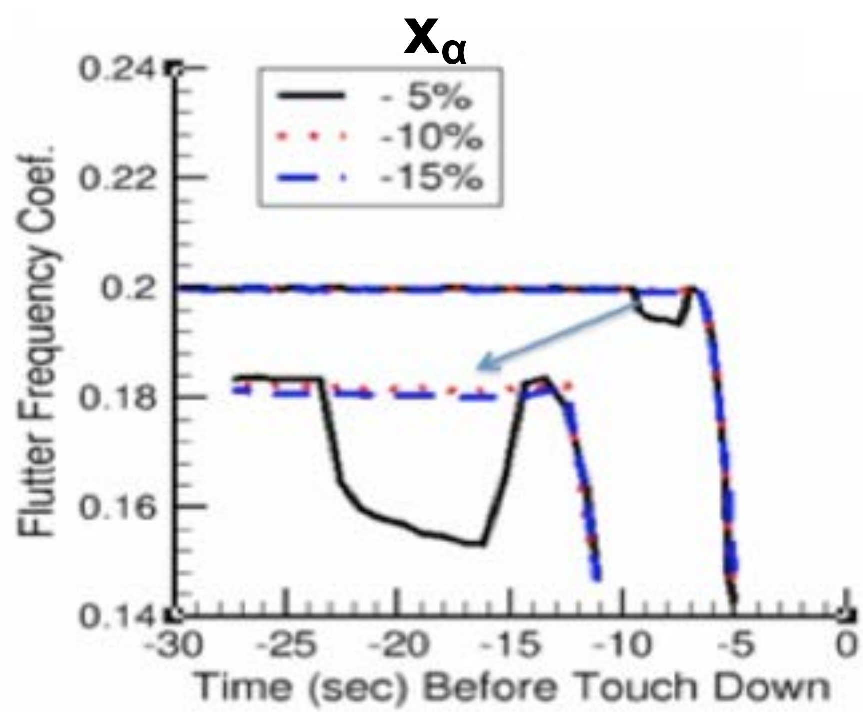

Flutter Boundary Computations during Reentry

Effect on Center of Pressure location

100 cases with M_∞ = 5.5 to 0.5, α = 12.0 to 2.0 degs

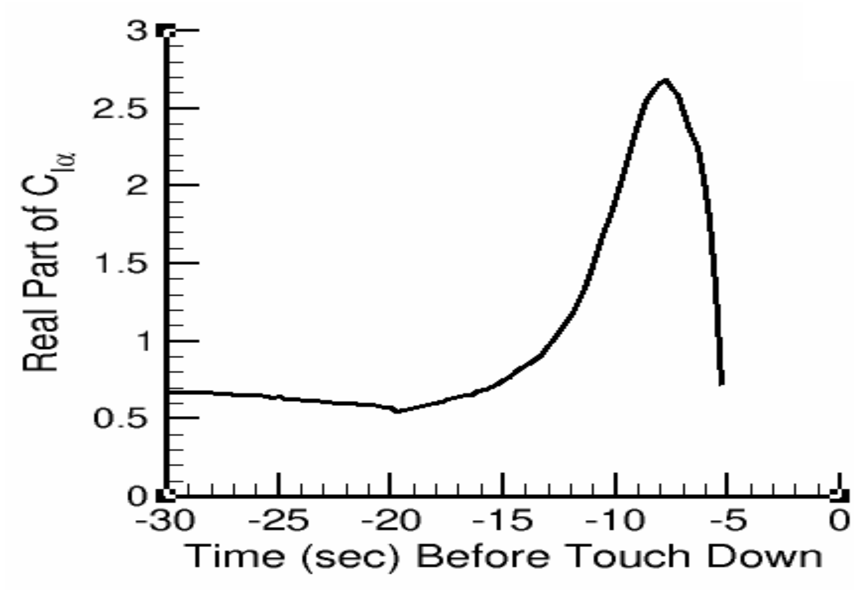

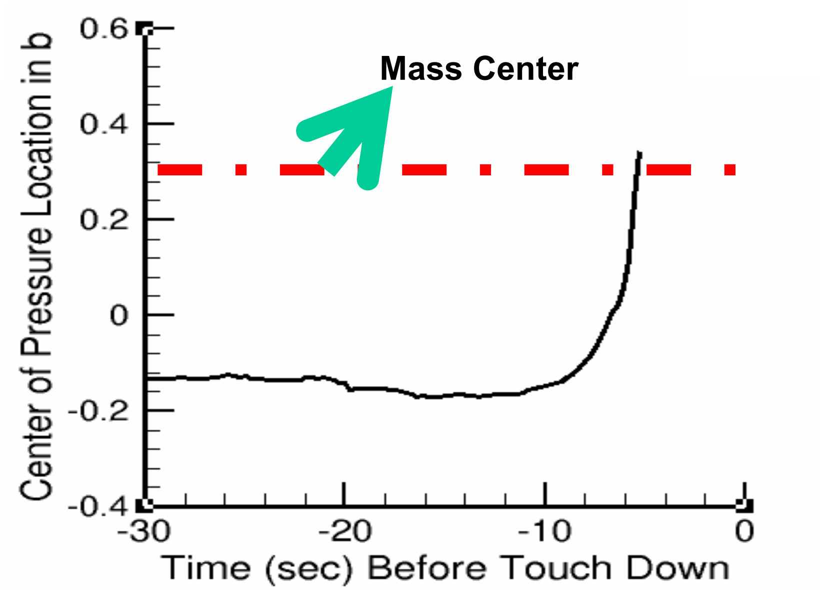

- **Based on Classical Theory**
  - **- Flutter speed decrease with increase in lift force**
  - **- Flutter speed increase as x_{CP} moves closer to mass center**
  - **- Phenomenon is similar to dip in flutter speed for wing of supersonic aircraft in the transonic regime**

LaRc BACT Model

Unsteady Computations on Oscillating Flap

M_∞ = 0.77, δ_0 = 0.0 deg, Re_c = 3.86 million

Sheared Grid Approach

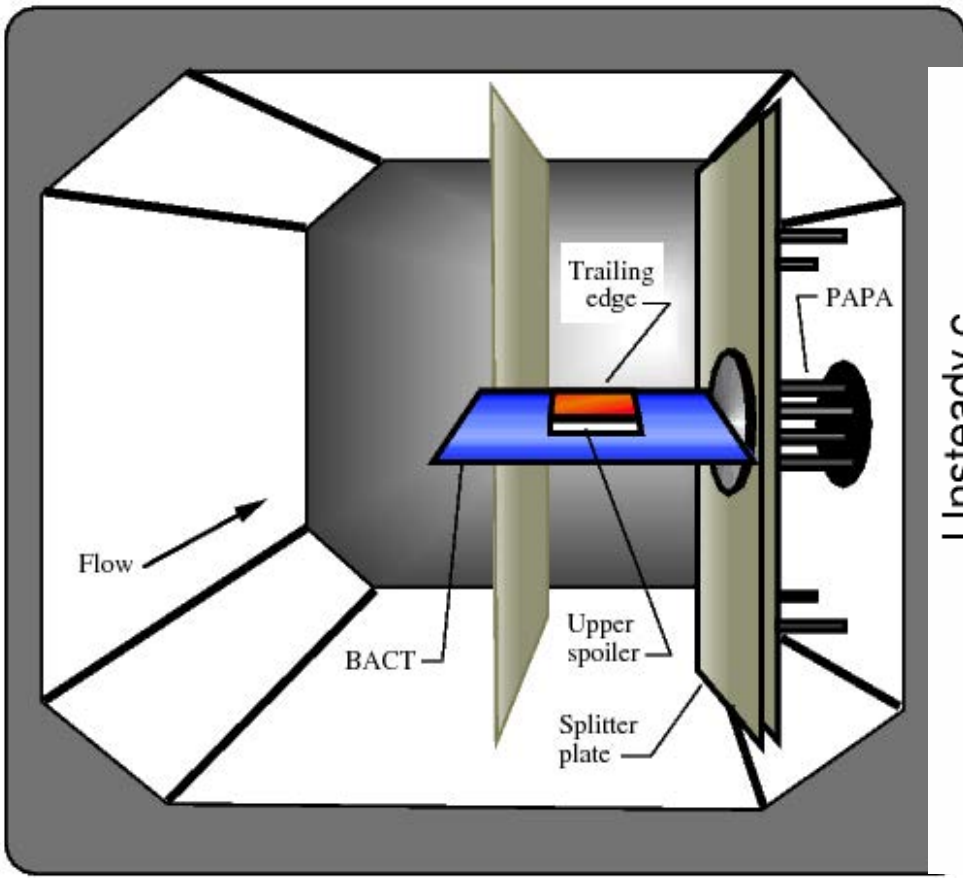

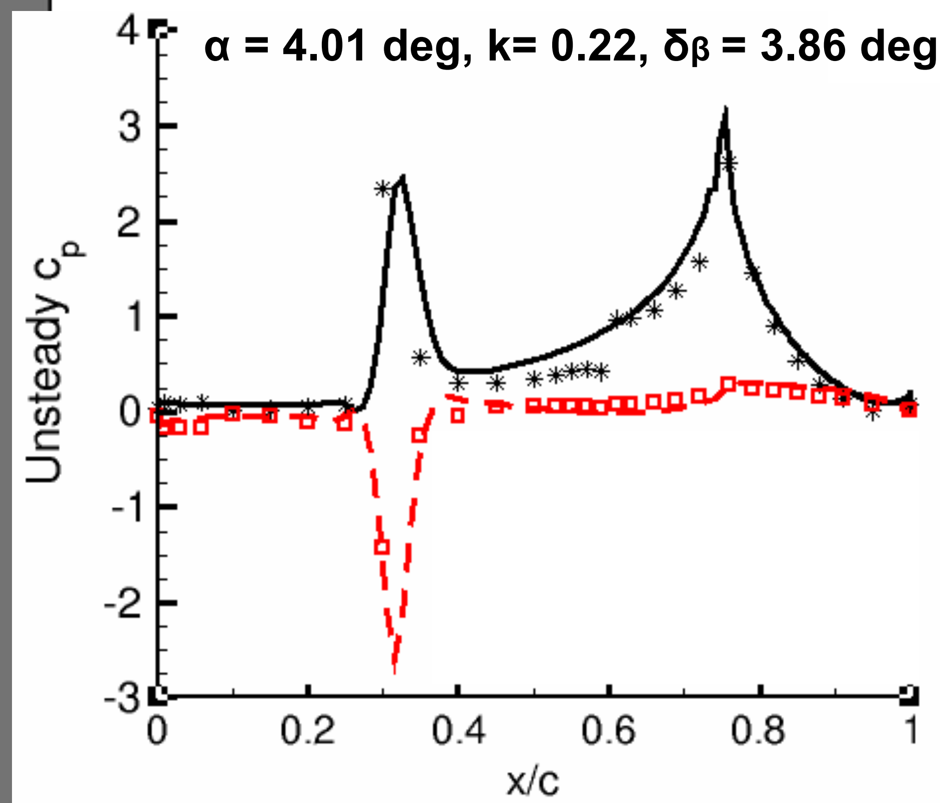

Wing Body with Oscillating Control Surfaces

FORCE COEFFICIENTS

$$M_\infty = 0.85,\ \mathrm{Re}_c = 9.5 \times 10^6,\ \alpha = 7.93^\circ$$

GRID: 1,020,800 POINTS
H-H TOPOLOGY

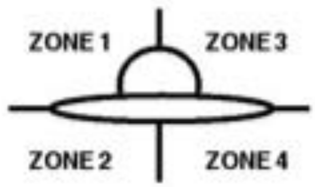

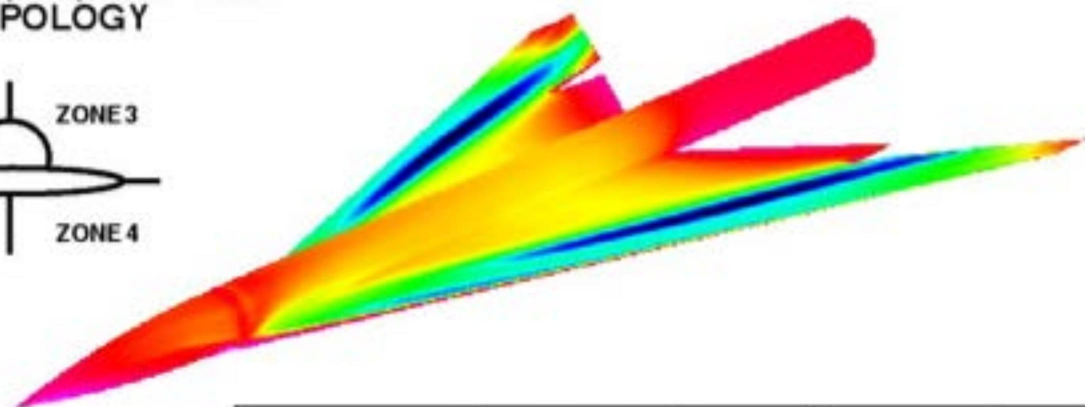

	$\alpha = 7.93^\circ,\ \delta = 0^\circ$		$\alpha = 7.93^\circ,\ \delta = 8.30^\circ$	
	C_N	C_{My}	C_N	C_{My}
Computation	0.298	–0.063	0.332	–0.092
Experiment, Manro et al.	0.295	–0.065	0.328	–0.093

Active Controls using TSP

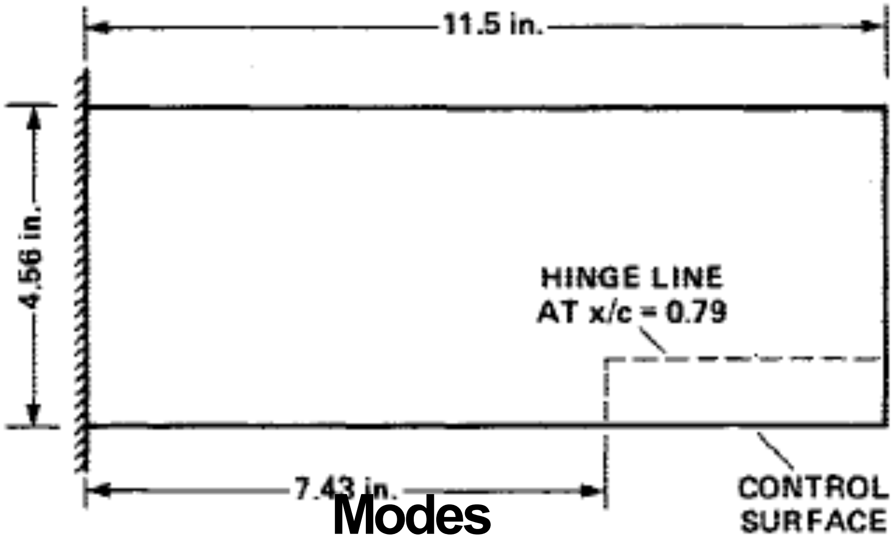

Modes

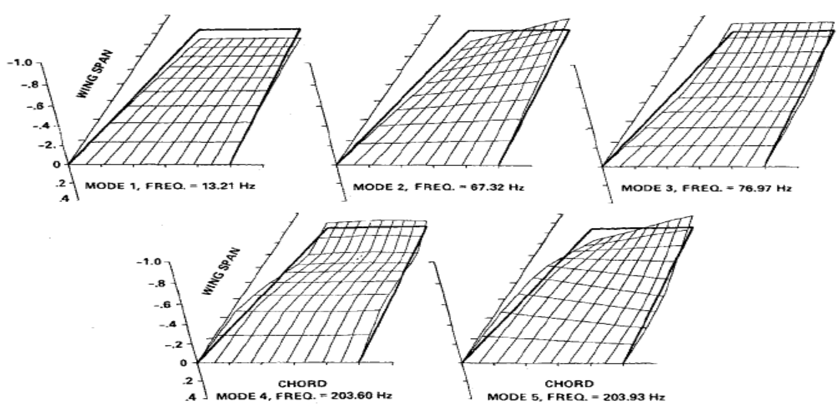

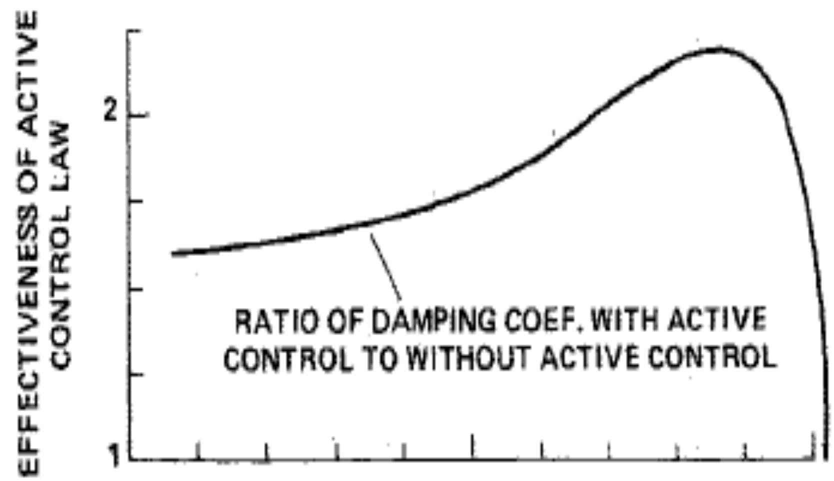

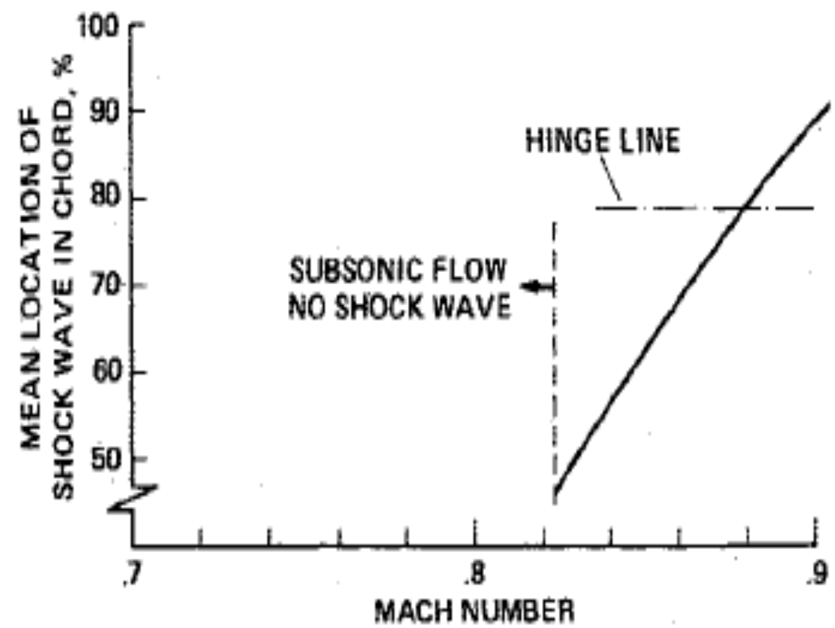

Demonstration of HiMAP for Wing-Body-Control Aeroelasticity

Processors

- **Fluid - 8**
- **Structures -1**
- **Controls -1**

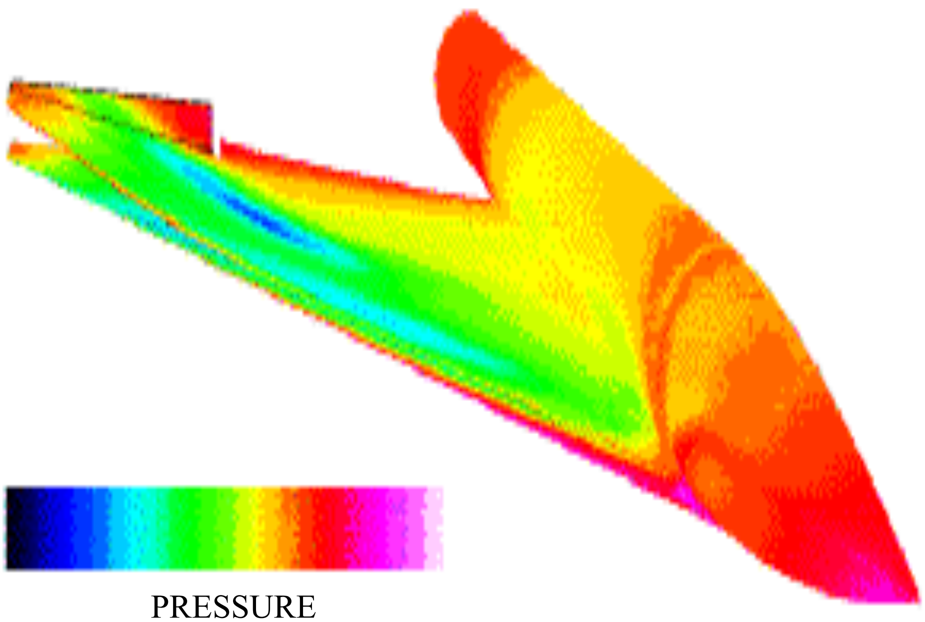

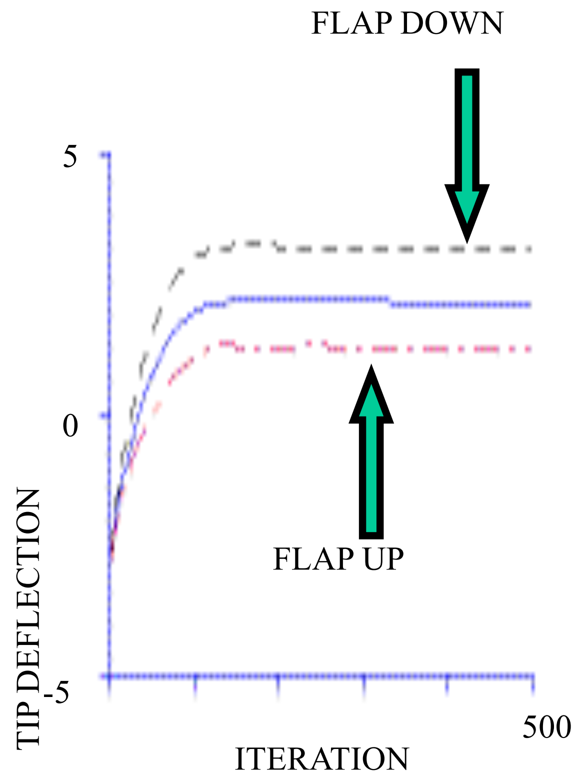

Summary of Results from Load Balancing Scheme

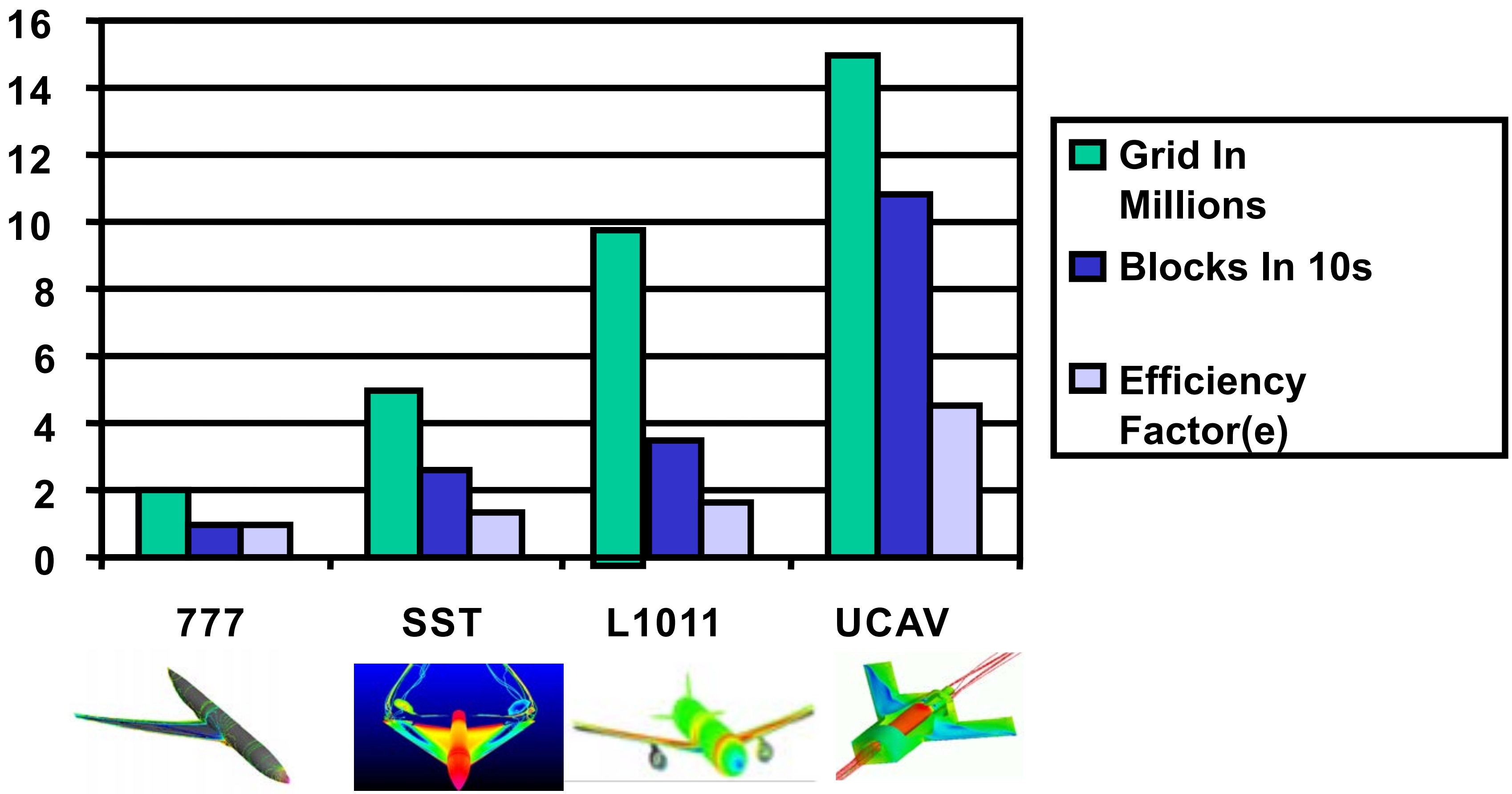

Efficiency factor 'E' is defined as $E = \left\{ \frac{ZO}{ZN} \right\}^2$

Where zo is number zones before load balancing and zn is the number of regrouped zones after load balancing.

Some Validation Efforts Since 1978

- CFD- based frequency domain uncoupled methods
- Classical methods such as Theodorsen's theory
- Linear aerodynamics theories
  - Kernel function method
  - Doublet-Lattice method (NASTRAN)
- Wind tunnel
  - NASA TND344: unsteady aero, rectangular wing
  - NASA TMX79: flutter of rectangular wing
  - NASA ARW: aeroelasticity of wing body
  - B-1 aircraft: vortex induced oscillations
  - F-18 aircraft: vertical tail buffet
  - HART II rotorcraft: blade vortex interaction
  - F5-wing: oscillating control surfaces
  - AFW: aeroelastic flexible wing, active controls
  - L1011: Nacelle oscillations
  - NASA/RAE/NLR – Moving control surfaces
- Flight tests
  - B-1 aircraft
  - F-18A -aircraft
  - UH-60A rotorcraft

What is Happening Elsewhere

- Rigorous Math models are being developed for FSI
  - Not yet proven better than engineering approaches

- Reduced order models for flows
  - Still as good as modal approach for Euler
  - Not robust for use with Navier-Stokes equations

- Using unstructured CFD
  - Computationally very slow
  - Still has issues in viscous zones

- Lattice Boltzmann equations based NS
  - Bookkeeping can be nightmare!
  -

- MDAO frameworks
  - One too many but still lack robust high fidelity MDA tools
  - Often end-up with low fidelity method
  - OpenMDAO supported by NASA has potential

Conclusions

- A summary of about 35-years, 100-person-year effort on development and applications of accurate coupled and uncoupled aeroelastic procedures using non-linear aerodynamic is presented.

- Case-by-case validations with either experiment or linear theory are shown to establish aeroelastic computations

- From this research it is observed that
  - Transonic small perturbation theory still useful for conceptual design
  - Euler/Navier Stokes equations and time accurate couplings are required to predict phase angles
  - Modal approach is adequate for responses
  - Staggered time integration is not necessary
  - Indicial method is better suited with NS than Reduced order modeling

- Given present computational resources, there is no need to hybridize CFD with linear/empirical aerodynamics
  - Introduces significant errors when inertial loads are present, which is common for flexible configurations
  - Not capable of predicting transient physics associated with coupling of non-linear flows with structures

- Classical Indicial method is robust and more efficient than reduced order method for RANS

Future Efforts

- Coupled procedures need higher fidelity CSD
  - 3-D FSI
  - Composites for all aerospace vehicles
  - Visco-thermoelastic for spacecrafts

- Faster and more accurate CFD
  - Better turbulence models
  - Robust moving grids
  - Larger time steps with no CPU time penalty
  - Robust codes with real-gas effects
  - Multi-Phase such as Cavitational flows for PoGO of Launch Vehicles)

- CFD/CSD method time accurately integrated with stability and maneuver dynamics equations is needed for full simulation

  Appa, K., Argyris J.H and Guruswamy G. P., "Aircraft Dynamics and Loads Computations Using CFD Methods," AIAA 96-1342.

Future Efforts

Hypersonic Inflatable Aerodynamic Decelerator

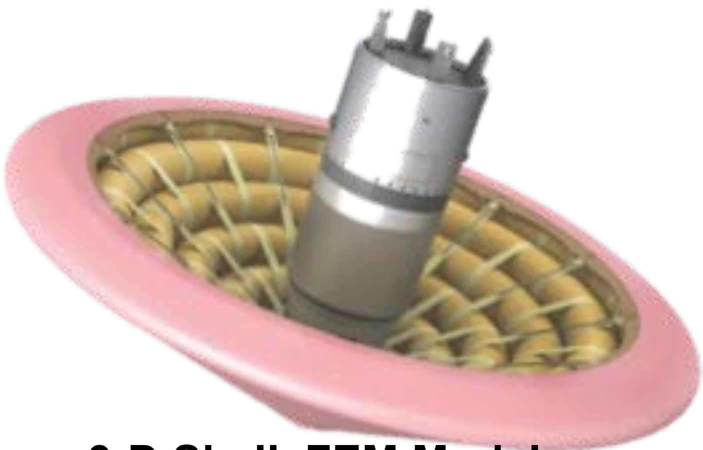

Simplified 1-D FEM Model Used Elsewhere

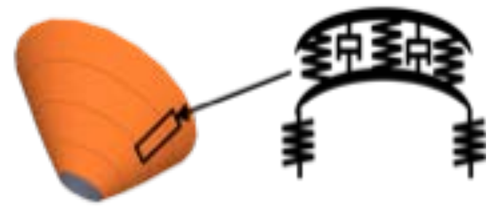

3-D Shell FEM Model Preliminary Results

DEMO COMPUTATIONS FOR HYPERSONIC RIGIME

- 18 DOF SHELL FEM, 920 ELEMENTS
- NOSE ASSUMED TO BE RIGID, OUTER BOUNDARY FREE TO MOVE
- Cp COMPUTED USING LEES FORMULA FOR NEWTONIAN FLOW

Structural Stresses Due to Aero-loads (red tension, green compression)

Quasi-Steady Radial Displacement Response While Oscillating with 1.5 deg amplitude